N84-33416
[redacted]

NASA CR-165949
R82AEB436

National Aeronautics and
Space Administration

Langley Research Center
Hampton, Virginia 23665

NOZZLE PERFORMANCE CALIBRATION AND TRUBOMACHINERY OPERATIONAL ANALYSIS OF TURBO-POWERED SIMULATORS (TPS) FOR THE NASA-LANGLEY EET PROPULSION AIRFRAME INTEGRATION INVESTIGATION

By

R. Kevin Rowe
General Electric Company
Aircraft Engine Business Group

Prepared for
National Aeronautics and Space Administration

[illegible]

Review for general release August 31, 1984.

NASA Langley Research Center
NAS1-15345

1. Report No.	2. Government Accession No.	3. Recipient's Catalog No.
NASA CR-165949		

4. Title and Subtitle
NOZZLE PERFORMANCE CALIBRATION AND TURBOMACHINERY OPERATIONAL ANALYSIS OF TURBOPOWERED SIMULATORS (TPS) FOR THE NASA-LANGLEY EET PROPULSION/AIRFRAME INTEGRATION INVESTIGATION

5. Report Date
August 1982

6. Performing Organization Code

7. Author(s)
R. Kevin Rowe

8. Performing Organization Report No.
R82AEB436

9. Performing Organization Name and Address
General Electric Company
Aircraft Engine Business Group
Advanced Technology Operations
Cincinnati, Ohio 45215

10. Work Unit No.

11. Contract or Grant No.
NAS1-15345

12. Sponsoring Agency Name and Address
National Aeronautics and Space Administration
Washington, D.C. 20546

13. Type of Report and Period Covered
Contractor Report

14. Sponsoring Agency Code

15. Supplementary Notes
Langley Technical Monitor; J.C. Patterson, Jr.
Final Report

16. Abstract

Calibration tests were conducted at the Boeing Flight Simulator Chamber facility in January 1979 for use in the NASA-Langley Engergy Efficient Transport (EET) Propulsion/Airframe Integration Investigation.

Two turbopowered simulators (TPS) were calibrated with four different nacelle configurations. Two nacelle configurations were calibrated on each TPS, each calibration simulating the full nozzle pressure ratio range encountered in a one atmosphere total pressure wind tunnel operating over a Mach number range from 0.70 to 0.90 Mach.

The configurations tested are 6% scale model versions of the CF6-50 Short Core and Long Core seperate flow nacelles, the CF6-50 Long Duct Mixed Flow nacelle, and a 6.2855% scale model of the Energy Efficient Engine (E^3) mixed flow nacelle. The results of the calibration test are in the form of velocity and discharge coeffecients used in determining the simulator thrust while the TPS is operating in the wind tunnel.

17. Key Words (Suggested by Author(s))
Turbopowered Simulator, Calibration Test, Nozzle Coefficients, Wind Tunnel Test, Turbomachinery Operation

18. Distribution Statement
[redacted]
Subject Category 07

19. Security Classif. (of this report)	20. Security Classif. (of this page)	21. No. of Pages	22. Price*
Unclassified	Unclassified	124	

[redacted]

Page intentionally left blank

Page intentionally left blank

TABLE OF CONTENTS

LIST OF ILLUSTRATIONS

LIST OF ILLUSTRATIONS (Concluded)

LIST OF TABLES

NOMENCLATURE

Symbol	Units SI	Units (British)	Definition
A_8	m^2	($in.^2$)	Primary Nozzle Exit Flow Area
A_{18}	m^2	($in.^2$)	Fan Nozzle Exit Flow Area
C_{D_8}	-	-	Primary Nozzle Discharge Coefficient
$C_{D_{18}}$	-	-	Fan Nozzle Discharge Coefficient
C_{f_g}	-	-	Thrust Coefficient
C_L	-	-	Airplane Lift Coefficient
C_{V_9}	-	-	Primary Nozzle Velocity Coefficient
$C_{V_{19}}$	-	-	Fan Nozzle Velocity Coefficient
F_{g9}	N	(lb)	Actual Primary Gross Thrust
F_{g9_i}	N	(lb)	Ideal Primary Gross Thrust
F_{g19}	N	(lb)	Actual Fan Gross Thrust
F_{g19_i}	N	(lb)	Ideal Fan Gross Thrust
F_{g_T}	N	(lb)	Total Simulator Gross Thrust
F_N	N	(lb)	Simulator Net Thrust
F_R	N	(lb)	Simulator Ram Drag
g	m/sec^2	(ft/sec^2)	Acceleration of Gravity, 9.8067 m/sec^2
M_∞	-	-	Tunnel Freestream Mach Number
$\bar{m}_8$	$\sqrt{\frac{m\text{-}Kmole\text{-}^\circ K}{sec^2\text{-}J}}$	$\left(\sqrt{\frac{lbm\text{-}^\circ R}{lbf\text{-}sec^2}}\right)$	Core Flow Function
$\bar{m}_{18}$	$\sqrt{\frac{m\text{-}Kmole\text{-}^\circ K}{sec^2\text{-}J}}$	$\left(\sqrt{\frac{lbm\text{-}^\circ R}{lbf\text{-}sec^2}}\right)$	Fan Flow Function

Symbol	Units SI	(British)	Definition
N_F	rad/sec	(rpm)	Physical Fan Speed
$N_F/\sqrt{\theta_F}$	rad/sec	(rpm)	Corrected Fan Speed
P_∞	N/m^2	($lb/in.^2$)	Tunnel Ambient Pressure
P_{S_8}	N/m^2	($lb/in.^2$)	Primary Exit Static Pressure
P_{T_N}	N/m^2	($lb/in.^2$)	ASME Nozzle Total Pressure
P_{T_∞}	N/m^2	($lb/in.^2$)	Tunnel Total Pressure
P_{T_4}	N/m^2	($lb/in.^2$)	Turbine Inlet Pressure
P_{T_5}	N/m^2	($lb/in.^2$)	Average Turbine Discharge Pressure
P_{T_8}	N/m^2	($lb/in.^2$)	Core Exit Total Pressure
$P_{T_{15}}$	N/m^2	($lb/in.^2$)	Average Fan Discharge Pressure
P_{T_4}/P_{T_5}	-	-	Turbine Pressure Ratio
P_{T_5}/P_∞	-	-	Core Nozzle Pressure Ratio
$P_{T_{15}}/P_\infty$	-	-	Fan Nozzle Pressure Ratio
$P_{T_{15}}/P_{T_\infty}$	-	-	Fan Pressure Ratio
R	$\frac{J}{Kmole\text{-}K}$	$\left(\frac{ft\text{-}lbf}{lbm\text{-}^\circ R}\right)$	Gas constant for air, $8314.34 \frac{J}{Kmole\text{-}K}$
$rpm/\sqrt{\theta}$	Rad/sec	(rpm)	TPS rpm Corrected to Ambient Total Temperature
T_{T_∞}	K	(° R)	Tunnel Total Temperature
T_{T_4}	K	(° R)	Turbine Inlet Temperature
T_{T_5}	K	(° R)	Average Turbine Discharge Temperature
$T_{T_{15}}$	K	(° R)	Average Fan Discharge Temperature
T_{T_4}/T_{T_5}	-	-	Turbine Temperature Ratio
$T_{T_{15}}/T_{T_\infty}$	-	-	Fan Temperature Ratio

Symbol	Units SI	(British)	Definition
V_∞	m/sec	(ft/sec)	Tunnel Freestream Velocity
V_{8_i}	m/sec	(ft/sec)	Ideal Core Exit Velocity
V_{9_i}	m/sec	(ft/sec)	Ideal Fully Expanded Core Flow Velocity
V_{19_i}	m/sec	(ft/sec)	Ideal Fully Expanded Fan Flow Velocity
W_5	kg/sec	(lb/sec)	Simulator Drive Weight Flow
W_8	kg/sec	(lb/sec)	Actual Core Weight Flow
W_{8_i}	kg/sec	(lb/sec)	Ideal Core Weight Flow
W_{18}	kg/sec	(lb/sec)	Actual Fan Weight Flow
W_{18_i}	kg/sec	(lb/sec)	Ideal Fan Weight Flow
$W_5\sqrt{\theta T}/\delta_T$	kg/sec	(lb/sec)	Corrected Turbine Weight Flow
$W_{18}\sqrt{\theta F}/\delta_F$	kg/sec	(lb/sec)	Corrected Fan Weight Flow
α	rad	(deg)	Fuselage Angle of Attack
α_{EI}	rad	(deg)	Engine Incidence Angle w.r.t. Fuselage
γ_F	-	-	Ratio of Specific Heats for Fan Air
γ_T	-	-	Ratio of Specific Heats for Turbine Air
δ_F	-	-	Pressure Correction Factor (P_{T_∞}/14.696)
δ_T	-	-	Pressure Correction Factor (P_{T_5}/14.696)
θ_F	-	-	Temperature Correction Factor (T_{T_∞}/518.7)
θ_T	-	-	Temperature Correction Factor (T_{T_5}/518.7)
ψ_E	-	-	Engine Cant Angle (Toe In)

1.0 SUMMARY

A turbo-powered simulator calibration test was conducted at the Boeing Company's Flight Simulation Chamber in conjunction with the NASA-Langley EET Propulsion/Airframe Integration Investigation wind tunnel test. The objectives of this test were to accurately determine the thrust and weight flow characteristics of the powered simulators with six nacelle configurations for use in the wind tunnel data reduction program and then to assure proper operation of the powered simulators in the wind tunnel.

This report presents the fan velocity and discharge coefficients derived from the calibration test data which were used in the wind tunnel test data reduction program. Also presented are the characteristic turbomachinery plots for each of the six nacelle configurations. These plots were used to check the turbo-powered simulator performance in the wind tunnel and make corrections to the final data as necessary.

2.0 INTRODUCTION

It has long been recognized that the proper installation of the propulsion system on an aircraft is a critical factor in achieving the desired level of aircraft performance. With the continuing advancement of both aircraft and propulsion technology, installation aerodynamics has become an even more important factor in achieving optimum aircraft performance. In the past, the standard methods of simulating the engine installation were by means of a flow-through nacelle or a blowing nacelle. The disadvantages of these methods are that the flow-through nacelle does not accurately simulate the geometry or exhaust effects of the real engine, and the blowing nacelle does not simulate the inlet effects on the installation. Recent developments have allowed the integration of the turbo-powered simulator (TPS) with conventional wind tunnel models to achieve a more realistic simulation of the installed engine effects on the airplane drag characteristics.

In order to measure and evaluate these installation effects, it is first necessary to know the thrust and airflow characteristics of the turbo-powered simulator. Since it is impractical to measure the thrust of the simulator while operating installed in the wind tunnel, the thrust is calculated from engine parameters that can be measured more easily. It is, therefore, necessary to calibrate the turbo-powered simulators in a test simulated static environment where the thrust can be measured directly and related to the quantities measured in the wind tunnel. This calibration was performed at the Boeing Flight Simulation Chamber facility. TPS calibration in this type of facility provides the means to statically calibrate the powered simulator over the complete range of inlet/exhaust pressure ratios that occur in an atmospheric total pressure wind tunnel.

This report documents the procedures, results, and data reduction methodology of the calibration of two TPS units with six nacelle configurations for use in the NASA-Langley EET Propulsion/Airframe Integration Wind Tunnel Test. The six nacelle configurations calibrated are:

- CF6-50 Long Core Nozzle
- CF6-50 Short Core Nozzle
- CF6-50 Long Duct Mixed Flow - preliminary design
- Energy Efficient Engine (E^3) - preliminary design
- E^3 Extended Nacelle
- E^3 Separate Flow.

In addition, this report presents comparison of the calibration data and the subsequent wind tunnel test data to verify the proper and consistent operation of the TPS units during the wind tunnel test.

3.0 MODEL DESCRIPTION

3.1 TURBO-POWERED SIMULATORS

The two turbo-powered simulators used in this test are model TD-441's manufactured at Tech Development, Inc., Dayton, Ohio. The TD-441 is a two-stage fan, three-stage turbine-powered simulator that operates at a design speed of 45,000 rpm and fan pressure ratio of 1.60.

3.2 NACELLES

The CF6-50 long core, short core, and long duct mixed flow nacelles are 6% scale models. Figure 1 shows the CF6-50 short core nacelle installed in the flight calibration chamber. The three E^3 nacelles are 6.2855% scale models. The nacelle contours for the six configurations tested are presented in the Appendix. Important parameters for the six nacelles are presented in Table I and Figures 2, 3, and 4. The engine station designation for all the nacelles is shown in Figure 5.

Because the TPS units receive their primary air from an external source (instead of through the fan as in the full scale engine), the E^3 model inlet (common to all three E^3 nacelles) was modified from the scaled production inlet contours in order to simulate the full scale mass flow ratio. This was done by reducing the inlet highlight area. In addition, the E^3 model inlet was lengthened slightly to prevent excessive internal diffuser angles (Figure 6). The CF6-50 TPS inlet, however, was designed by Boeing to simulate the full scale external nacelle pressure profiles rather than simulating the correct mass flow ratio. Therefore, care must be taken to assure that any spillage drag be accounted for in the wind tunnel data reduction.

3.3 TPS INSTRUMENTATION

The TPS units are instrumented with two rake assemblies. Both rakes are instrumented to measure total pressures and total temperatures. The rakes were located directly behind the fan and the turbine discharge. The fan rake is common to all six nacelles and consists of 54 total pressure probes which are manifolded in threes to give 18 total pressure readings. Figure 7 shows the location of the probes in the rake and the order of manifolding. The fan rake also contains six thermocouples to give six discreet total temperature readings. There are two primary rakes, one for the three CF6-50 nacelles and the E^3 separate flow nacelle and an integral rake in the E^3 core nozzles. Both primary rakes contain 16 total pressure probes which are not manifolded and four thermocouples for total temperature measurement. Figure 8 shows the primary rake assembly and instrumentation.

No nacelle static pressure/instrumentation was connected for the calibration.

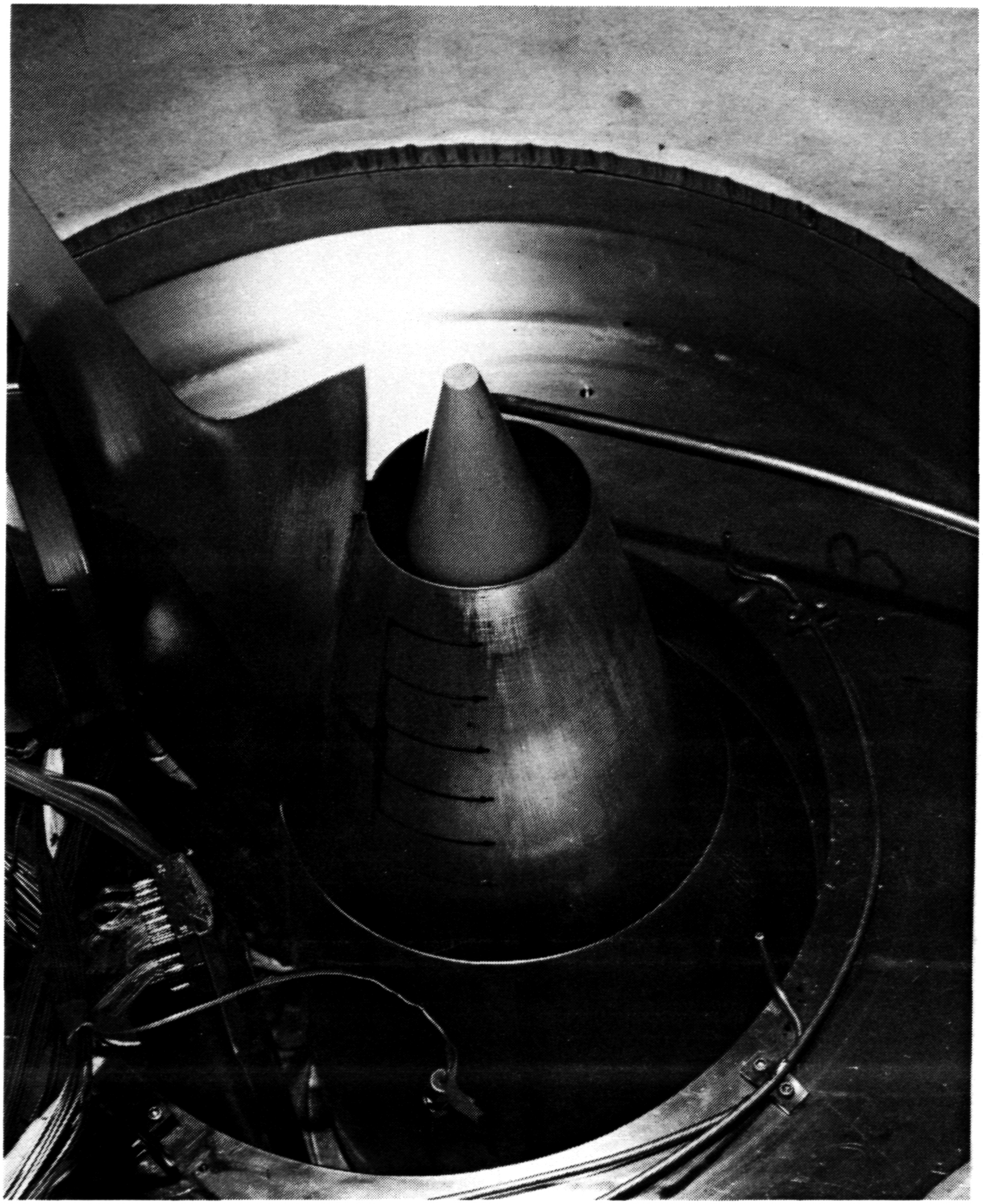

Figure 1. CF6-50 Short Core Nacelle Installed in Flight Calibration Chamber.

Table I. Important Nacelle Dimensions.

Dimensions	CF6-50 Short Core		CF6-50 Long Core		CF6-50 LDMF		E^3		E^3 Extended		E^3 Separate Flow	
	cm^2, cm	$in.^2$, in.	cm^2, cm	$in.^2$, in.	cm^2, cm	$in.^2$, in.	cm^2, cm	$in.^2$, in.	cm^2, cm	$in.^2$, in.	cm^2, cm	$in.^2$, in.
Fan Exit Flow Area	51.774	8.025	51.774	8.025	53.684	8.321(2)	54.406	8.433	57.258	8.875	53.729	8.328
Core Exit Flow Area	20.477	3.174	19.981	3.097	20.058	3.109	20.735	3.214	20.735	3.214	18.019	2.793
Max. Nacelle Diameter	17.475	6.880	17.475	6.880	17.475	6.880	15.646	6.160	15.646	6.160	15.646	6.160
Inlet Highlight Diameter	12.695	4.998	12.695	4.998	12.695	4.998	12.202	4.804	12.202	4.804	12.202	4.804
Inlet Throat Diameter	11.372	4.477	11.372	4.477	11.372	4.477	10.932	4.304	10.932	4.304	10.932	4.304
Fan Forebody Length	15.062	5.930	15.062	5.930	15.062	5.930	12.949	5.098	12.949	5.098	12.949	5.098
Fan Afterbody Length	12.482	4.914	12.482	4.914	33.147	13.050	27.478	10.818	29.073	11.446	16.657	6.558
Total Fan Cowl Length(1)	27.544	10.844	27.544	10.844	48.209	18.980	40.427	15.916	42.022	16.544	29.606	11.656
Total Nacelle Length(1)	45.136	17.770	46.700	18.386	48.946	19.270	42.131	16.587	42.131	16.587	49.538	19.503

(1) Along engine top centerline (inlet is drooped 4°)

(2) This is the design exit area for the LDMF nacelle. In the data reduction programs, it was changed to 55.226 cm^2 (8.560 $in.^2$) to account for damage incurred by the model.

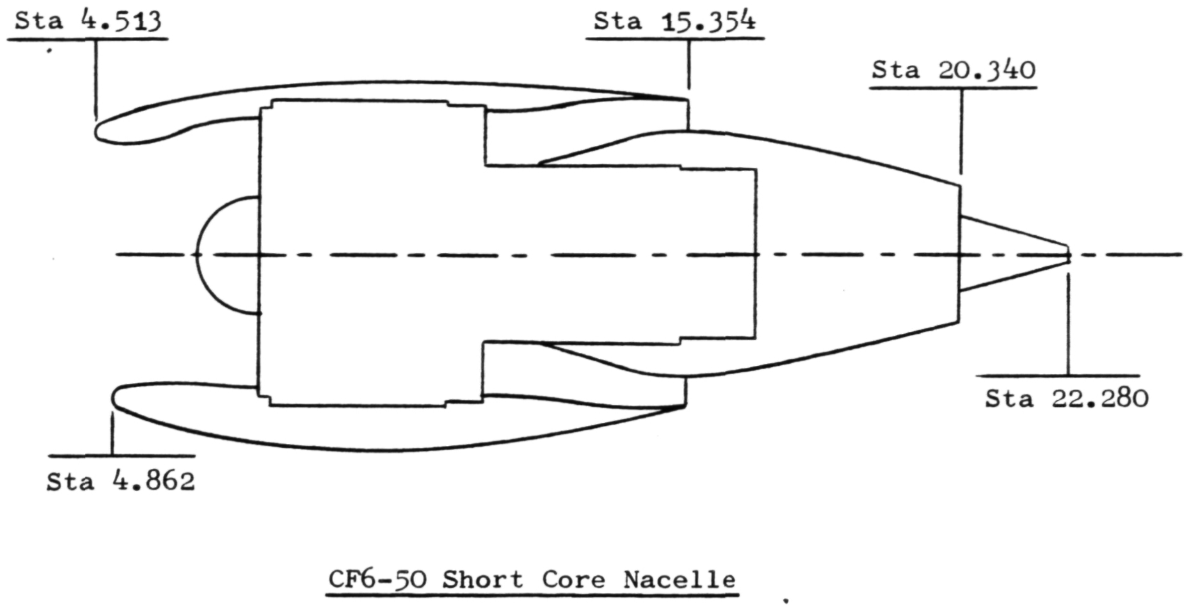

Figure 2. CF6-50 Short and Long Core Nacelle Stations.

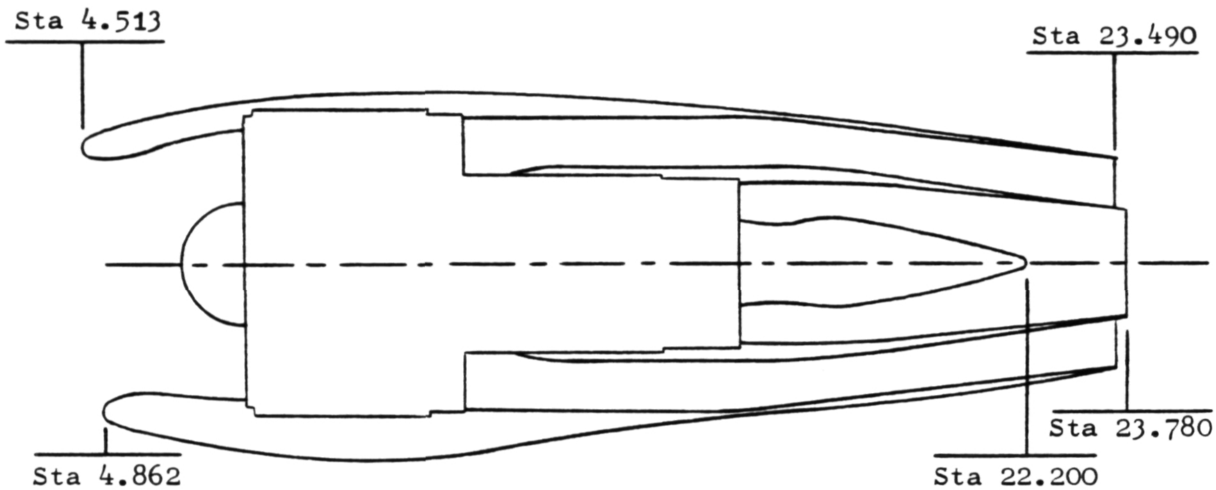

CF6-50 LDMF Nacelle

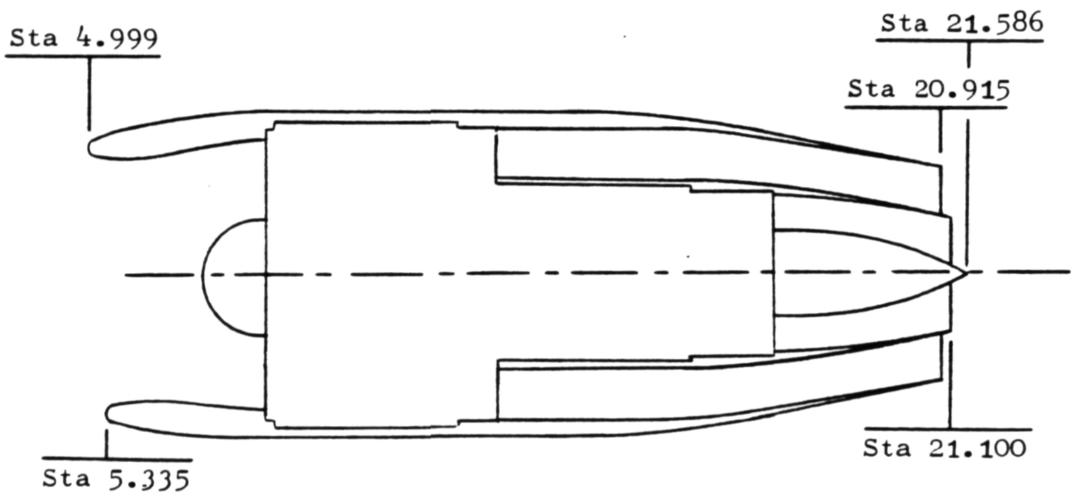

E^3 Nacelle

Figure 3. CF6-50 LDMF and E^3 Nacelle Stations.

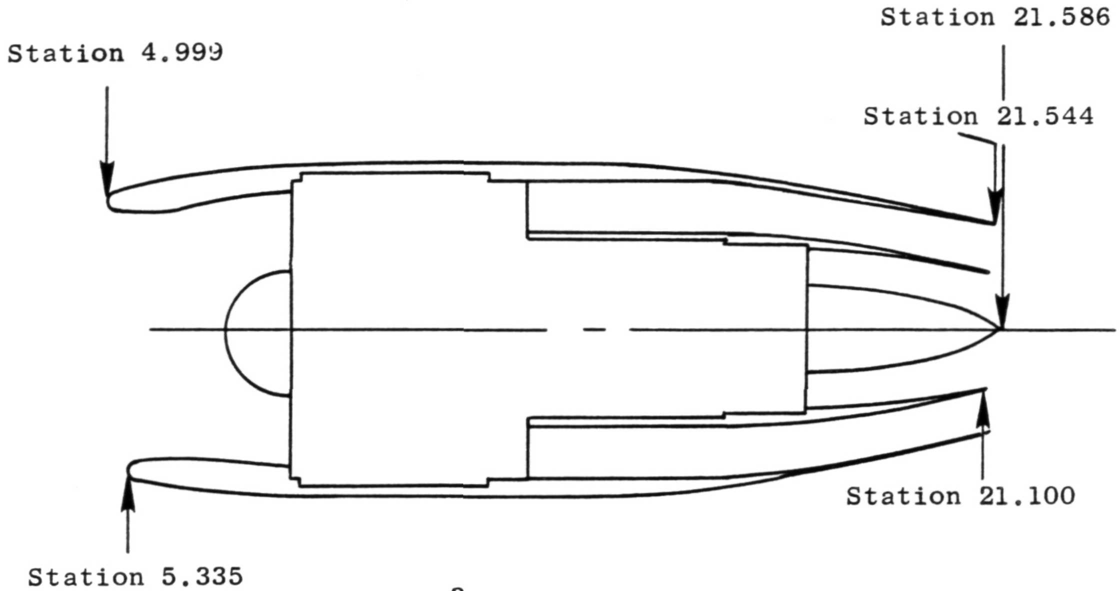

E^3 Extended

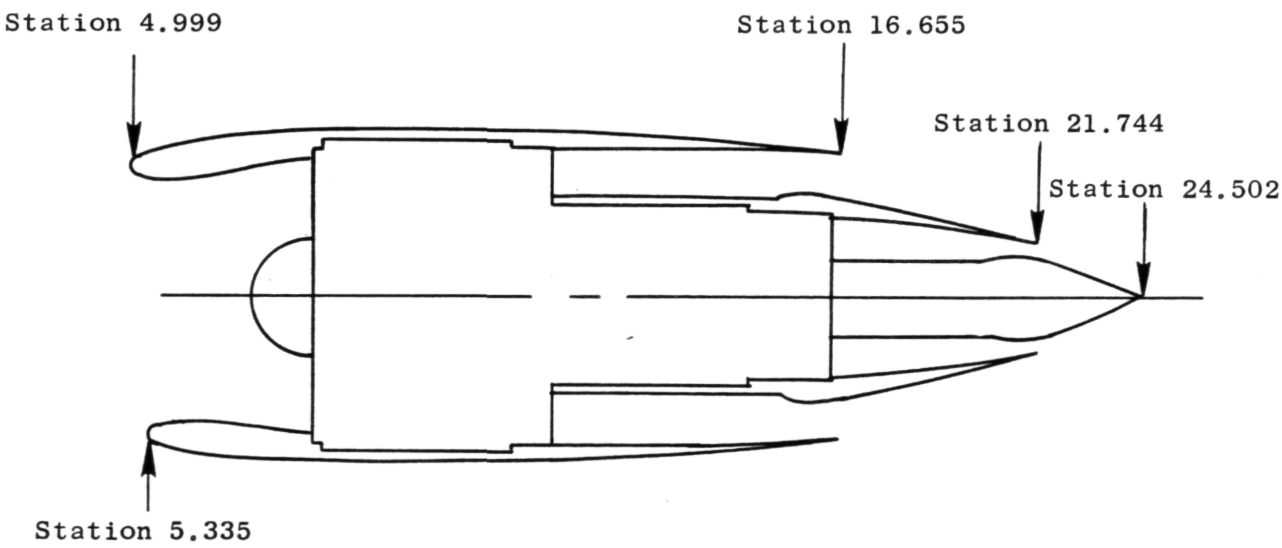

E^3 Separate Flow

Figure 4. E^3 Extended and E^3 Separate Flow Nacelle Stations.

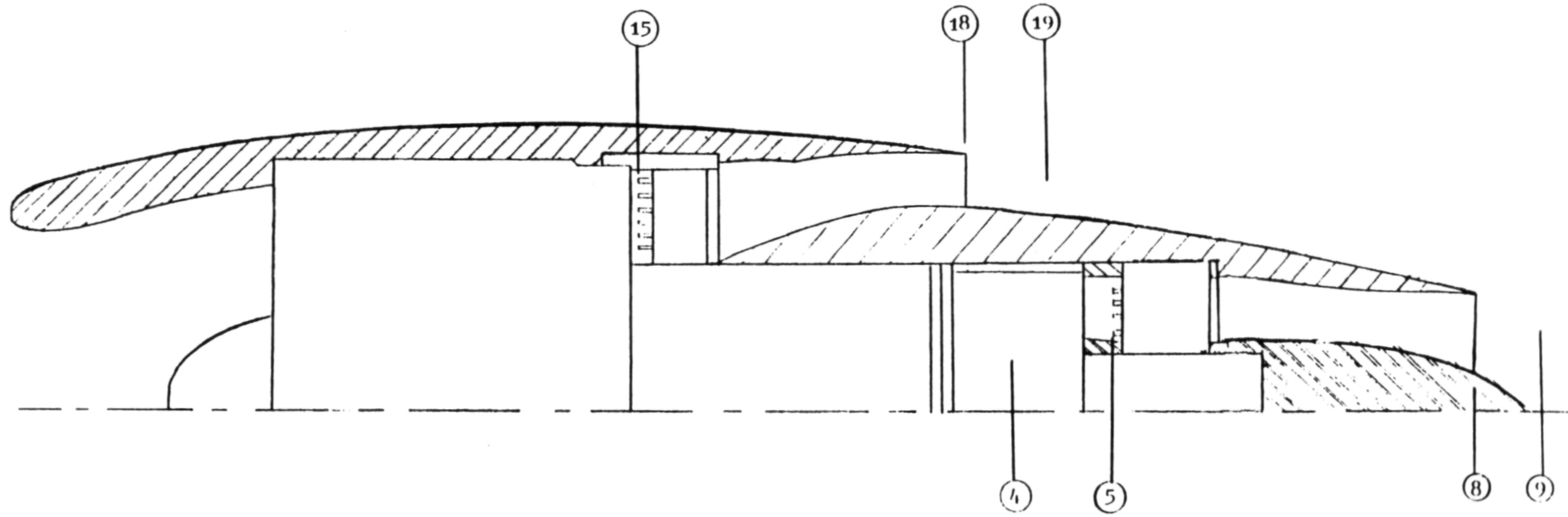

4 - Turbine Inlet
5 - Primary Rake Charging Station
8 - Primary Nozzle Exit
9 - Fully Expanded Primary Flow
15 - Fan Rake Charging Station
18 - Fan Nozzle Exit
19 - Fully Expanded Fan Flow

Figure 5. Engine Station Designation.

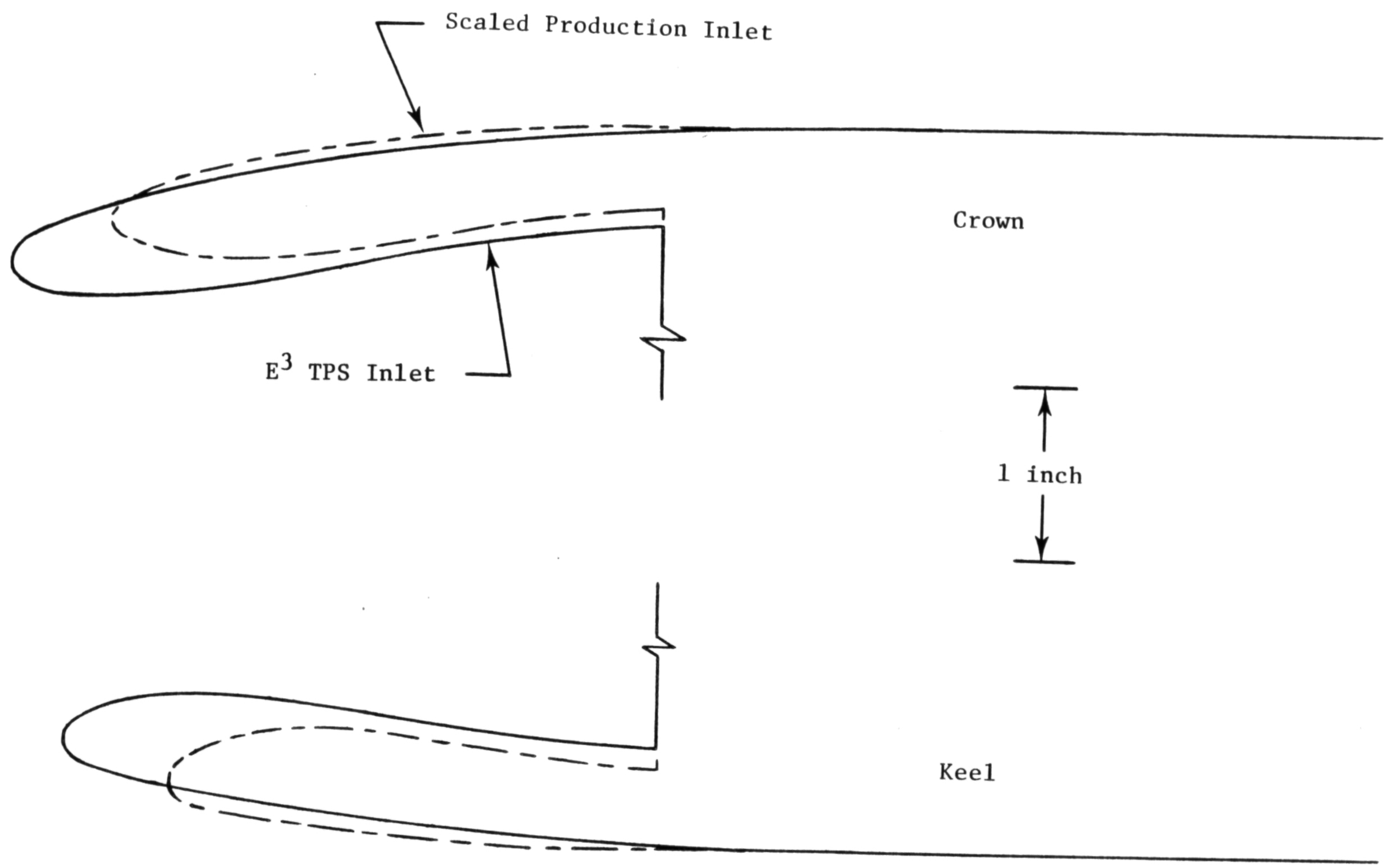

Figure 6. E^3 TPS Inlet Modification.

CF6-50 AND E^3 FAN EXIT RAKE

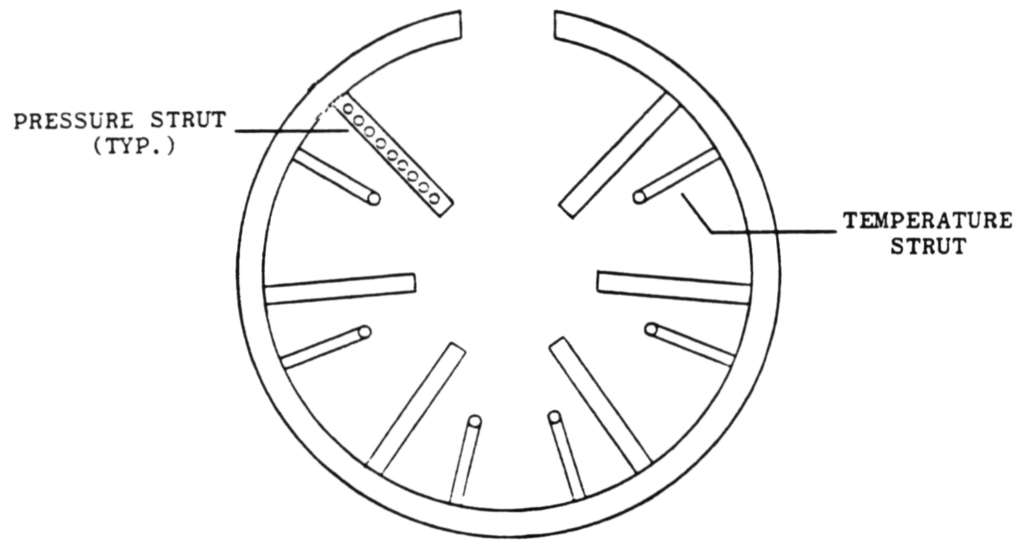

PRESSURE TUBE NUMBERS				
RADIUS	MANIFOLD 3 PROBES 43°-95°-146°		MANIFOLD 3 PROBES 214°-265°-317°	
1.724	20	P_{T15} - 1	29	P_{T15} - 10
1.869	21	2	30	11
2.003	22	3	31	12
2.128	23	4	32	13
2.246	24	5	33	14
2.358	25	6	34	15
2.466	26	7	35	16
2.568	27	8	36	17
2.667	28	9	37	18

ORIENTATION

top vertical ℄

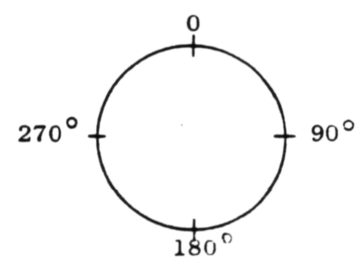

aft looking forward

TEMPERATURE PROBES						
RADIUS	60°	112°	163°	197°	248°	300°
2.175	84	85	86	87	88	89

Figure 7. Fan Exit Rake Instrumentation.

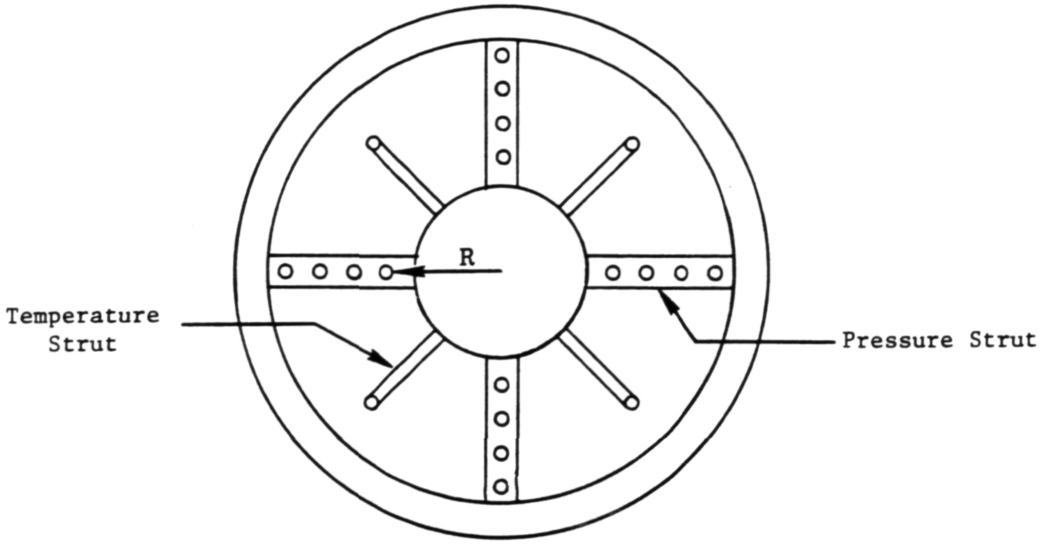

E^3 Pressure Tube Numbers				
Radius	0°	90°	180°	270°
0.908	300	304	308	312
1.087	301	305	309	313
1.240	302	306	310	314
1.376	303	307	311	315
Temperature Probes				
Radius	45°	135°	225°	315°
1.130	320	321	322	323

Orientation

top vertical ℄

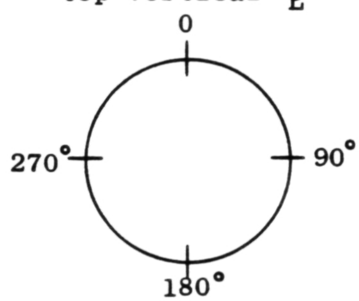

aft looking forward

CF6-50 Pressure Tube Numbers				
Radius	0°	90°	180°	270°
0.875	40	44	48	52
1.070	41	45	49	53
1.233	42	46	50	54
1.377	43	47	51	55
Temperature Probes				
Radius	45°	135°	225°	315°
1.150	56	57	58	59

Orientation

top vertical ℄

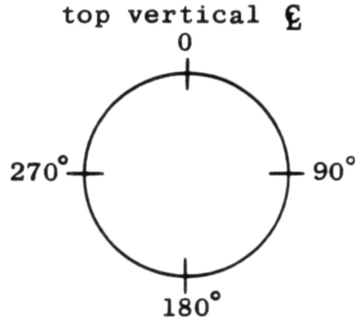

aft looking forward

Figure 8. Primary Exit Rake Instrumentation.

4.0 CALIBRATION FACILITY DESCRIPTION

The Boeing Flight Simulation Chamber (Figure 9) was used to calibrate turbo-powered simulators for this test. The Flight Simulation Chamber consists of five major components:

- Force balance assembly
- Vacuum tank assembly
- High pressure multiple critical venturi (MCV)
- Low pressure multiple critical venturi (MCV)
- Air ejector suction system.

The force balance assembly is mounted at the upstream end of the vacuum tank and consists of a dual balance rig utilizing two six-component strain gage balances for thrust measurement. The high pressure air line used to provide the simulator drive air is brought across a series of three bellows flexures in order to eliminate momentum tares on the balance. Phenolic spacers are used to isolate the balance from the tank assembly in order to eliminate thermal transients being transmitted to the balance. These transients are produced in the model support frame and tank assembly by the airflow to the model, and the work of compression in the powered simulator fan.

The vacuum tank assembly provides the exhaust environment for the TPS thereby simulating the stream conditions for the various test Mach numbers (Figure 10). The interior of the tank is fitted with a series of screens to:

- Minimize recirculation effects on the exhaust nozzle
- Prevent the direct impact of the exhaust jet on the inlets to the low pressure multiple critical venturi
- Provide thermal mixing of the fan and primary flow.

A high pressure multiple critical venturi (MCV) is used to meter the powered simulator primary drive air. By changing combinations of the six individual venturi's in the MCV (i.e., setting an MCV code), a range of airflows can be measured to within an accuracy of ±0.1%.

At the exhaust end of the vacuum tank assembly is the low pressure multiple critical venturi used to measure the total powered simulator airflow (Figure 10). As with the high pressure MCV, the low pressure MCV utilizes eight individual critical venturis to provide a range of nozzle back pressures for complete performance mapping over the ranges of nozzle pressure ratios experienced in the wind tunnel.

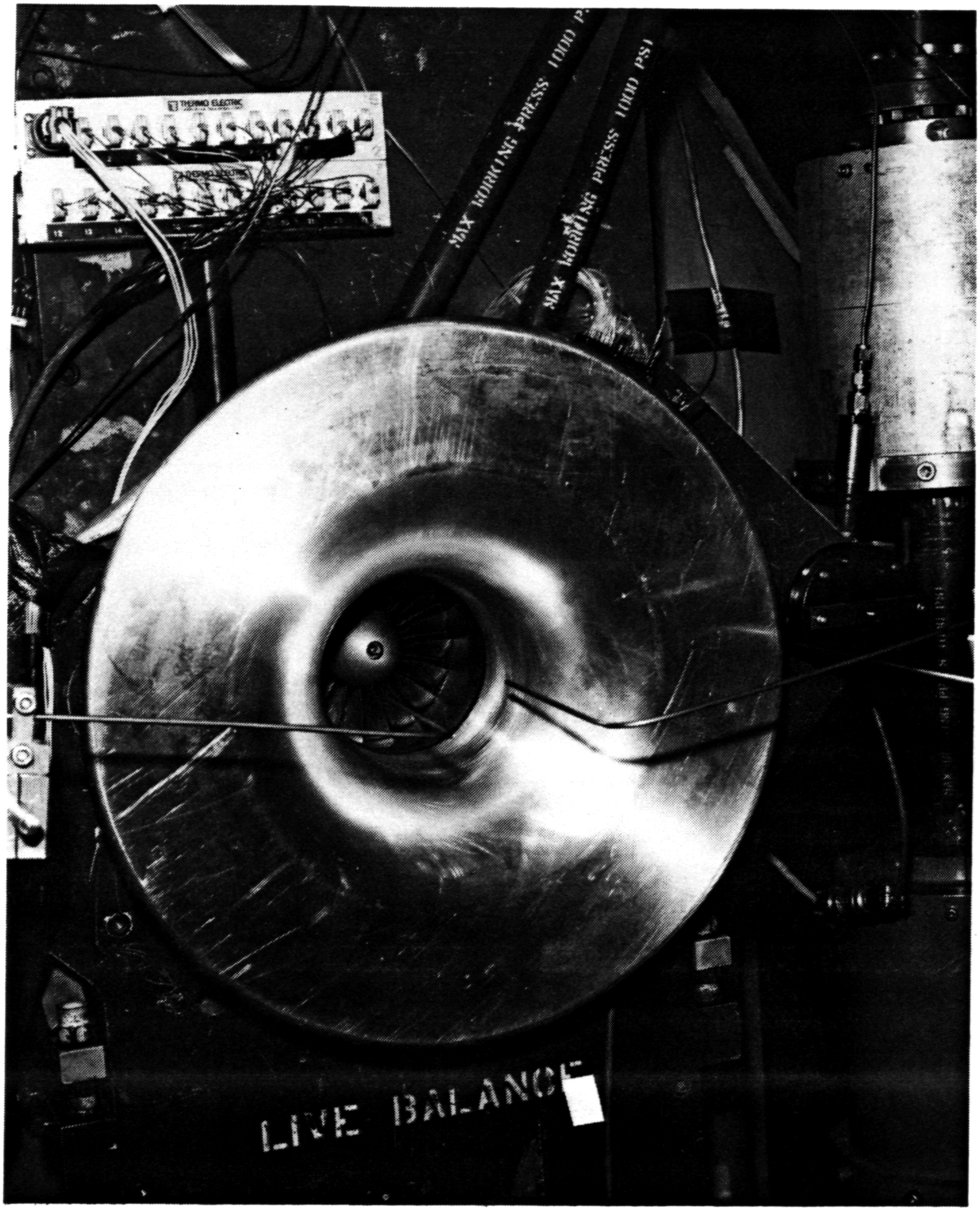

Figure 9. TPS Unit with Bellmouth in Flight Calibration Chamber.

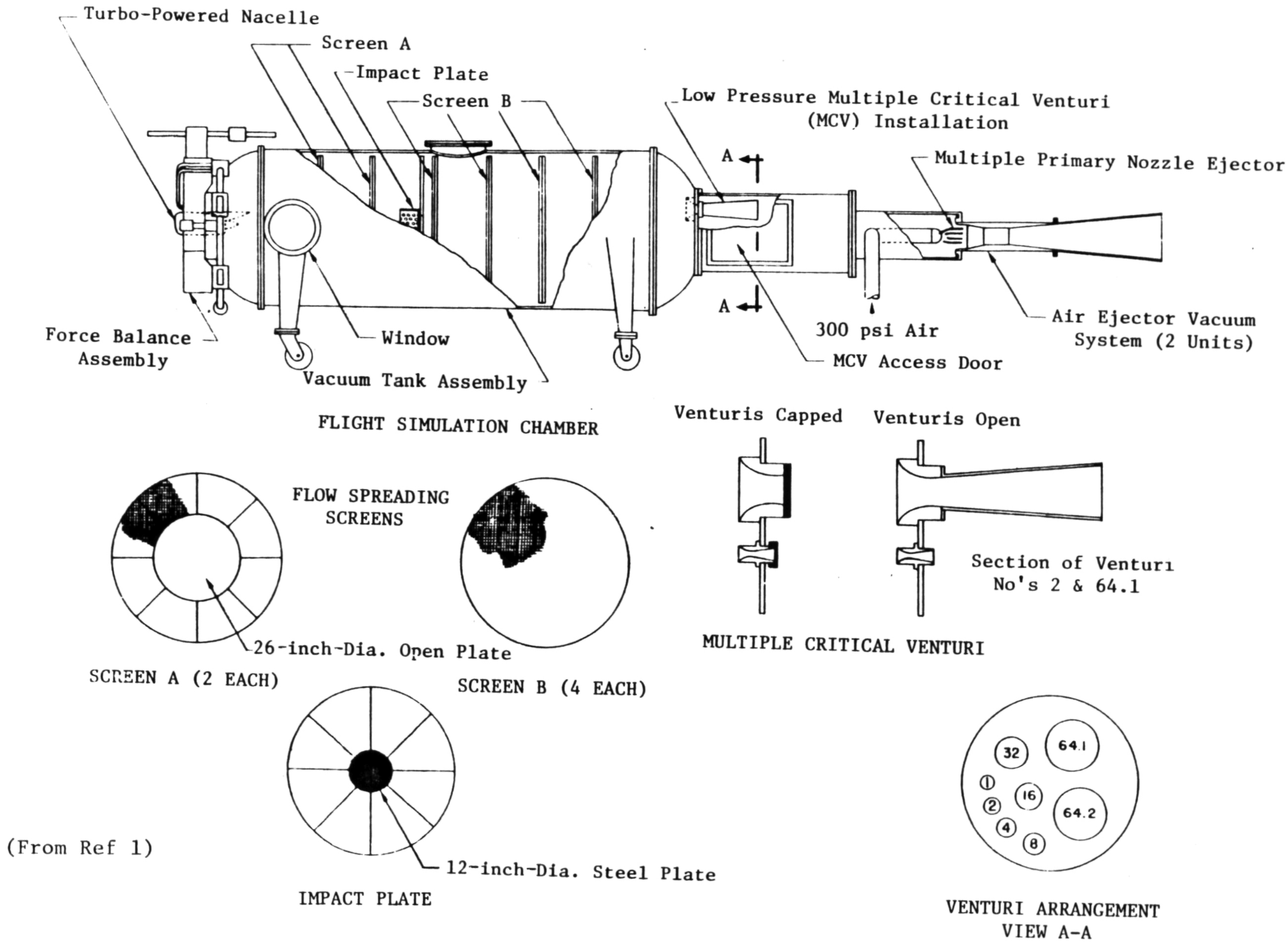

(From Ref 1)

Figure 10. Calibration Facility Tank Assembly.

Two air ejectors are used to exhaust the flow from the downstream end of the vacuum tank to provide the desired tank pressure and assure critical flow in the MCV.

The Boeing Flight Simulation Chamber provides an excellent means for accurately calibrating TPS units over the required range of Mach number, rpm, and nozzle pressure ratio.

5.0 ASME VALIDATION TEST

The accuracy of the Boeing Flight Simulation Chamber is verified by using a 3.004-inch ASME long-radius flow nozzle (Figure 11). The use of this nozzle verifies the accuracy of both the force balance system and the exhaust airflow metering system. This test was scheduled to be run at the beginning and end of the calibration test. Unfortunately, the air ejector system compressor became inoperative at the end of the test; therefore, the second ASME nozzle run was not obtained. The data for the first ASME nozzle test are presented in the form of thrust and flow coefficients in Figure 12. It is compared against the General Electric - FluiDyne predicted values of velocity and discharge coefficient. The data above a choked nozzle condition shows good correlation with the predicted values verifying the accuracy of the facility.

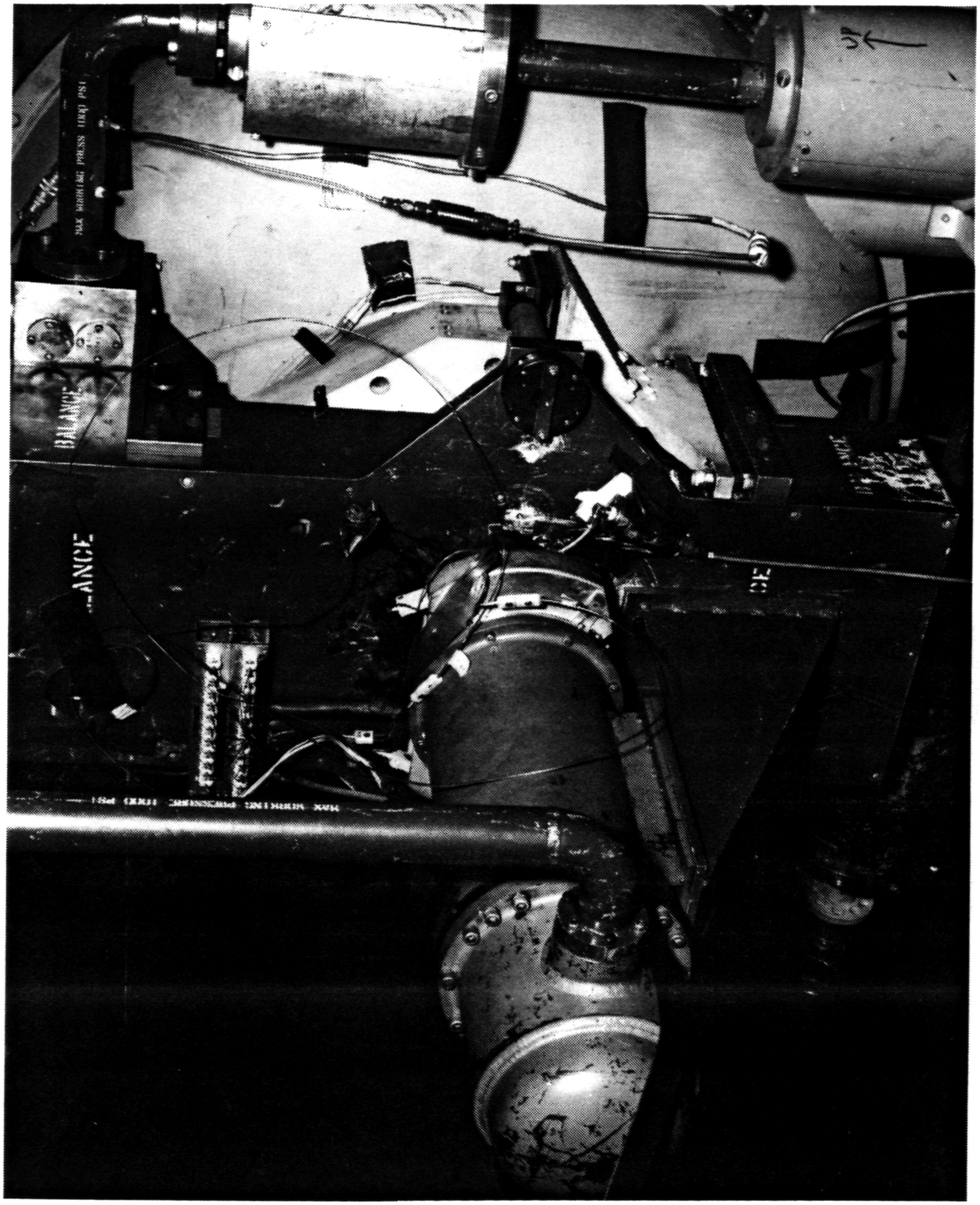

Figure 11. ASME Nozzle Installed in Flight Simulation Chamber.

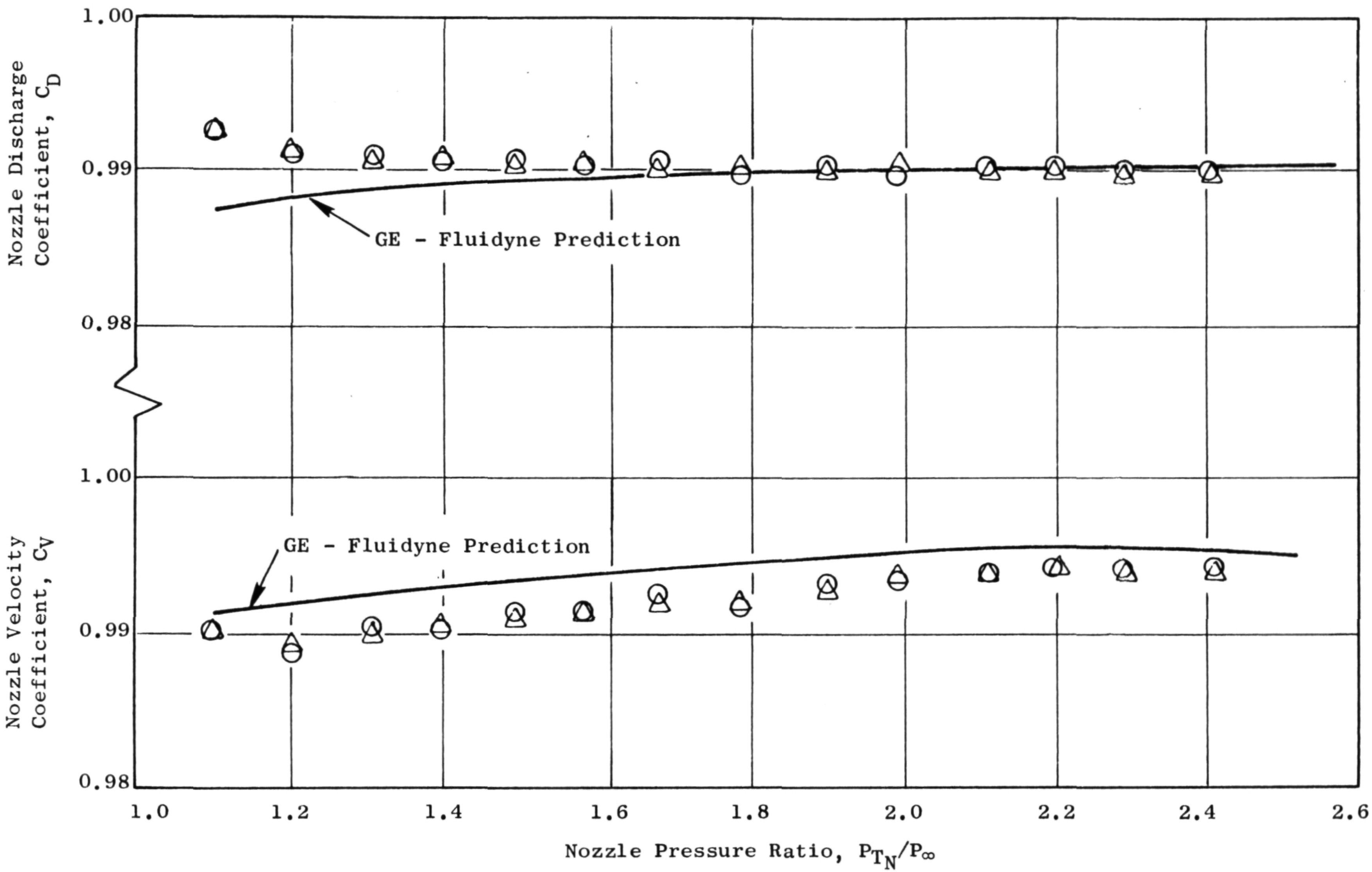

Figure 12. Calibration Facility Checkout with ASME Nozzle.

6.0 DISCUSSION OF CALIBRATION TEST

6.1 GENERAL

Six nacelle configurations were calibrated at the Boeing Flight Simulation Chamber for subsequent use in the Propulsion/Airframe Integration Wind Tunnel Test to be conducted at the NASA-Langley Research Center in the 8 Foot Transonic Pressure Tunnel. The configurations tested are:

- CF6-50 Long Core
- CF6-50 Short Core (primary reverser removed)
- CF6-50 Long Duct Mixed Flow (LDMF)
- Energy Efficient Engine (E^3)
- E^3 Extended Nacelle
- E^3 Separate Flow.

6.2 TEST PROCEDURE

For reasons mentioned previously, it is necessary to calibrate the simulators over the range of equivalent Mach numbers, rpm, and nozzle pressure ratios that will be encountered in the wind tunnel test. For this particular wind tunnel test, it was intended that the simulators be run at the following conditions:

1. Windmilling - no drive air to the turbine
2. Flow Through - simulate a flow through nacelle by running at a fan pressure ratio of 1.0
3. Max. Cruise - simulate the inlet/exhaust effects by running the TPS at the cruise nozzle pressure ratios of the full scale engine.

In order to run these conditions in the wind tunnel, it was necessary to calibrate the simulators over the following ranges:

1. Equivalent Mach number - 0.5 to 0.9
2. Rpm - 12,000 to 45,000
3. Nozzle Pressure Ratio - 1.4 to 2.6

This is accomplished by setting an MCV-Code with the venturis and running the TPS through an rpm sweep. Data points were taken at intervals of between 500 and 1000 rpm. The data recorded at each point included all the rake pressures and temperatures, the balance forces and moments, ambient and tank conditions, TPS plenum conditions, primary and total airflows, and engine rpm. This is repeated until the complete TPS operating envelope is tested. This procedure is shown graphically in Figure 13 (obtained from Reference 1). This was done for the six nacelle configurations installed on their respective TPS unit.

6.3 FLOW SUPPRESSION

There was concern during the course of this test that flow suppression experienced in the wind tunnel, due to the external flow which is not present in the calibration test, would introduce an error into the TPS thrust calculation. Test data have shown that flow suppression is negligible if the nozzle is choked. Since the fan nozzle is choked when operating at maximum rpm (the area of primary interest) but the primary nozzle is unchoked, the following discussion centers on the primary nozzle and the possible error introduced in the thrust calculation when flow suppression is present.

The present method for finding the TPS thrust while operating in the wind tunnel is to calculate the momentum term based on ambient static pressure (P_∞), and neglect the pressure-area term. The more rigorous way of calculating the thrust is to calculate the exit momentum based on the exit static pressure (P_S) and add to it the pressure-area term as depicted below:

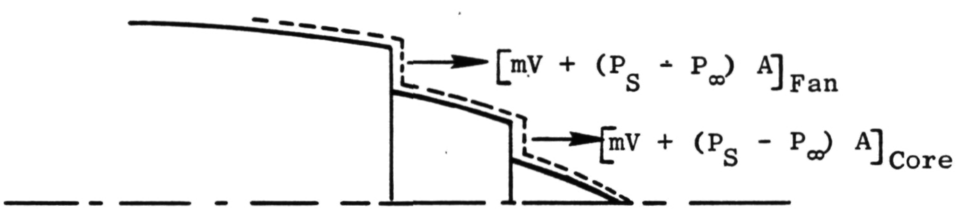

Flow supprssion affects the value of thrust by changing the rate of mass flow through the nozzle and by changing the exit static pressure (P_S). Since the mass flow rate is measured in the wind tunnel, any error in the thrust would be introduced by neglecting the pressure-area term as is done in the present method of thrust calculation. To assess the accuracy of using the present method of calculating thrust and find whether any error is introduced when flow suppression is present, two runs were chosen for analysis from each of the following:

- Calibration Test at Boeing-static
- Wind Tunnel Test - isolated nacelle, wind on
- Wind Tunnel Test - installed nacelle, wind on.

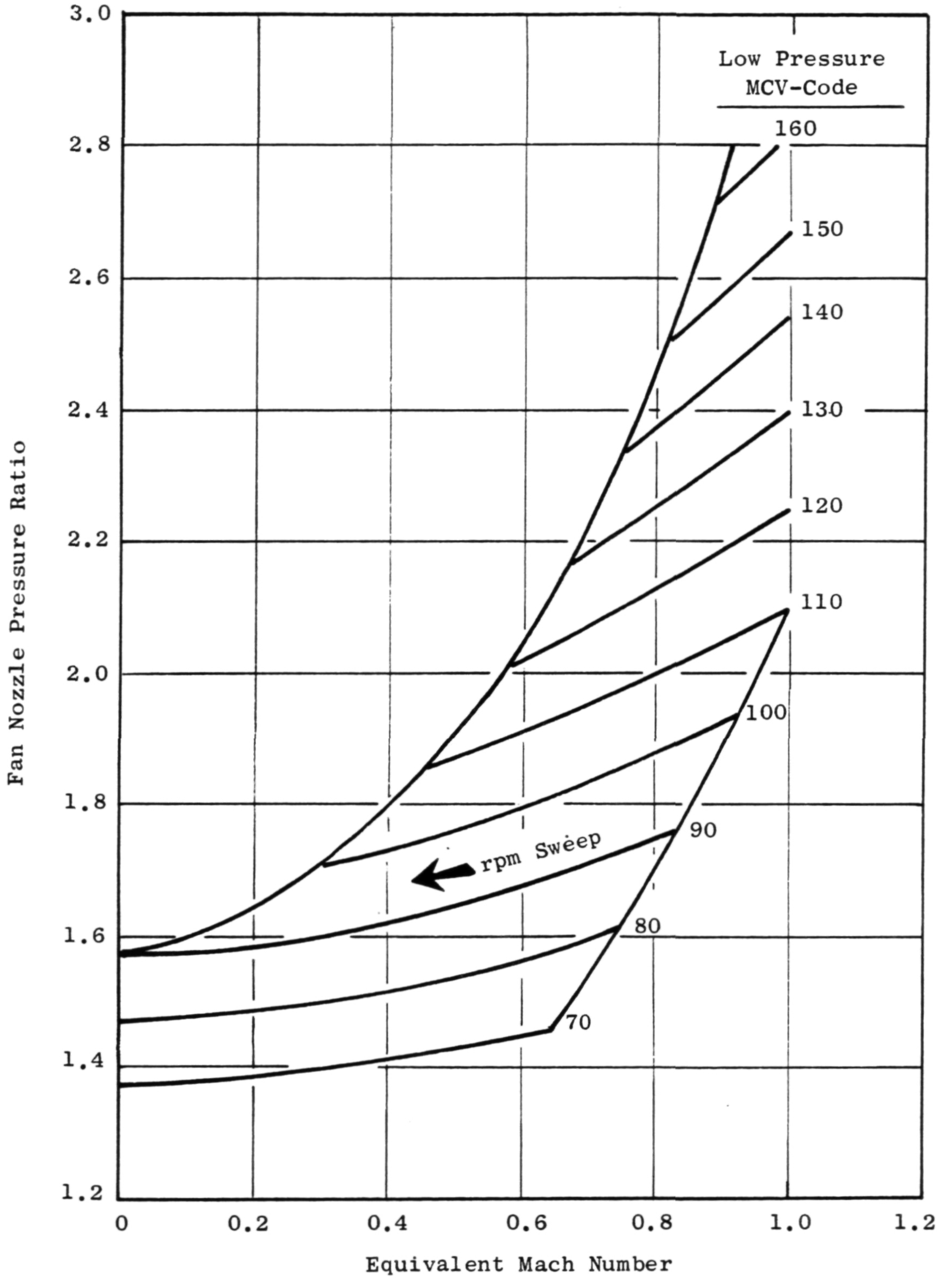

Figure 13. Typical TPS Operating Envelope.

The runs were chosen so that they were reasonably close to the same operating condition (M = 0.82, max. rpm). In order to negate the effects of slightly different temperatures and pressures, the comparisons were made in terms of coefficients. The present method for calculating thrust uses the coefficient C_{V_9} as defined in Section 8.0. In order to assess the effect of flow suppression, a thrust coefficient C_{f_g} which is based on P_S will be used. This thrust coefficient is defined as:

$$C_{f_g} = \frac{F_{g_{act}}}{F_{g9i}}$$

where:

$$F_{g_{act}} = \text{Actual Primary Thrust}$$

$$= W_8 \, C_{V_9} \, V_{8i} + (P_{S8} - P_\infty) A_8$$

$$F_{g9i} = \text{Ideal Primary Thrust}$$

$$= W_8 \, V_{9i}$$

giving:

$$C_{f_g} = \frac{W_8 \, C_{V_9} \, V_{8i} + (P_{S8} - P_\infty) A_8}{W_8 \, V_{9i}}$$

where: W_8 is the measured primary weight flow.

The ideal velocities are defined as:

$$V_{8i} = \left(\frac{2g\gamma R}{\gamma - 1} T_{T_5}\right)^{1/2} \left[1 - \left(P_{S_8}/P_{T_8}\right)^{\frac{\gamma-1}{\gamma}}\right]^{1/2}$$

and

$$V_{9i} = \left(\frac{2g\gamma R}{\gamma - 1} T_{T_5}\right)^{1/2} \left[1 - \left(P_\infty/P_{T_5}\right)^{\frac{\gamma-1}{\gamma}}\right]^{1/2}$$

Since the nozzle exit static pressure (P_{S_8}) was not measured in the test, it must be calculated using the mass flow function:

$$\overline{m}_8 = \frac{W_8 \sqrt{T_{T_5}}}{P_{T_8} \; A_8} \quad \text{and } P_{S8} = f\left(M_8\right) = f\left(\overline{m}_8\right)$$

where W_8 and T_{T_5} are measured and P_{T_8} can be found from the measured quantity P_{T_5} and analytically applying duct losses.

The difference between the calculated values of C_{f_g} and C_{V_9} will be the error in the present method of calculating thrust while operating in the wind tunnel. Table II presents the results of this study. As can be seen from the table, the errors in the thrust calculation are negligible (less than 0.1% in total thrust). Therefore, the present method for calculating thrust is accurate even in the case where a small amount of primary flow suppression is present.

6.4 TEST ANOMALIES

Two incidences encountered while calibrating the simulators are worth discussing for consideration in future tests. The first was compressor stall at high rpm (above approximately 40,000 rpm) on the separate flow nacelles. This was caused by a fan exit area which was undersized for the mass flow requirements of this TPS model. This is shown on the fan map for the Model TD-441 turbo-powered simulator in Figure 14. The fan exit flow area for the separate flow nacelles (CF6-50 Long and Short Core) is 51.977 cm^2 (8.05 $in.^2$) which lies outside the area of demonstrated good calibration characteristics. The impact of this on the wind tunnel test was to limit the maximum nozzle pressure ratio that was attainable. At the highest rpm attainable without experiencing compressor stall, the maximum fan pressure ratio was $P_{T15}/P_{T\infty}$ = 1.49 This is lower than the nominal full scale engine fan pressure ratio but was determinied to be adequate for the purposes of this test. Although the CF6-50 LDMF and the three E^3 nacelles encountered no compressor stall (because of their larger fan exit areas), they were also run at this limited fan pressure ratio for consistency and comparison with the seperated flow nacelles.

The second incidence encountered in the course of calibrating these nacelles was ice buildup on the core nozzle and plug. Figure 15 shows the ice that formed on the CF6-50 LDMF nacelle during calibration testing. This is a common problem caused by the very cold core nozzle air freezing the moisture in the room air flowing through the fan. One proposed solution to this problem is to use a nonconducting material to fabricate the core nozzle. Unfortunately, this eliminates the option of having pressure instrumentation on the core nozzle, and there is also some concern about the ability of the material to hold its contours under stress. For this test, the problem was alleviated by bringing the TPS down to low rpm between short test runs to warm up and dry off the core nozzle. This was time consuming but worked effectively.

Table II. Results of Primary Thrust Investigation (at M = 0.82), CF6-50 Long Core Nacelle.

Test	Run	PNT	P_{S_8}, N/m² (lb/in.²)	C_{f_g}	C_{V_9}	$C_{f_g} - C_{V_9}$	ΔF_{g_9} N (lb)	Correction to W.T. Test N (lb)
Calibration	143	12	64,472.8 (9.351)	0.98279	0.98173	0.00106	0.13 (0.030)	---
	143	11	64,279.8 (9.323)	0.98275	0.98137	0.00138	0.13 (0.03)	---
Isolated Wind Tunnel	540	19	72,332.9 (10.491)	0.98824	0.98256	0.00568	0.71 (0.16)	0.58 (0.13)
	523	22	72,312.2 (10.488)	0.98828	0.98275	0.00553	0.71 (0.16)	0.58 (0.13)
Installed Wind Tunnel	338	25	70,705.7 (10.255)	0.98668	0.98263	0.00405	0.53 (0.12)	0.40 (0.09)
	340	21	70,105.9 (10.168)	0.98608	0.98244	0.00364	0.44 (0.10)	0.31 (0.07)

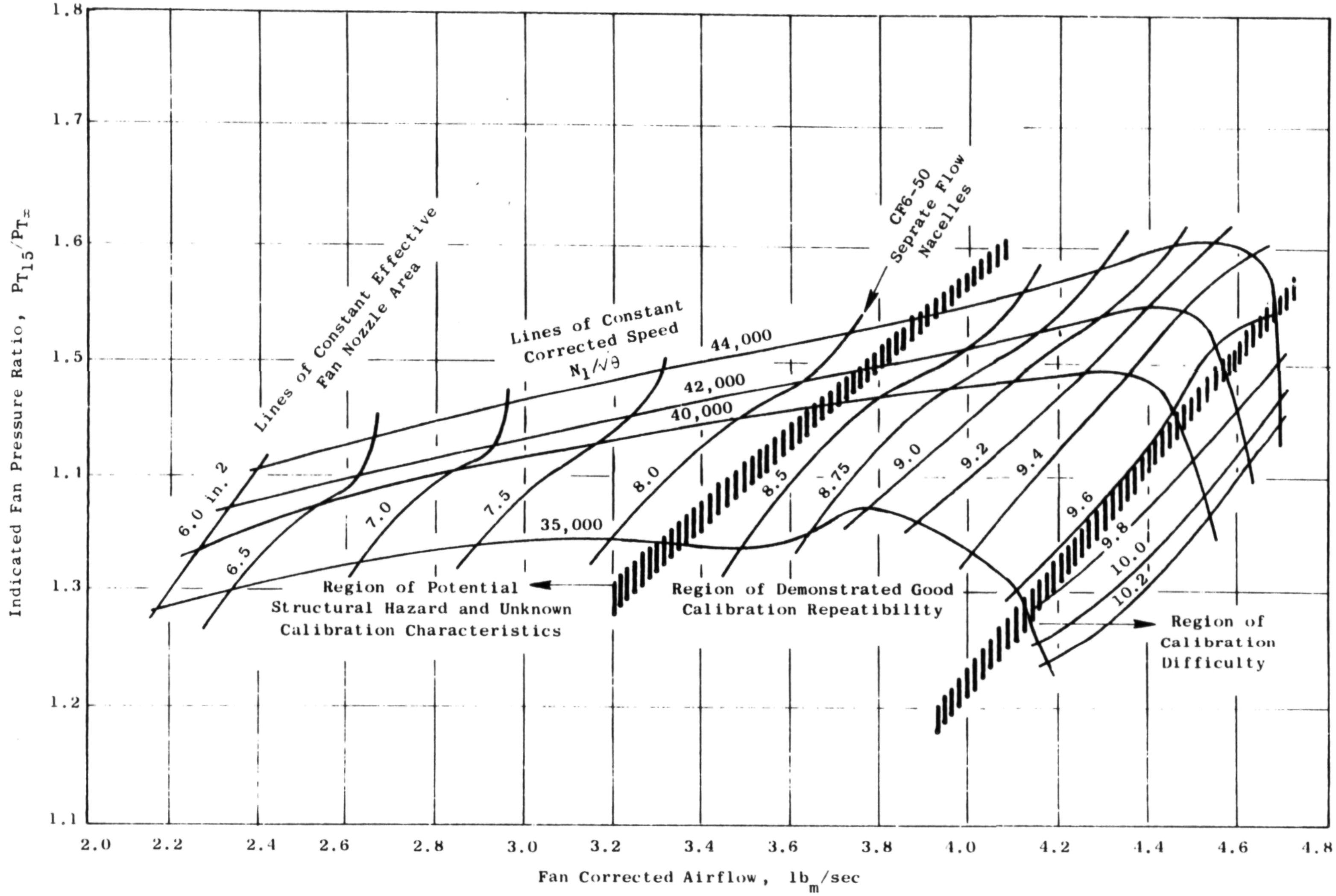

Figure 14. Fan Map for Typical Turbo-Powered Simulator Model TD-441.

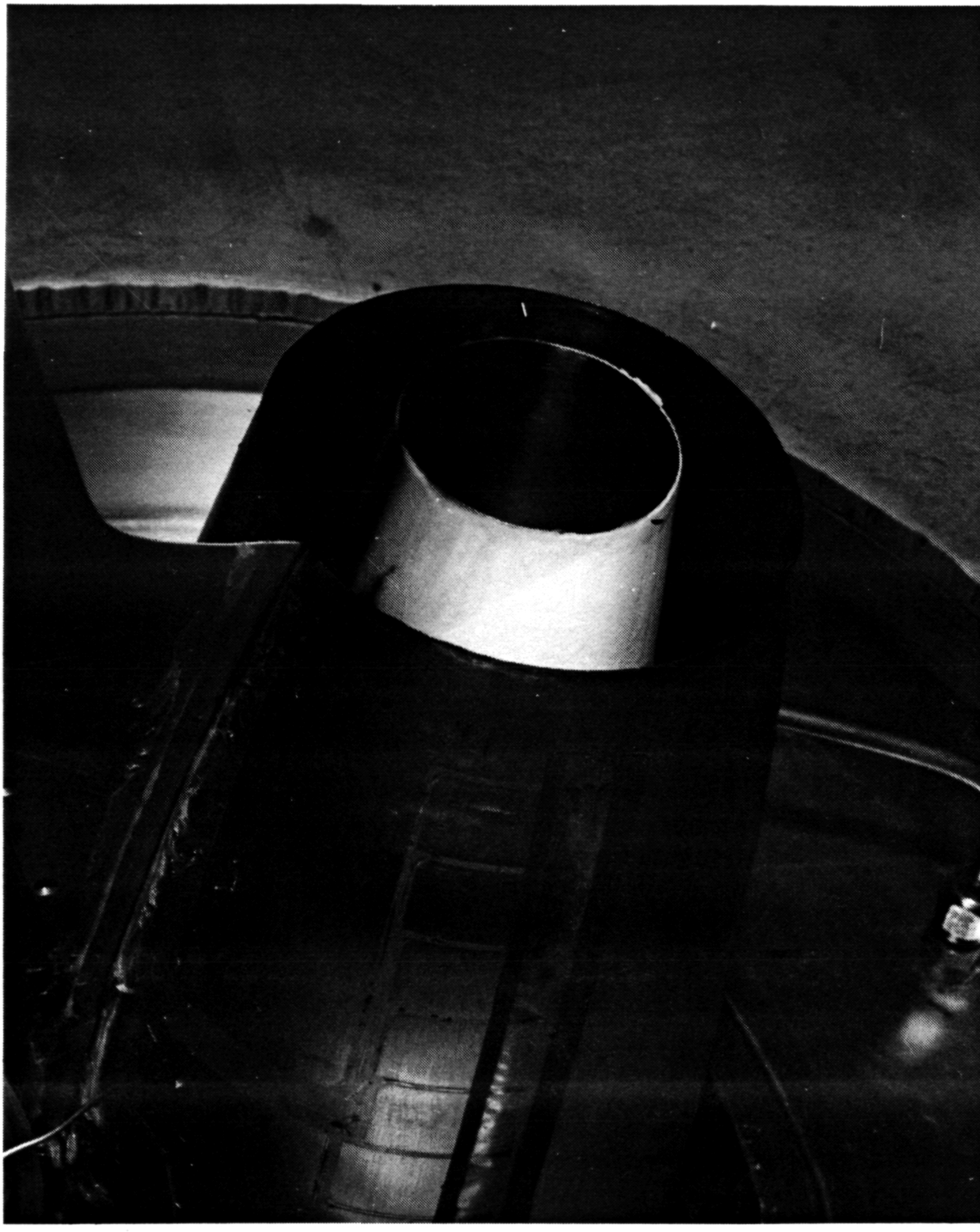

Figure 15. Ice Buildup on the CF6-50 LDMF Primary Nozzle.

7.0 CALIBRATION TEST RESULTS

The results of the calibration test are in the form of fan velocity and fan discharge coefficients. These coefficients are defined as follows:

$$\text{Fan Velocity Coefficient} \equiv C_{V_{19}} = \frac{\text{Measured Fan Thrust}}{\text{Ideal Fan Thrust}}$$

$$\text{Fan Discharge Coefficient} \equiv C_{D_{18}} = \frac{\text{Measured Fan Weight Flow}}{\text{Ideal Fan Weight Flow}}$$

where the ideal fan thrust and ideal fan weight flow are defined in Section 8.0. The measured fan thrust is derived from estimating analytically the core thrust and subtracting it from the total thrust force measured on the calibration balance. The analytical core thrust is calculated using the velocity coefficients in Figure 16 as follows:

$$\text{Core Thrust} \equiv F_{g_9} = C_{V_9} W_5 V_{9_i}$$

where W_5 and V_{9_i} are defined in Section 8.0 and $C_{V_{19}}$ is the core thrust coefficient. The C_{V_9} estimates are obtained by calculating the internal core nozzle friction drag, pressure and temperature rake and strut drag and estimating the external plug scrubbing drag. Since the total thrust is measured in the calibration chamber, any errors in estimating C_{V_9} are accounted for in the fan thrust coefficient $C_{V_{19}}$ thus giving an accurate value for the total thrust in the wind tunnel.

The measured fan weight flow is calculated by taking the total airflow measured by the venturis at the downstream end of the tank and subtracting the measured core drive airflow. Since the core drive airflow is measured in both the calibration test and the wind tunnel test, no core discharge coefficient is necessary.

The final fan velocity and discharge coefficients are presented versus fan nozzle pressure ratio in Figures 17 through 22 for the six nacelle configurations. Tables III through VIII present these curves in equation form.

Caution must be observed in trying to compare the levels of $C_{V_{19}}$ and $C_{D_{18}}$ for the six configurations since two TPS units were used, each having different characteristics. In addition, the exit of the CF6-50 long duct mixed flow nacelle was damaged prior to testing and the exit flow area could only be estimated. Since the same numerical value of area is used in both the calibration test and the wind tunnel test, this problem did not affect the thrust calculation. However, it does affect the level of the fan discharge coefficient.

The use of these coefficients in the wind tunnel data reduction is explained in Section 8.0.

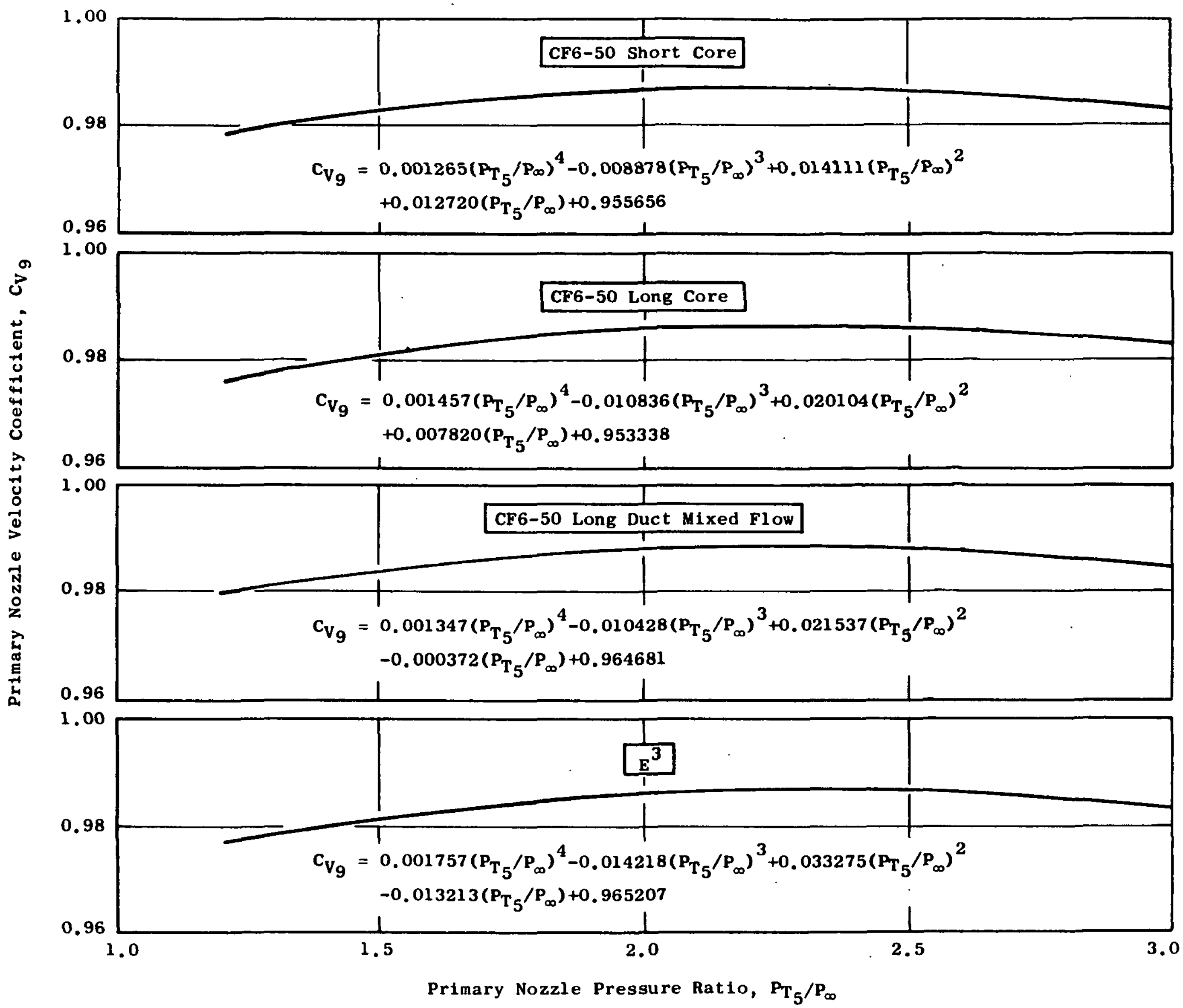

Figure 16a. Primary Nozzle Velocity Coefficients.

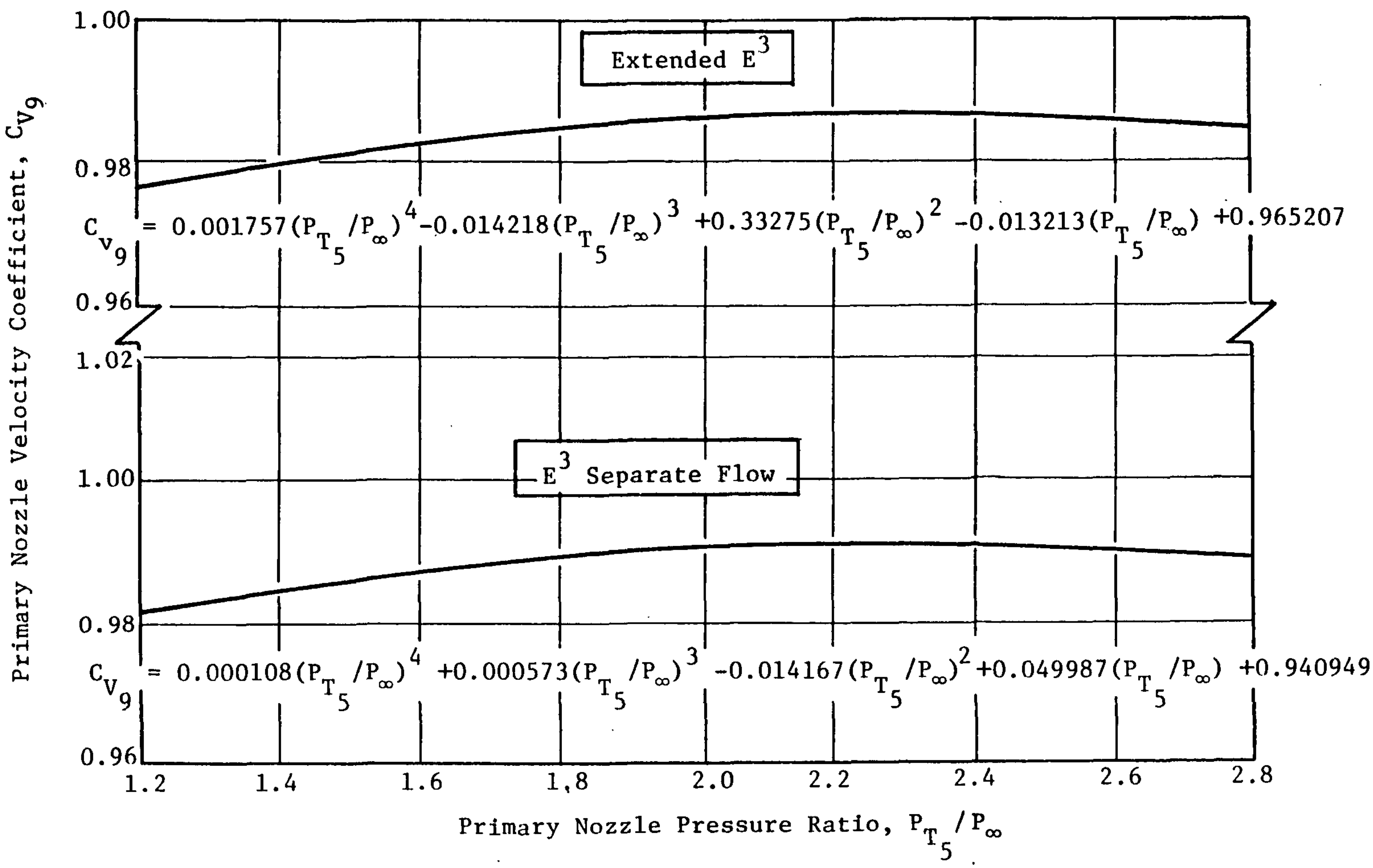

Figure 16b. Primary Nozzle Velocity Coefficient.

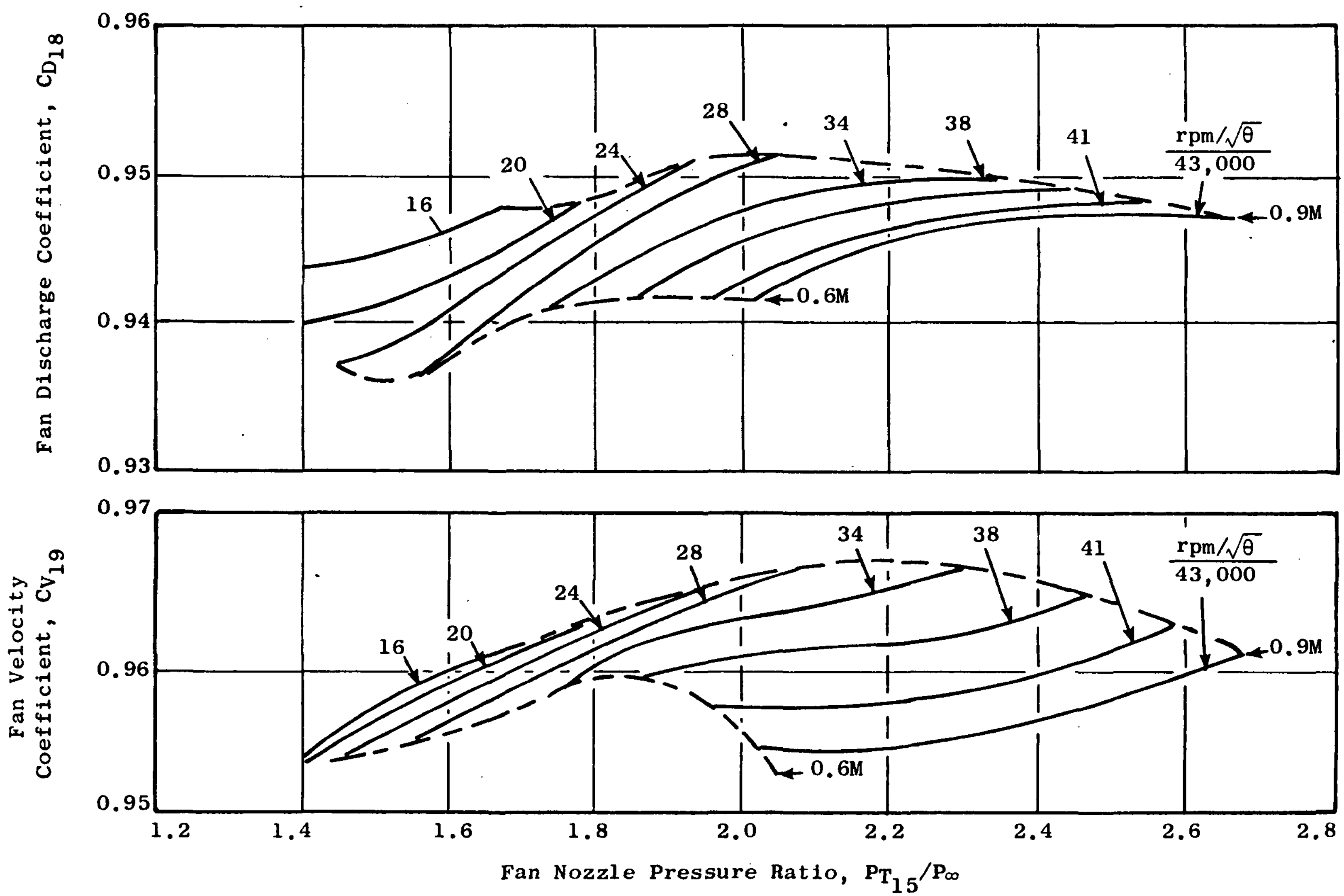

Figure 17. CF6-50 Short Core Velocity and Discharge Coefficients.

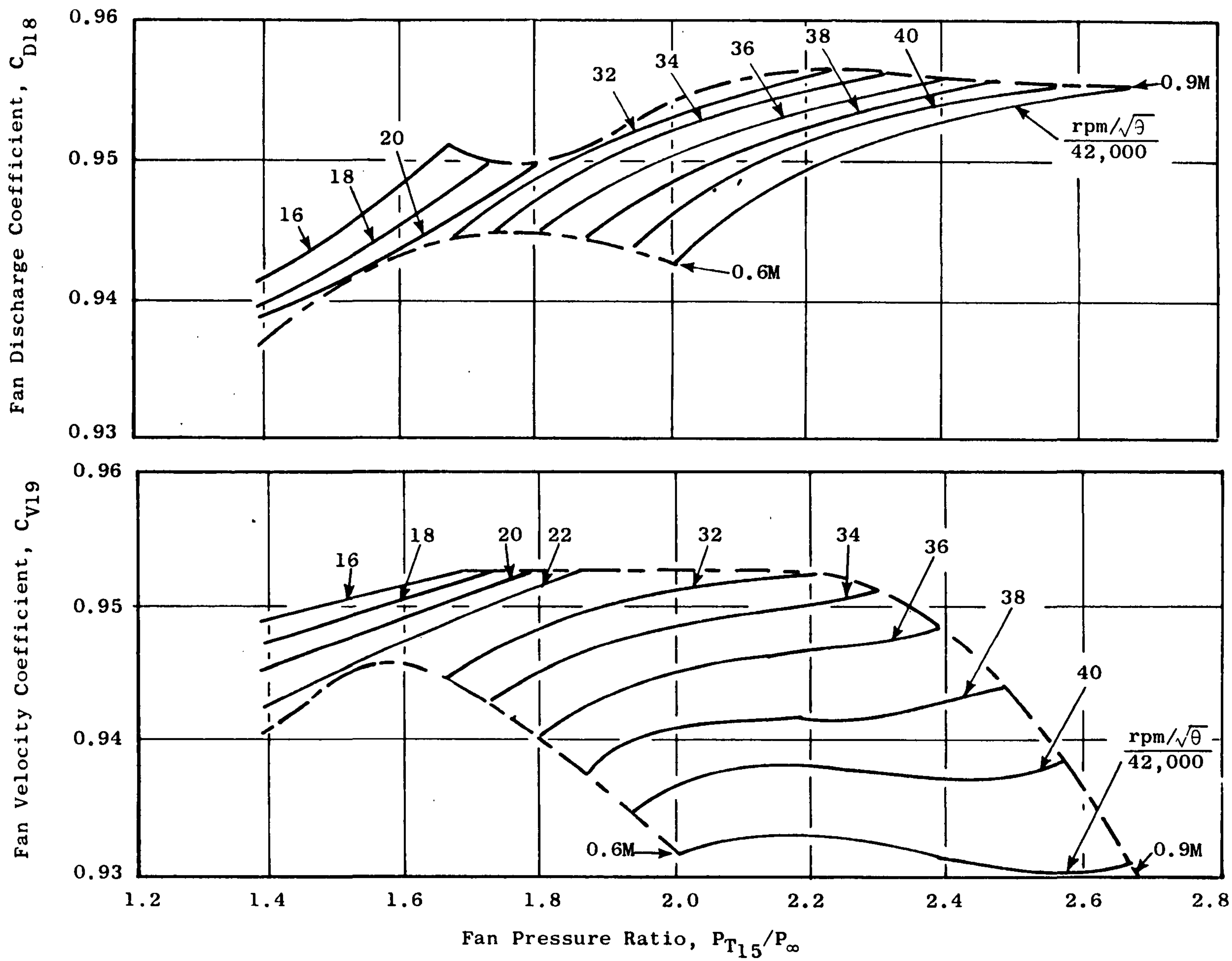

Figure 18. CF6-50 Long Core Velocity and Discharge Coefficients.

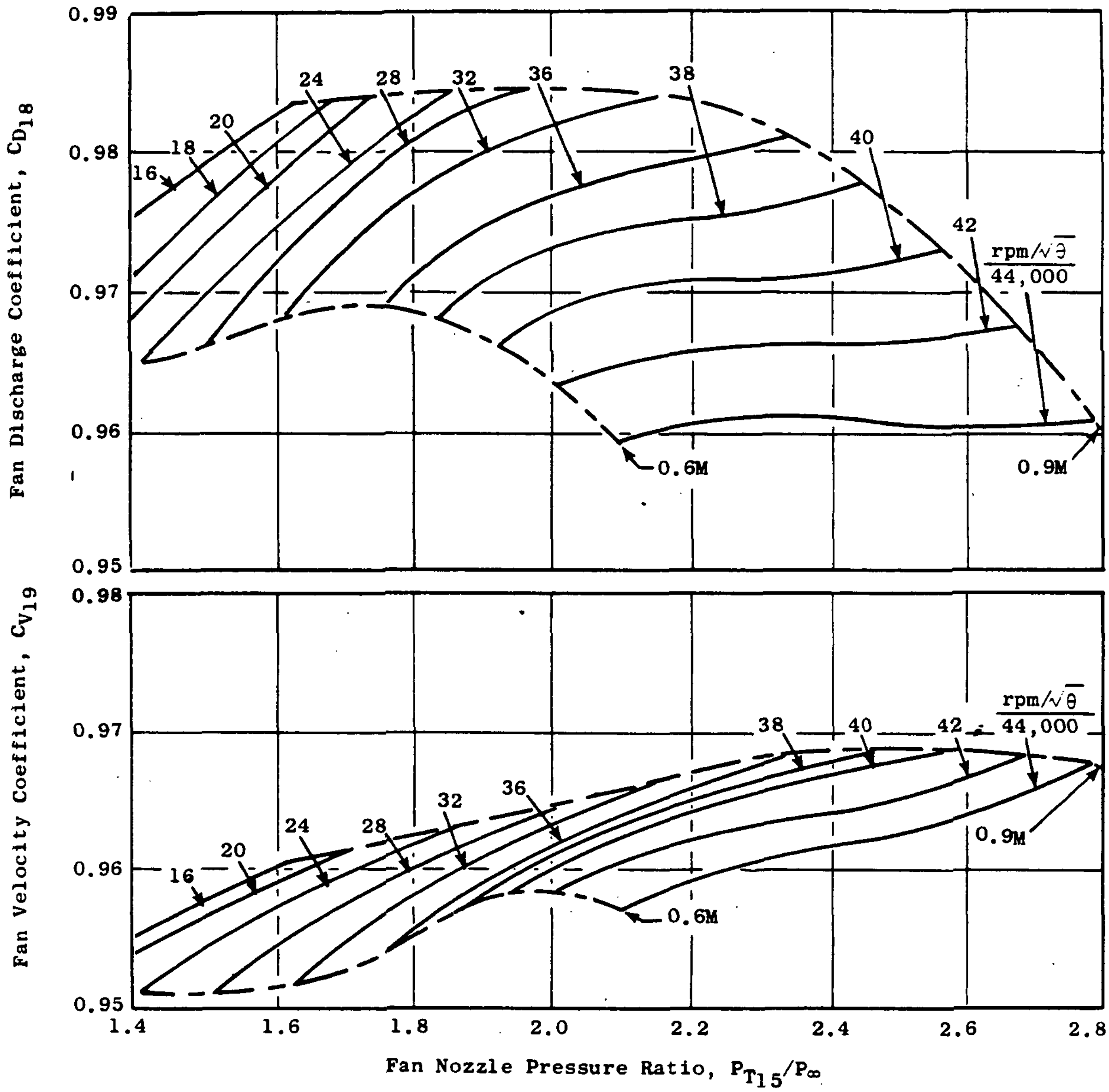

Figure 19. CF6-50 LDMF Velocity and Discharge Coefficients.

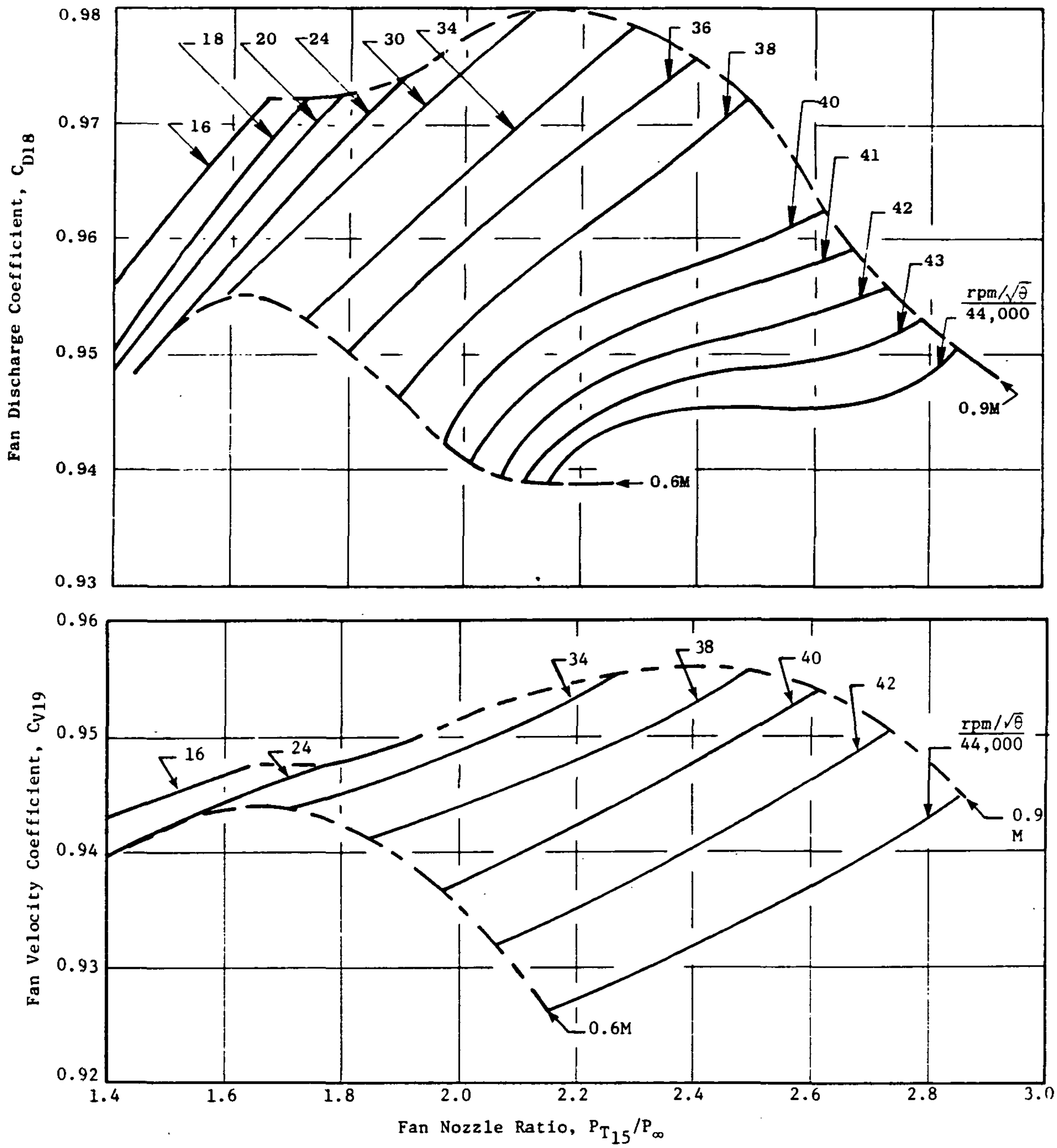

Figure 20. E^3 Velocity and Discharge Coefficients.

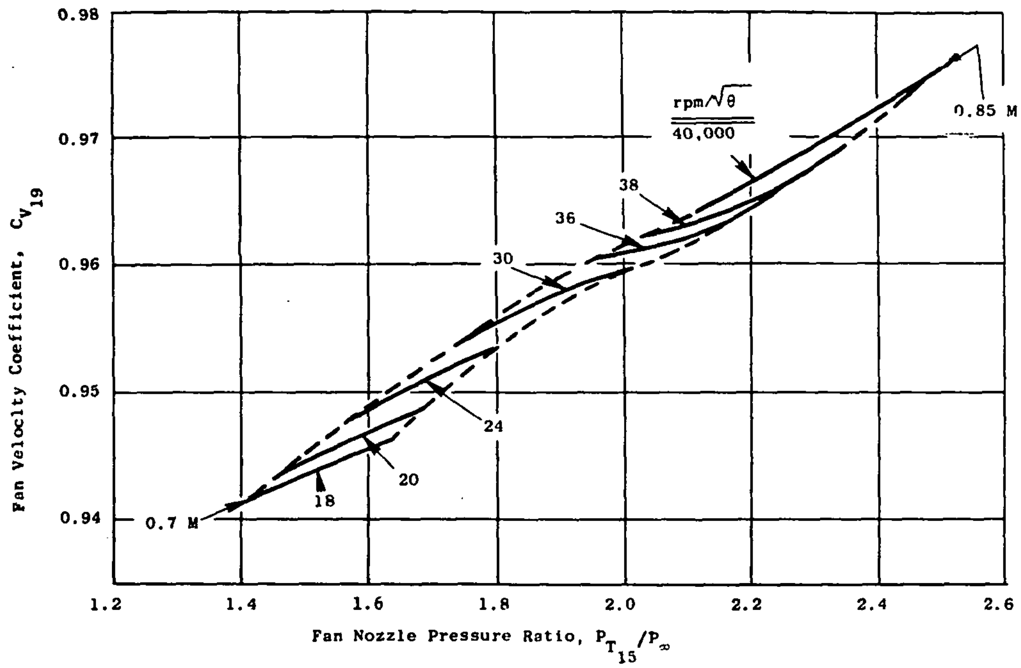

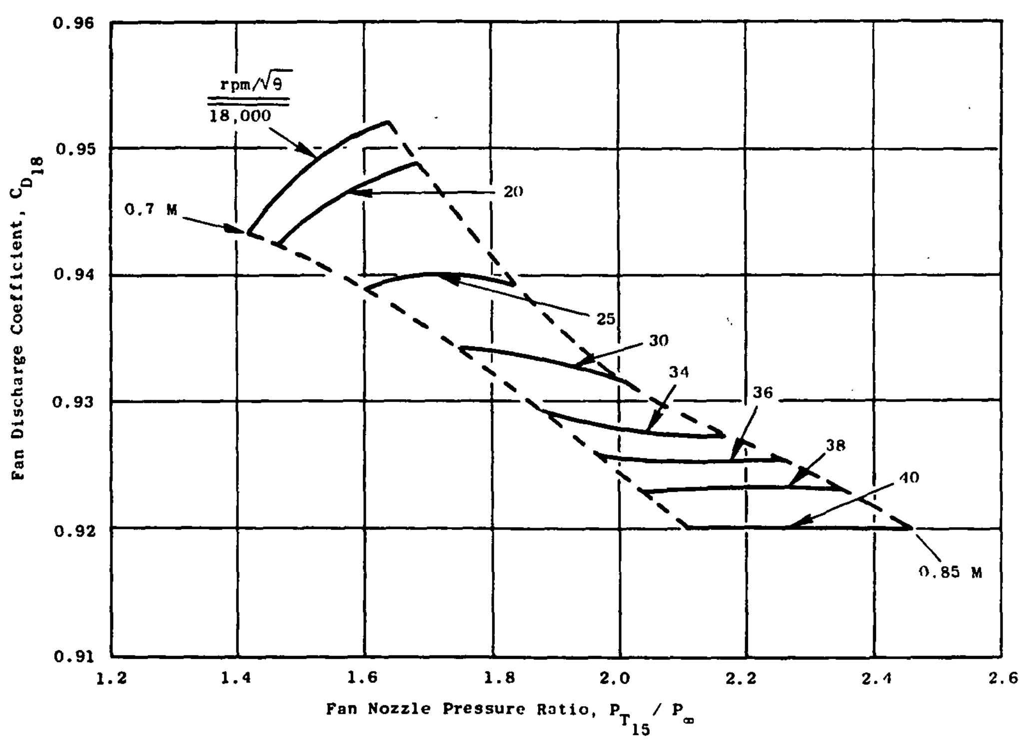

Figure 21. E^3 Extended Nacelle Velocity and Discharge Coefficients.

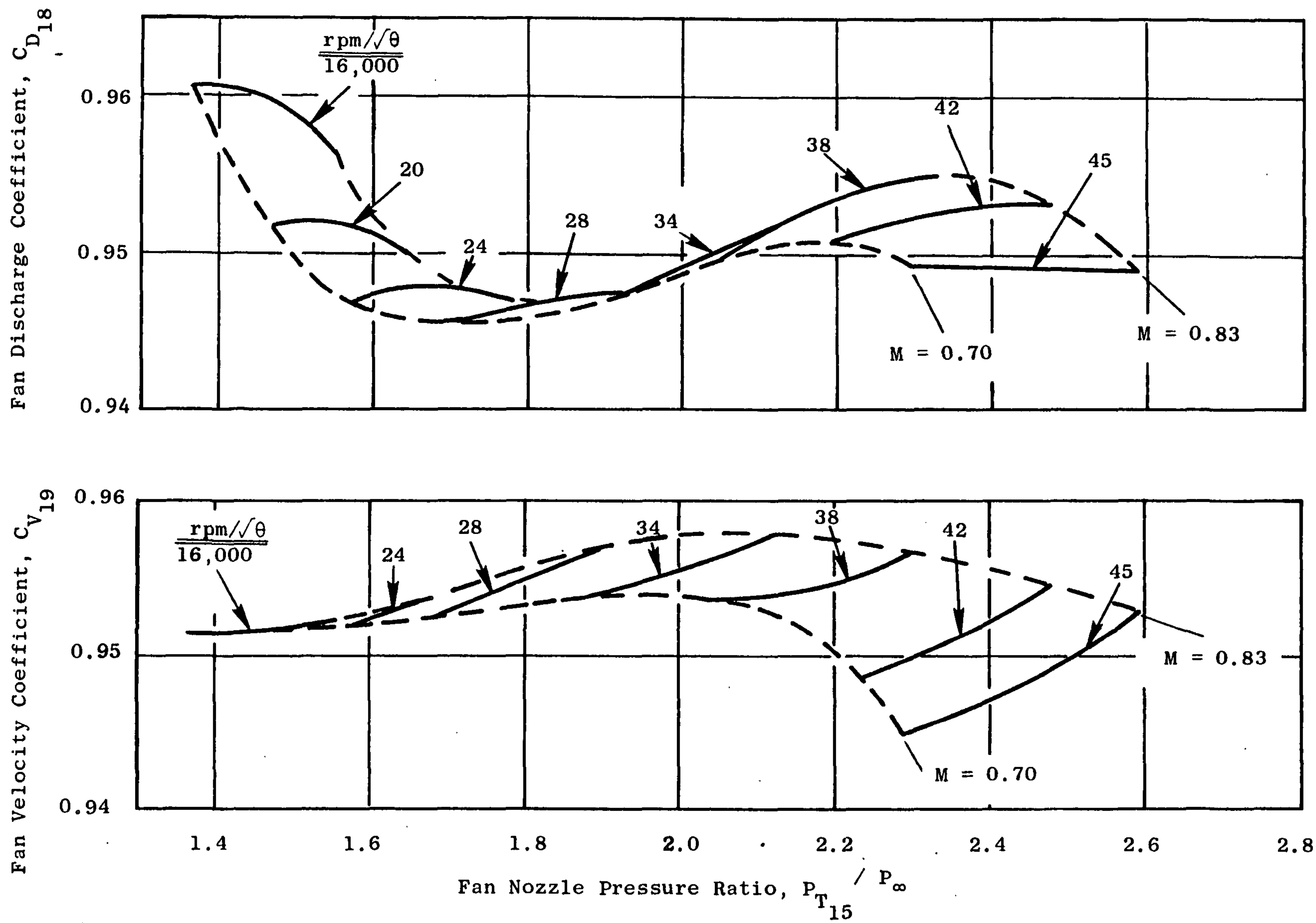

Figure 22. E^3 Separate Flow Velocity and Discharge Coefficients.

Table III. CF6-50 Short Core C_D and C_V Curve Fit Equations.

$$C_{D_{18}} = A\,(P_{T_{15}}/P_\infty)^3 + B(P_{T_{15}}/P_\infty)^2 + C(P_{T_{15}}/P_\infty) + D$$

$$C_{V_{19}} = E(P_{T_{15}}/P_\infty)^3 + F(P_{T_{15}}/P_\infty)^2 + G(P_{T_{15}}/P_\infty) + H$$

$rpm/\sqrt{\theta}$	A	B	C	D	E	F	G	H
16000	-0.69030	3.28625	-5.19133	3.66699	0.12402	-0.61818	1.04518	0.36228
20000	-0.09354	0.47724	-0.78384	1.35846	0.10125	-0.49514	0.82833	0.48659
24000	-0.09019	0.46417	-0.76217	1.34109	-0.01676	0.08208	-0.10951	0.99156
28000	-0.04061	0.19316	-0.26763	1.03787	-0.00533	0.01829	0.00896	0.91733
34000	-0.00310	-0.01305	0.10624	0.81181	0.08220	-0.51259	1.07388	0.20870
38000	0.02926	-0.21767	0.54032	0.50110	0.05933	-0.37801	0.80639	0.38555
41000	-0.00139	-0.01412	0.09597	0.81817	0.01104	-0.05464	0.08533	0.91704
43000	0.03456	-0.26851	0.69406	0.35008	-0.02164	0.17135	-0.43491	1.31244

Table IV. CF6-50 Long Core C_D and C_V Curve Fit Equations.

$$C_{D_{18}} = A\,(P_{T_{15}}/P_\infty)^3 + B(P_{T_{15}}/P_\infty)^2 + C(P_{T_{15}}/P_\infty) + D$$

$$C_{V_{19}} = E(P_{T_{15}}/P_\infty)^3 + F(P_{T_{15}}/P_\infty)^2 + G(P_{T_{15}}/P_\infty) + H$$

$rpm/\sqrt{\theta}$	A	B	C	D	E	F	G	H
16000	0.00531	0.00622	-0.02253	0.94589	0.01247	-0.05102	0.08026	0.90261
18000	0.02620	-0.10822	0.17522	0.83432	0.00046	-0.00521	0.02807	0.91714
20000	0.00586	-0.01711	0.03669	0.90439	0.00239	-0.01387	0.04405	0.90438
22000	---	---	---	---	0.00135	-0.01614	0.06390	0.88098
32000	0.00451	-0.04896	0.16140	0.79007	0.03532	-0.23719	0.53321	0.55133
34000	0.01433	-0.11290	0.29944	0.69003	0.08844	-0.55666	1.17442	0.11911
36000	0.02579	-0.18118	0.43648	0.59547	0.09482	-0.61820	1.34784	-0.03594
38000	0.02790	-0.20617	0.51732	0.51511	0.11897	-0.78903	1.74398	-0.34255
40000	0.03342	-0.25601	0.66112	0.38006	0.11065	-0.76452	1.75467	-0.39969
42000	0.04148	-0.32103	0.83601	0.22229	0.08031	-0.57020	1.33996	-0.10983

Table V. CF6-50 LDMF C_D and C_V Curve Fit Equations.

$$C_{D_{18}} = A\,(P_{T_{15}}/P_\infty)^3 + B(P_{T_{15}}/P_\infty)^2 + C(P_{T_{15}}/P_\infty) + D$$

$$C_{V_{19}} = E(P_{T_{15}}/P_\infty)^3 + F(P_{T_{15}}/P_\infty)^2 + G(P_{T_{15}}/P_\infty) + H$$

rpm/$\sqrt{\theta}$	A	B	C	D	E	F	G	H
16000	0.10477	-0.48644	0.78656	0.53974	-0.10938	0.49224	-0.71331	1.28898
18000	-0.00666	0.01494	0.04669	0.89403	---	---	---	---
20000	-0.00636	0.00828	0.06779	0.87371	-0.05060	0.22067	-0.29415	1.07176
24000	-0.03573	0.14771	-0.15134	0.98424	0.02630	-0.14788	0.29768	0.75140
28000	-0.05082	0.20628	-0.21216	0.99026	0.03299	-0.19494	0.40516	0.66975
32000	0.06592	-0.42505	0.92607	0.30231	0.04226	-0.26487	0.57406	0.53627
36000	0.08092	-0.53372	1.18352	0.09701	0.02944	-0.20140	0.47698	0.57754
38000	0.09423	-0.62869	1.40442	-0.07522	0.03558	-0.24727	0.58724	0.49082
40000	0.08214	-0.56682	1.30609	-0.03408	0.01853	-0.14037	0.36503	0.64304
42000	0.05500	-0.39586	0.95011	0.20585	0.05711	-0.40418	0.96213	0.19346
44000	0.05423	-0.40607	1.00937	0.12779	0.05815	-0.42210	1.03027	0.11629

Table VI. E^3 C_D and C_V Curve Fit Equations.

$$C_{D_{18}} = A\,(P_{T_{15}}/P_\infty)^3 + B(P_{T_{15}}/P_\infty)^2 + C(P_{T_{15}}/P_\infty) + D$$

$$C_{V_{19}} = E(P_{T_{15}}/P_\infty)^3 + F(P_{T_{15}}/P_\infty)^2 + G(P_{T_{15}}/P_\infty) + H$$

rpm/$\sqrt{\theta}$	A	B	C	D	E	F	G	H
16000	0.00012	-0.02049	0.12363	0.82283	-0.02635	0.11854	-0.15851	1.00477
18000	0.02332	-0.12995	0.30170	0.71883	---	---	---	---
20000	0.01603	-0.09331	0.23688	0.75588	---	---	---	---
24000	0.01954	-0.11574	0.27806	0.72982	-0.00002	-0.01490	0.06835	0.87328
30000	-0.03993	0.21079	-0.31936	1.09042	---	---	---	---
34000	-0.00198	0.00734	0.04002	0.87229	0.15868	-0.94565	1.89235	-0.32238
36000	0.01353	-0.09898	0.27851	0.69062	---	---	---	---
38000	0.05062	-0.34780	0.83302	0.27282	0.02039	-0.12223	0.26314	0.74362
40000	0.13676	-0.97531	2.33206	-0.91174	-0.00002	0.00727	-0.00615	0.92085
41000	0.09927	-0.73279	1.81640	-0.55592	---	---	---	---
42000	0.11141	-0.82940	2.06797	-0.77454	0.00275	-0.01179	0.03656	0.88268
43000	0.12016	-0.90286	2.26674	-0.95241	---	---	---	---
44000	0.15466	-1.16411	2.91767	-1.48946	0.00565	-0.03420	0.09060	0.83340

Table VII. E^3 Extended C_D and C_V Curve Fit Equations.

$$C_{D_{18}} = A(P_{T_{15}}/P_\infty)^3 + B(P_{T_{15}}/P_\infty)^2 + C(P_{T_{15}}/P_\infty) + D$$

$$C_{V_{19}} = E(P_{T_{15}}/P_\infty)^3 + F(P_{T_{15}}/P_\infty)^2 + G(P_{T_{15}}/P_\infty) + H$$

rpm/$\sqrt{\theta}$	A	B	C	D	E	F	G	H
18,000	0.18126	−0.94878	1.66666	−0.02914	−0.07101	0.32580	0.47699	1.16551
20,000	0.23267	−1.17269	1.98885	−0.18611	0.00309	−0.01782	0.05683	0.88879
24,000	---	---	---	---	−0.14909	0.73013	−1.16364	1.55188
25,000	0.00828	−0.11984	0.33875	0.66957	---	---	---	---
30,000	0.08804	−0.51428	0.98873	0.30686	0.008102	−0.08161	0.24279	0.73556
34,000	0.02133	−0.10153	0.14146	0.88014	---	---	---	---
36,000	−0.14433	0.92772	−1.98597	2.34086	0.00300	0.06781	−0.22689	1.16735
38,000	0.0	−0.00997	0.04473	0.87287	0.05000	−0.28101	0.53325	0.61941
40,000	0.0	0.0	0.0	0.91980	−0.00068	0.00485	0.01755	0.91156

Table VIII. E^3 Separate Flow C_D and C_V Curve Fit Equations.

$$C_{D_{18}} = A(P_{T_{15}}/P_\infty)^3 + B(P_{T_{15}}/P_\infty)^2 + C(P_{T_{15}}/P_\infty) + D$$

$$C_{V_{19}} = E(P_{T_{15}}/P_\infty)^3 + F(P_{T_{15}}/P_\infty)^2 + G(P_{T_{15}}/P_\infty) + H$$

$rpm/\sqrt{\theta}$	A	B	C	D	E	F	G	H
16,000	-0.00863	-0.12072	0.38441	0.68282	0.46996	-2.03438	2.93571	-0.46053
20,000	-0.28670	1.19706	-1.65105	1.70281	---	---	---	---
24,000	0.48852	-2.53083	4.36212	-1.55380	-0.18024	0.89986	-1.47939	1.75400
28,000	-0.12129	0.66499	-1.20468	1.66782	-0.00119	0.00636	0.00862	0.92567
34,000	0.06660	-0.37388	0.71717	0.47758	0.13327	-0.78536	1.55683	-0.08285
38,000	0.04675	-0.34792	0.86997	0.22571	0.08379	-0.49602	0.97925	0.30878
42,000	-0.07213	0.47599	-1.03323	1.68840	0.03897	-0.25108	0.55853	0.51933
45,000	0.01505	-0.10982	0.26570	0.73601	-0.41786	3.06824	-7.47910	7.00033

8.0 WIND TUNNEL THRUST ACCOUNTING DATA REDUCTION EQUATIONS

The following section presents the equations and data logic that are used with the wind tunnel data reduction program to calculate the powered simulator thrust for the appropriate operating condition. The values for the velocity and discharge coefficents are provided from the calibration test and the remaining variables are measured in the wind tunnel. The definitions for the variables contained in this section are presented in the Nomenclature section.

The following measurements are obtained from the TPS instrumentation rakes and are averaged to give one reading:

$$P_{T_{15}} = \frac{\sum_{i=1}^{18} P_{T_{15i}}}{18} \qquad \text{(Average of 18 } P_{T_{15}} \text{ readings)}$$

$$T_{T_{15}} = \frac{\sum_{i=1}^{6} T_{T_{15i}}}{6} \qquad \text{(Average of 6 } T_{T_{15}} \text{ readings)}$$

$$P_{T_5} = \frac{\sum_{i=1}^{16} P_{T_{5i}}}{16} \qquad \text{(Average of 16 } P_{T_5} \text{ readings)}$$

$$T_{T_5} = \frac{\sum_{i=1}^{4} T_{T_{5i}}}{4} \qquad \text{(Average of 4 } T_{T_5} \text{ readings)}$$

The fan airflow is calculated using:

if, $P_{T_{15}}/P_\infty < 1.893$:

$$\bar{m}_{18} = \left(\frac{P_\infty}{P_{T_{15}}}\right)^{\frac{1}{\gamma_F}} \left\{\frac{2g}{R}\left(\frac{\gamma_F}{\gamma_F - 1}\right)\left[1 - \left(\frac{P_\infty}{P_{T_{15}}}\right)^{\frac{\gamma_F - 1}{\gamma_F}}\right]\right\}^{1/2}$$

if, $P_{T_{15}}/P_\infty \geqq 1.893$:

$$\bar{m}_{18} = \left[\frac{2g}{R}\left(\frac{\gamma_F}{\gamma_F + 1}\right)\right]^{1/2}\left(\frac{2}{\gamma_F + 1}\right)^{\frac{1}{\gamma_F - 1}}$$

Then,

$$W_{18i} = \bar{m}_{18}\, P_{T_{15}} A_{18}/\sqrt{T_{T15}}$$

$$W_{18} = C_{D_{18}}\, W_{18i}$$

where $C_{D_{18}}$ is provided from the calibration test and γ_F is a function of $T_{T_{15}}$.

The primary discharge coefficient can be found from:

if, $P_{T_5}/P_\infty < 1.893$:

$$\bar{m}_8 = \left(\frac{P_\infty}{P_{T_5}}\right)^{\frac{1}{\gamma_T}} \left\{ \frac{2g}{R} \left(\frac{\gamma_T}{\gamma_T - 1}\right) \left[1 - \left(\frac{P_\infty}{P_{T_5}}\right)^{\frac{\gamma_T - 1}{\gamma_T}} \right] \right\}^{1/2}$$

if, $P_{T_5}/P_\infty \geqq 1.893$:

$$\bar{m}_8 = \left[\frac{2g}{R} \left(\frac{\gamma_T}{\gamma_T + 1}\right)\right]^{1/2} \left(\frac{2}{\gamma_T + 1}\right)^{\frac{1}{\gamma_T - 1}}$$

Then,

$$W_{8i} = \bar{m}_8\, P_{T_5}\, A_8/\sqrt{T_{T_5}}$$

$$C_{D_8} = W_5/W_{8i}$$

where W_5 is measured primary drive airflow and γ_T is a function of T_{T_5}.

The core gross thrust is then:

$$V_{9i} = \left(\frac{2g\ \gamma_T\ R\ T_{T5}}{\gamma_T - 1}\right)^{1/2} \left\{ 1 - \left(\frac{P_\infty}{P_{T_5}}\right)^{\frac{\gamma_T - 1}{\gamma_T}} \right\}^{1/2}$$

$$F_{g9i} = W_5\, V_{9i}$$

$$F_{g9} = C_{V_9}\, F_{g9i}$$

And the fan gross thrust is:

$$V_{19i} = \left(\frac{2g\ \gamma_F\ R\ T_{T15}}{\gamma_F - 1}\right)^{1/2} \left\{ 1 - \left(\frac{P_\infty}{P_{T_{15}}}\right)^{\frac{\gamma_F - 1}{\gamma_F}} \right\}^{1/2}$$

$$F_{g_{19i}} = W_{18} V_{19i}$$

$$F_{g_{19}} = C_{V_{19}} F_{g_{19i}}$$

Giving the total simulator gross thrust of:

$$F_{g_T} = F_{g_9} + F_{g_{19}}$$

The ram drag on the simulator is:

$$F_R = W_{18} V_\infty$$

Finally, the net simulator thrust in the freestream direction is found from:

$$F_N = F_{g_T} \cos(\alpha + \alpha_{ei}) \cos(\psi_e) - F_R$$

where:

α = Fuselage angle of attack

α_{ei} = Engine incidence (angle of attack) w.r.t. the fuselage reference line

ψ_e = Engine cant angle (+ for engine toed outboard)

8.1 HAND CALCULATION CHECKCASE

The following case was arbitrarily taken from the calibration data in order to check the validity of the thrust accounting data reduction equations. The measured TPS thrust will be compared to the value of thrust computed from the quantities that will be measured in the wind tunnel.

Given from Calibration Test

Run 160 Test Point 11 (Picked at random)

$M = 0.828$

rpm = 39,950

$P_{T_{15}}/P_\infty = 2.4061$

$P_{T_5}/P_\infty = 1.7526$

$W_5 = 0.668569$ kg/sec

$T_{T_\infty} = 291.95$ K

$T_{T_{15}} = 334.04$ K

$T_{T_5} = 163.69$ K

$F_{g_9} = 148.98$ N

$F_{g_{19}} = 664.39$ N

$F_{g_T} = 813.36$ N

<u>From the Calibration C_V and C_D Curves</u>

$$\left.\begin{aligned} C_{V_9} &= 0.9843 \\ C_{V_{19}} &= 0.94868 \\ C_{D_{18}} &= 0.9597 \end{aligned}\right. \quad \text{at} \quad \left\{\begin{aligned} \text{rpm} &= 39{,}950 \\ P_{T_{15}}/P_\infty &= 2.4061 \\ P_{T_5}/P_\infty &= 1.7526 \end{aligned}\right.$$

Using the equations given in Section 8.0 for calculating the thrust and the above data:

$W_{18i} = 1.8895$ kg/sec

$W_{18} = 1.8134$ kg/sec

$V_{19i} = 385.88$ m/sec

$F_{g_{19i}} = 699.75$ N

$F_{g_{19}} = 663.85$ N

$V_{9i} = 220.72$ m/sec

$F_{g_{9i}} = 147.57$ N

$F_{g_9} = 145.25$ N

$F_{g_T} = 809.10$ N

This compares with the actual measured thrust of 813.36 N. The difference (0.5%) is due to some scatter in the calibration data.

This comparison shows excellent agreement between the measured and computed values of thrust verifying the data reduction methodology and the accuracy of the calibration coefficients.

9.0 TPS CHARACTERISTIC PARAMETER WIND TUNNEL CHECKOUT

This section presents plots of the characteristic parameters reflecting the turbomachinery performance, Figures 23 through 28. A comparison is made between the calibration test and the wind tunnel test to assure consistent operation between the two tests. Any discrepancy between the calibration and wind tunnel test in these characteristics would require that an adjustment be made to assure correct thrust calculation in the wind tunnel. These characteristic plots are:

- Fan pressure ratio ($P_{T_{15}}/P_{T_\infty}$) versus corrected rpm ($rpm/\sqrt{\theta}$)
- Fan temperature ratio ($T_{T_{15}}/T_{T_\infty}$) versus corrected rpm
- Fan temperature ratio ($T_{T_{15}}/T_{T_\infty}$) versus fan pressure ratio
- Fan corrected airflow ($W_{18}\sqrt{\theta F}/\delta_F$) versus corrected rpm
- Turbine temperature ratio (T_{T_4}/T_{T_5}) versus turbine pressure ratio (P_{T_4}/P_{T_5})
- Turbine corrected airflow ($W_5\sqrt{\theta T}/\delta_T$) versus turbine pressure ratio.

The calibration data are presented as a mean data line with dotted lines defining the total data scatter bands. Wind tunnel data are shown plotted as points for comparison with the calibration lines. The wind tunnel data points were taken from runs at a pressure ratio of $P_{T_{15}}/P_{T_\infty}$ = 1.49-1.50 (area of primary interest) and from the limited number of power sweeps run. The plotted data reflect the turbomachinery operation at the beginning, middle, and end of each configuration.

With a few exceptions, the data show good correlation between the calibration test data and the wind tunnel test data. The discrepancies noted are as follows:

- CF6-50 long core fan rake total temperatures ($T_{T_{15}}$) appear too low as compared to the calibration data (Figures 24b and c). At the high pressure ratios, the error in $T_{T_{15}}$ is 0.8%. This discrepancy introduces an error in the ram drag calculation which affects the final drag value. The error in airplane drag caused by a 0.8% error in $T_{T_{15}}$ is approximately 1.5 drag counts. This error is significant enough to require adjusting the wind tunnel data to eliminate the discrepancy in $T_{T_{15}}$.
- The core airflow measurement (W_5) appears to be in error at the high pressure ratios for the three CF6-50 nacelle configurations, the E^3 extended and the E^3 separate flow nacelles.

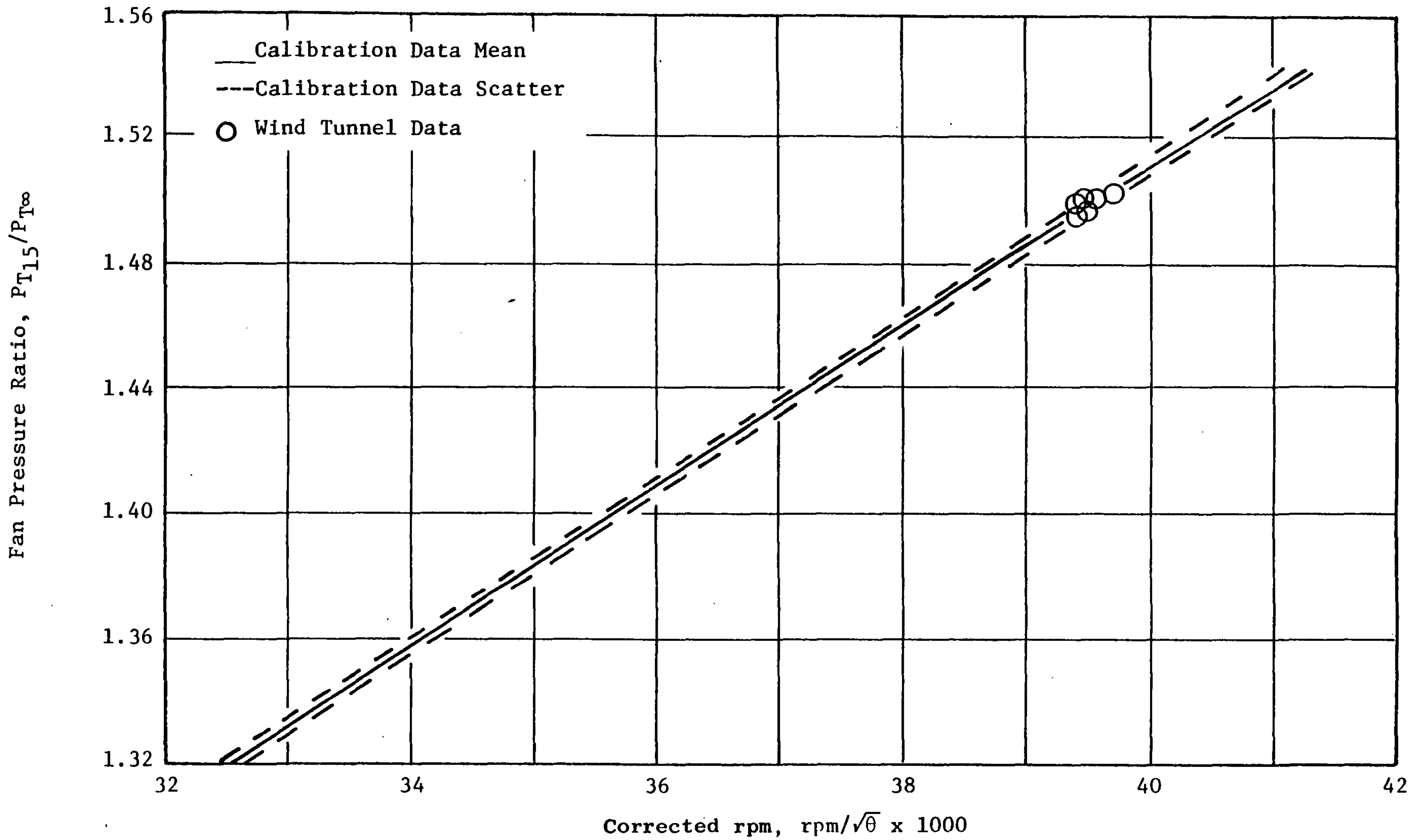

Figure 23a. Short Core Turbomachinery Characteristics.

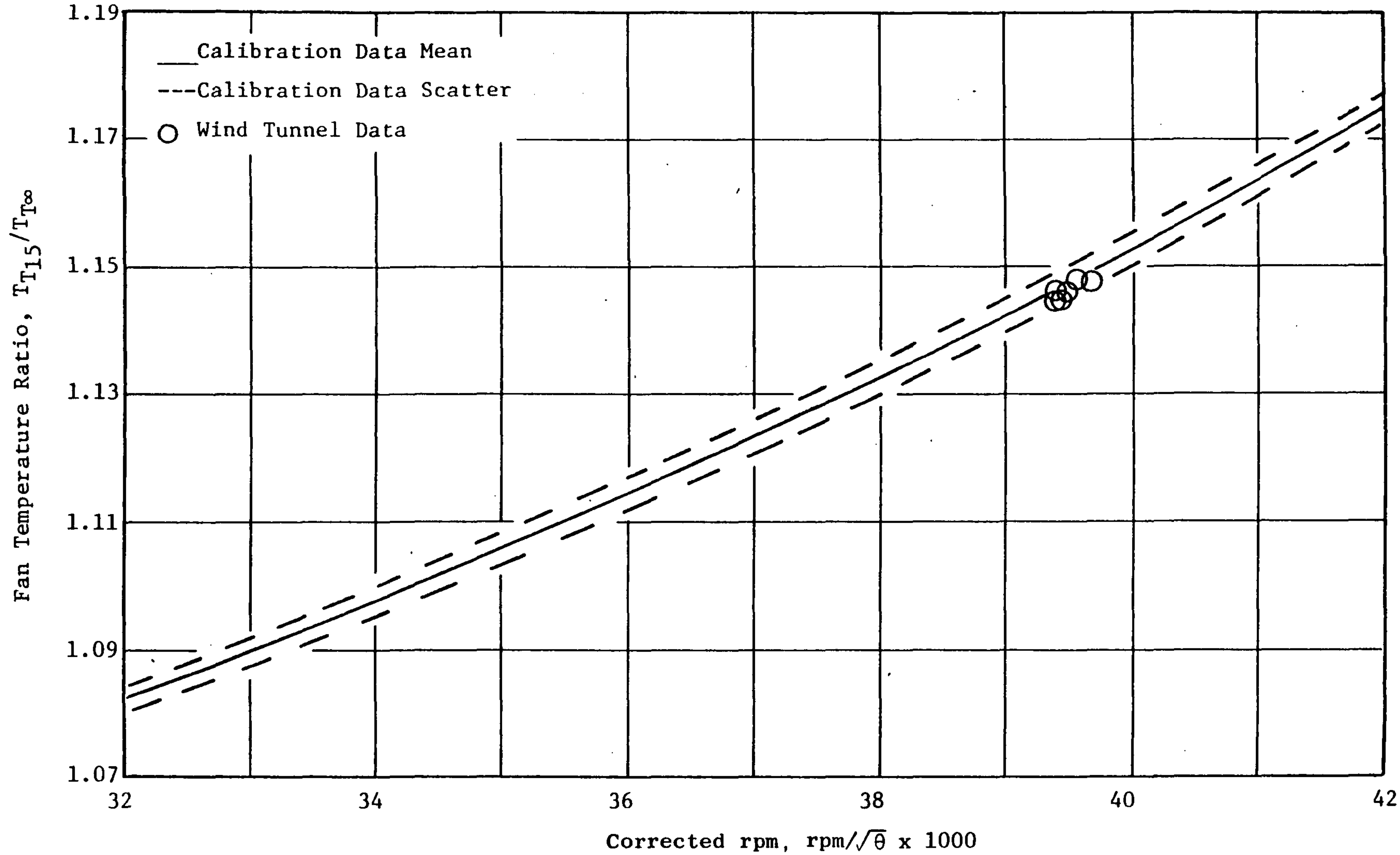

Figure 23b. Short Core Turbomachinery Characteristics.

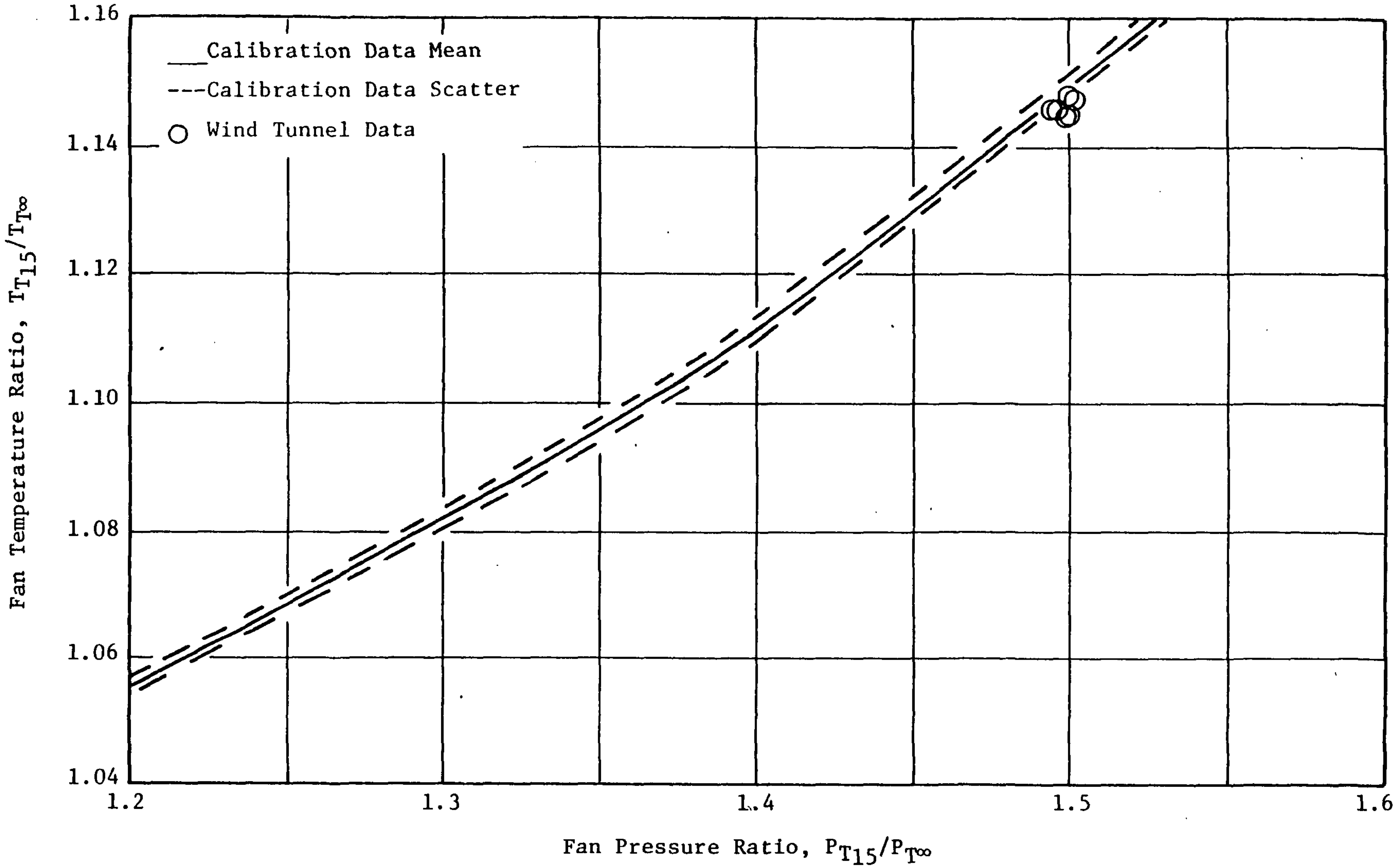

Figure 23c. Short Core Turbomachinery Characteristics.

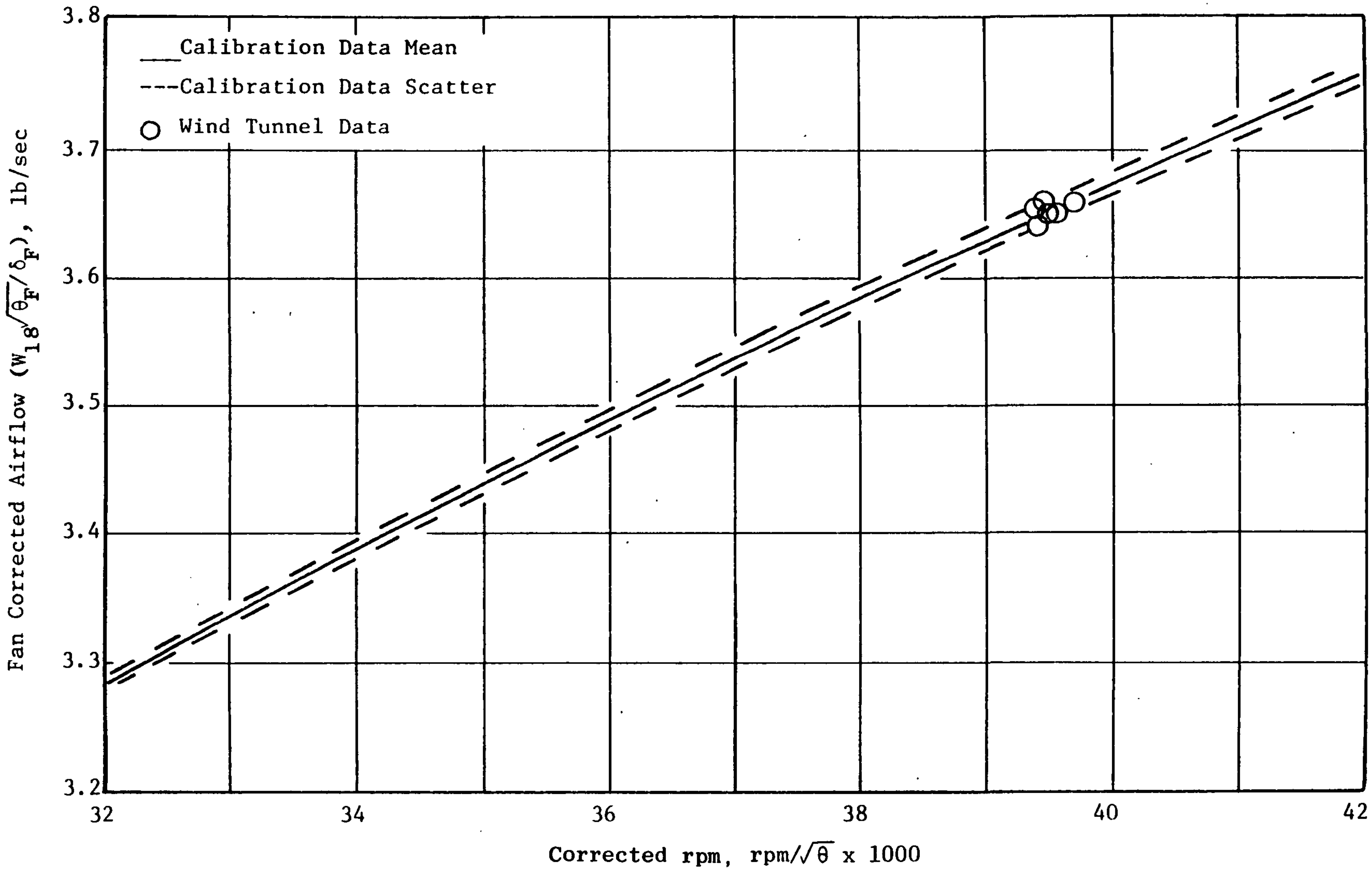

Figure 23d. Short Core Turbomachinery Characteristics.

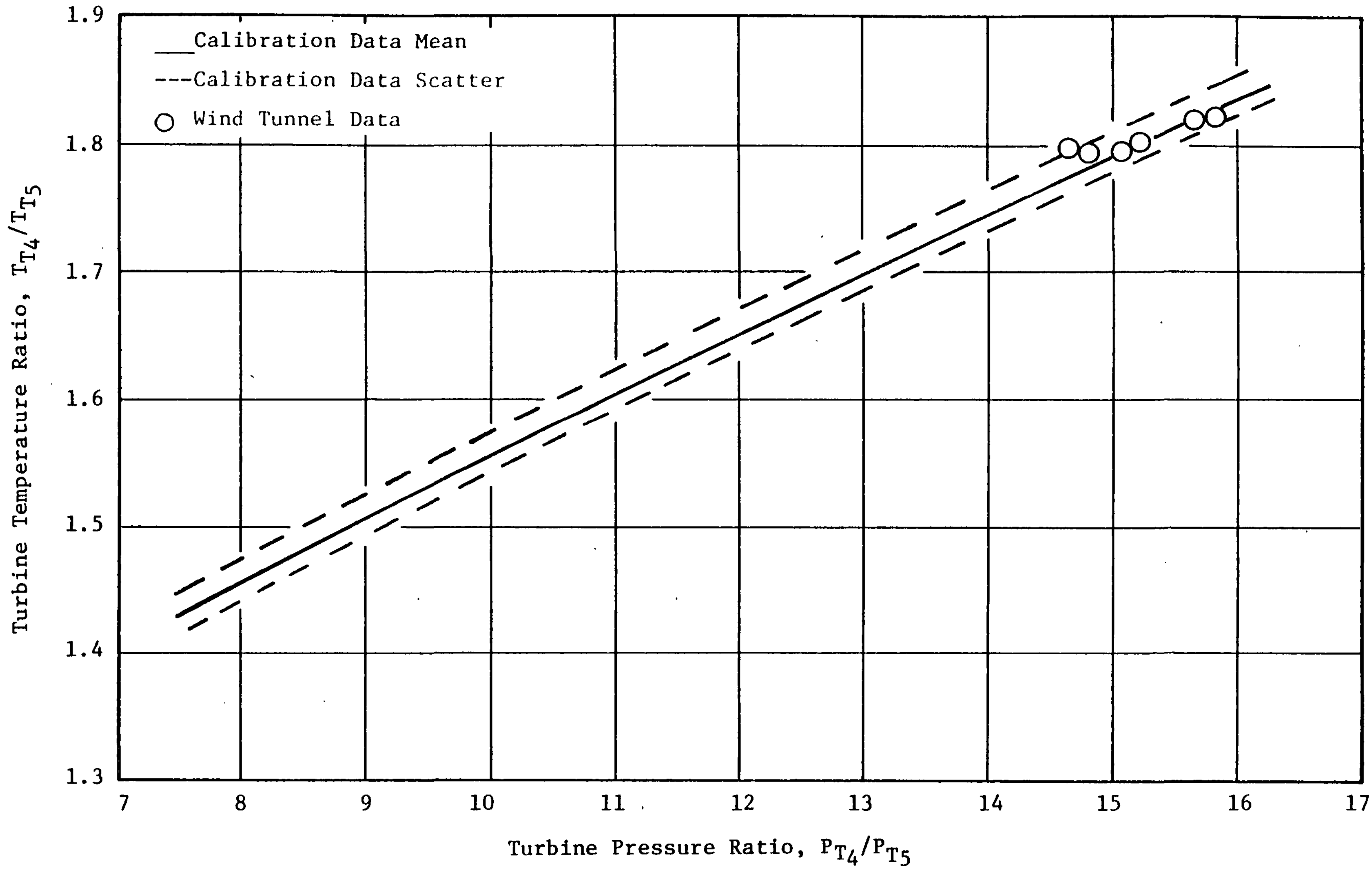

Figure 23e. Short Core Turbomachinery Characteristics.

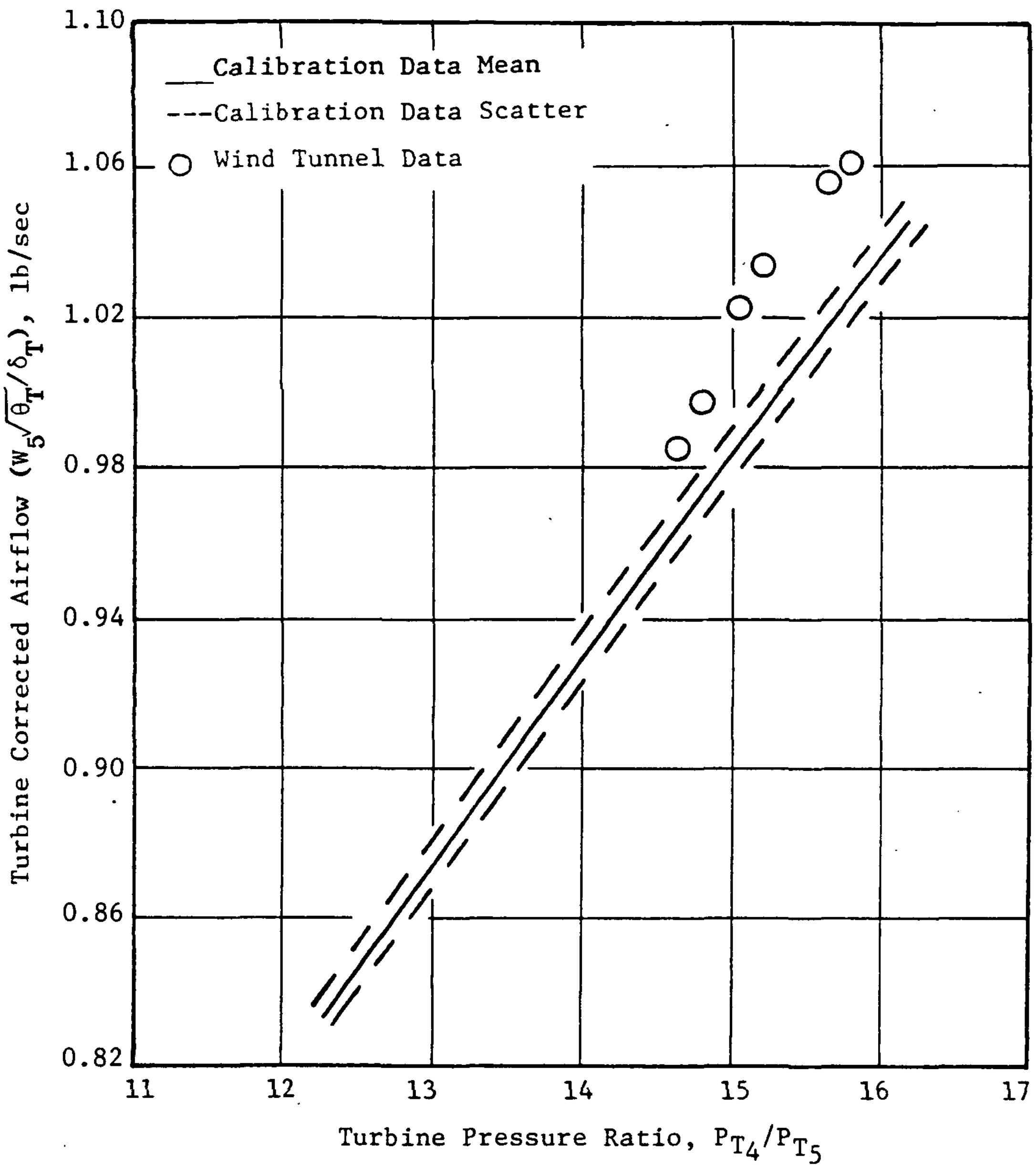

Figure 23f. Short Core Turbomachinery Characteristics.

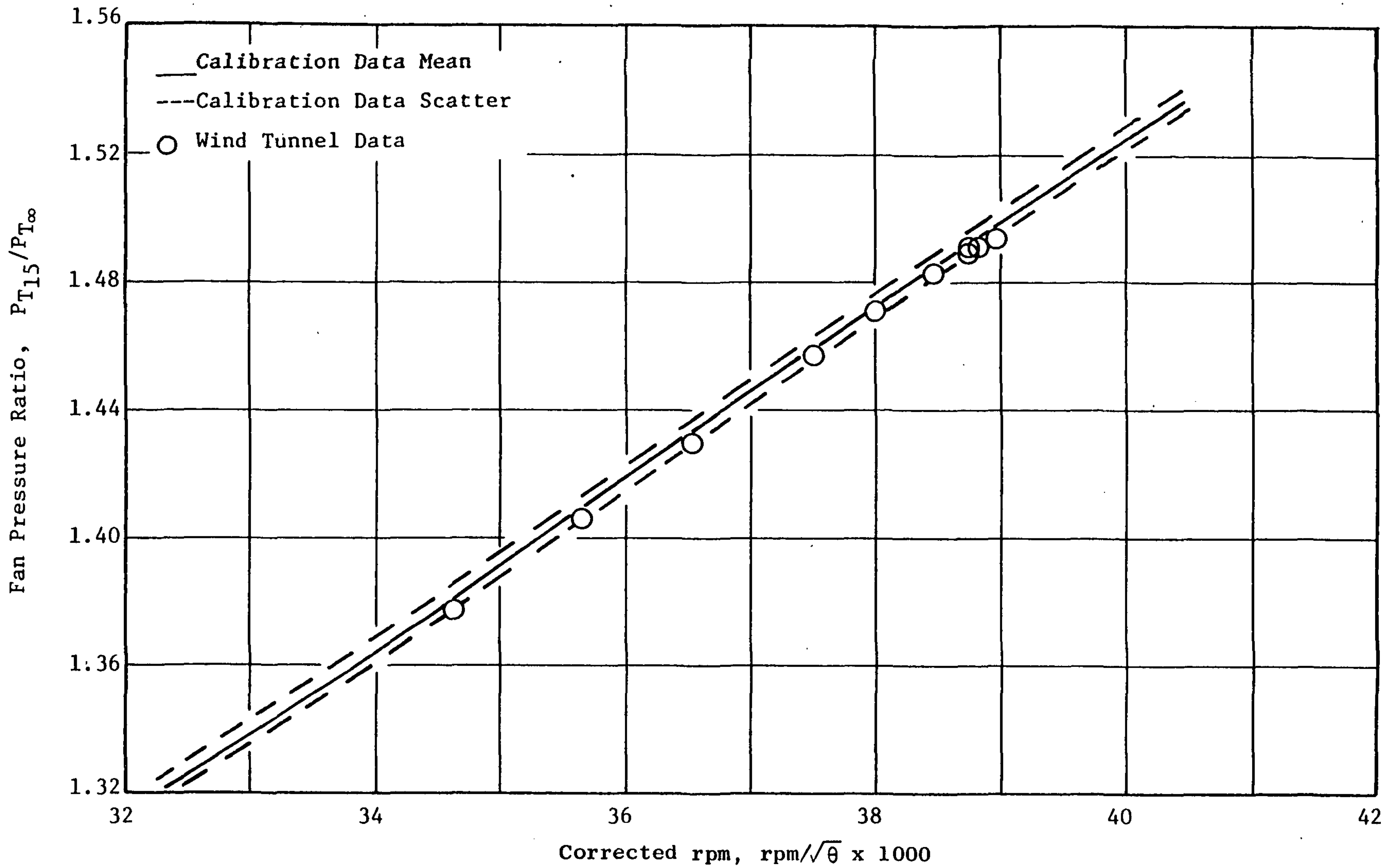

Figure 24a. Long Core Turbomachinery Characteristics.

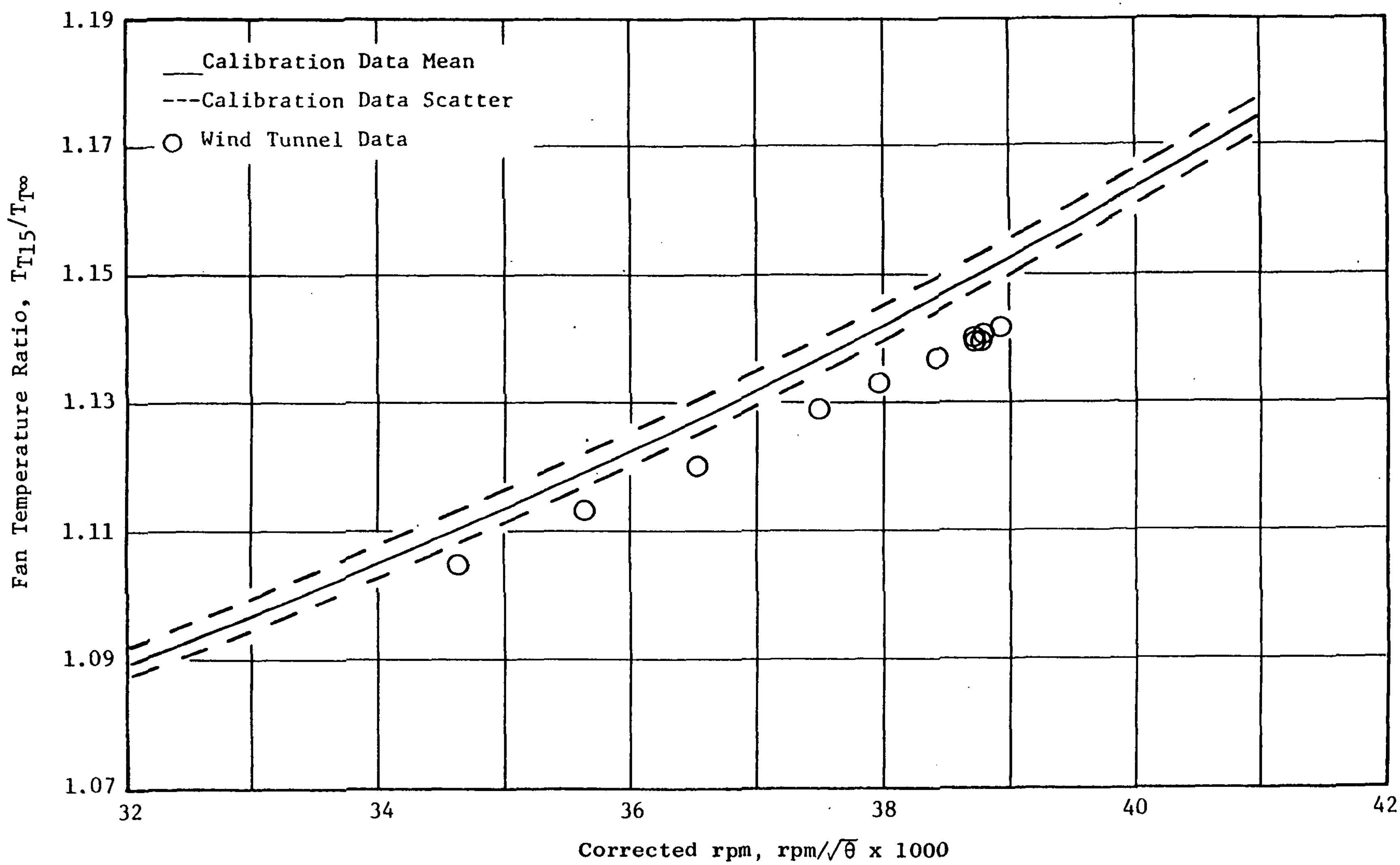

Figure 24b. Long Core Turbomachinery Characteristics.

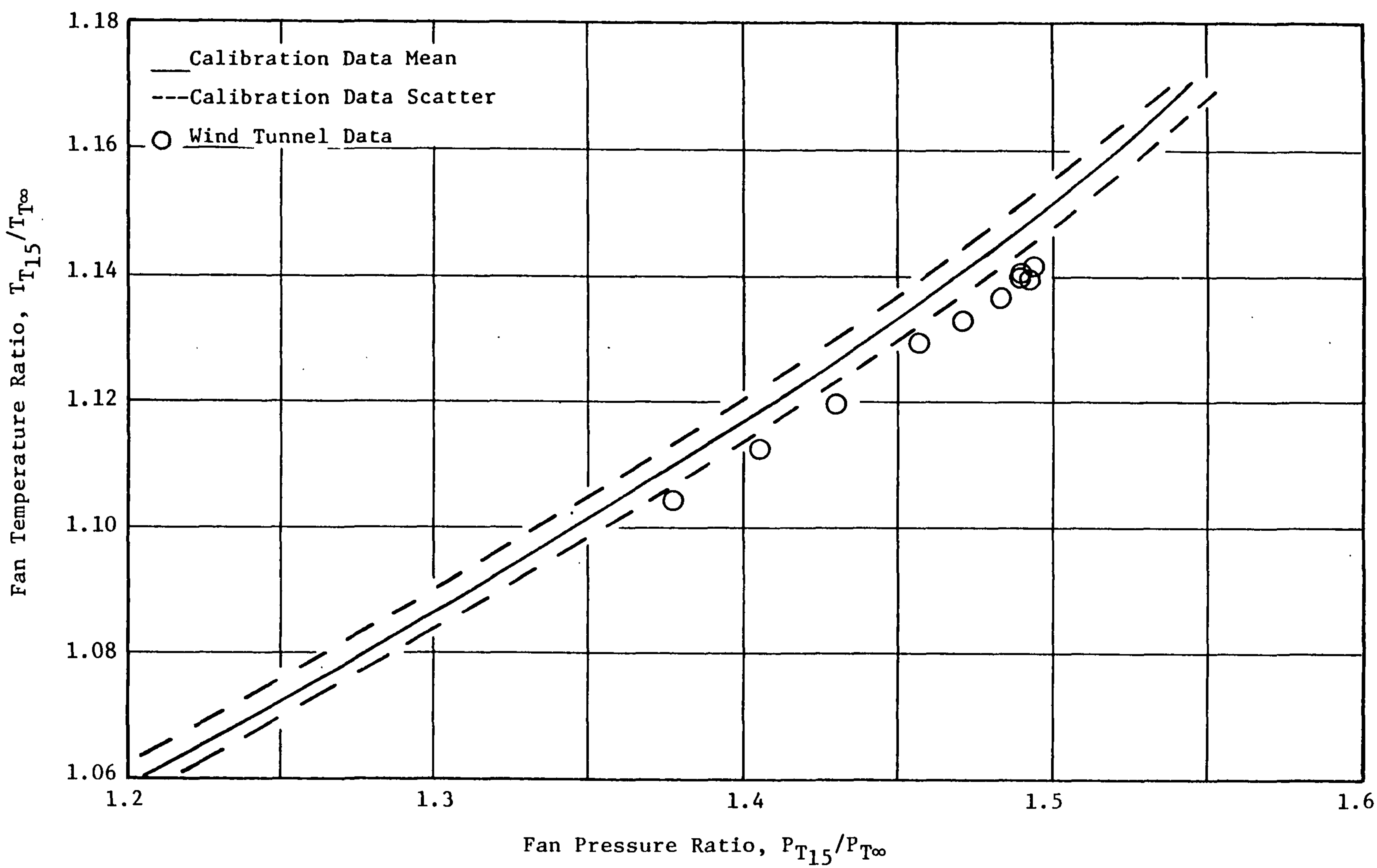

Figure 24c. Long Core Turbomachinery Characteristics.

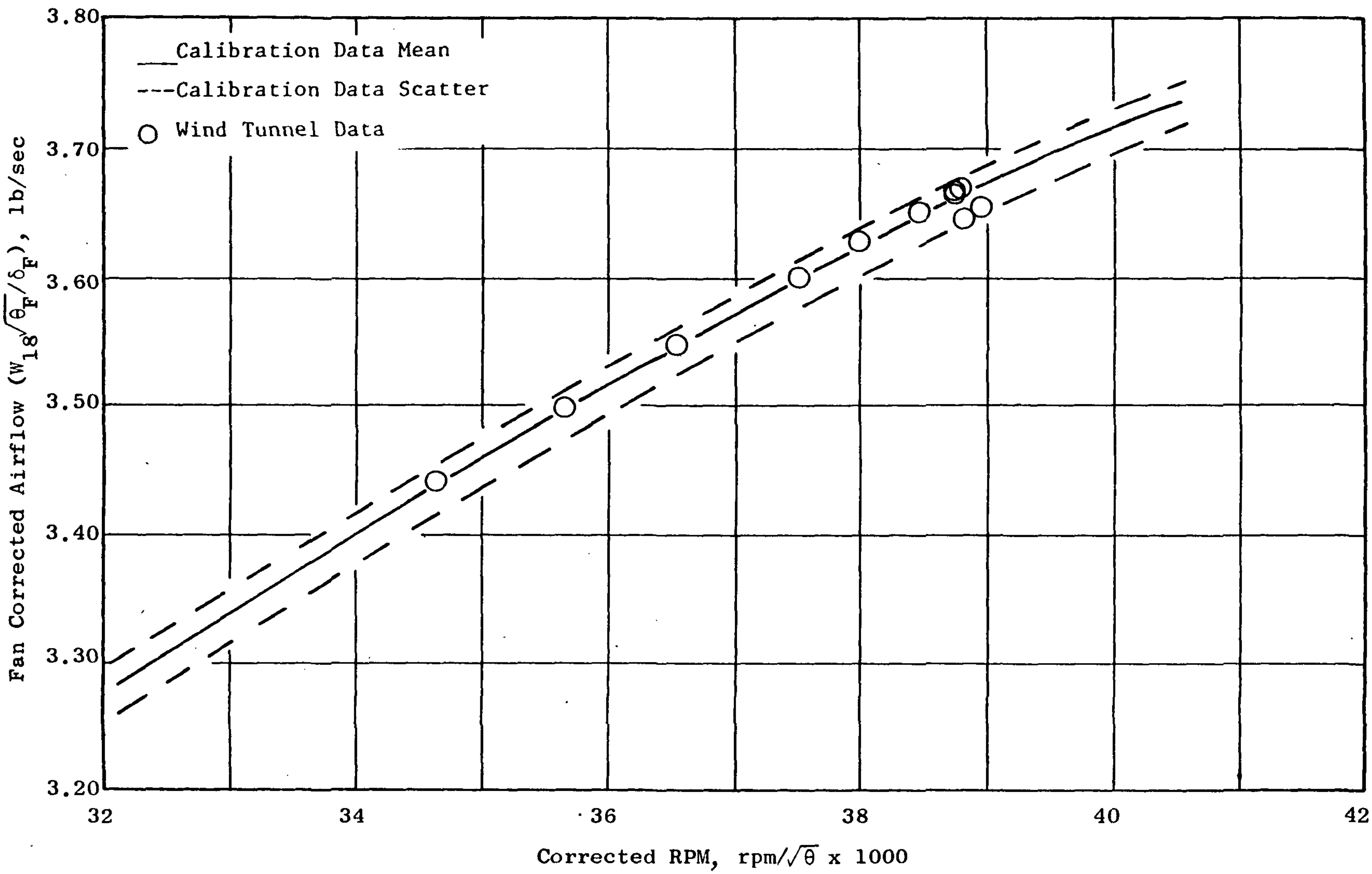

Figure 24d. Long Core Turbomachinery Characteristics.

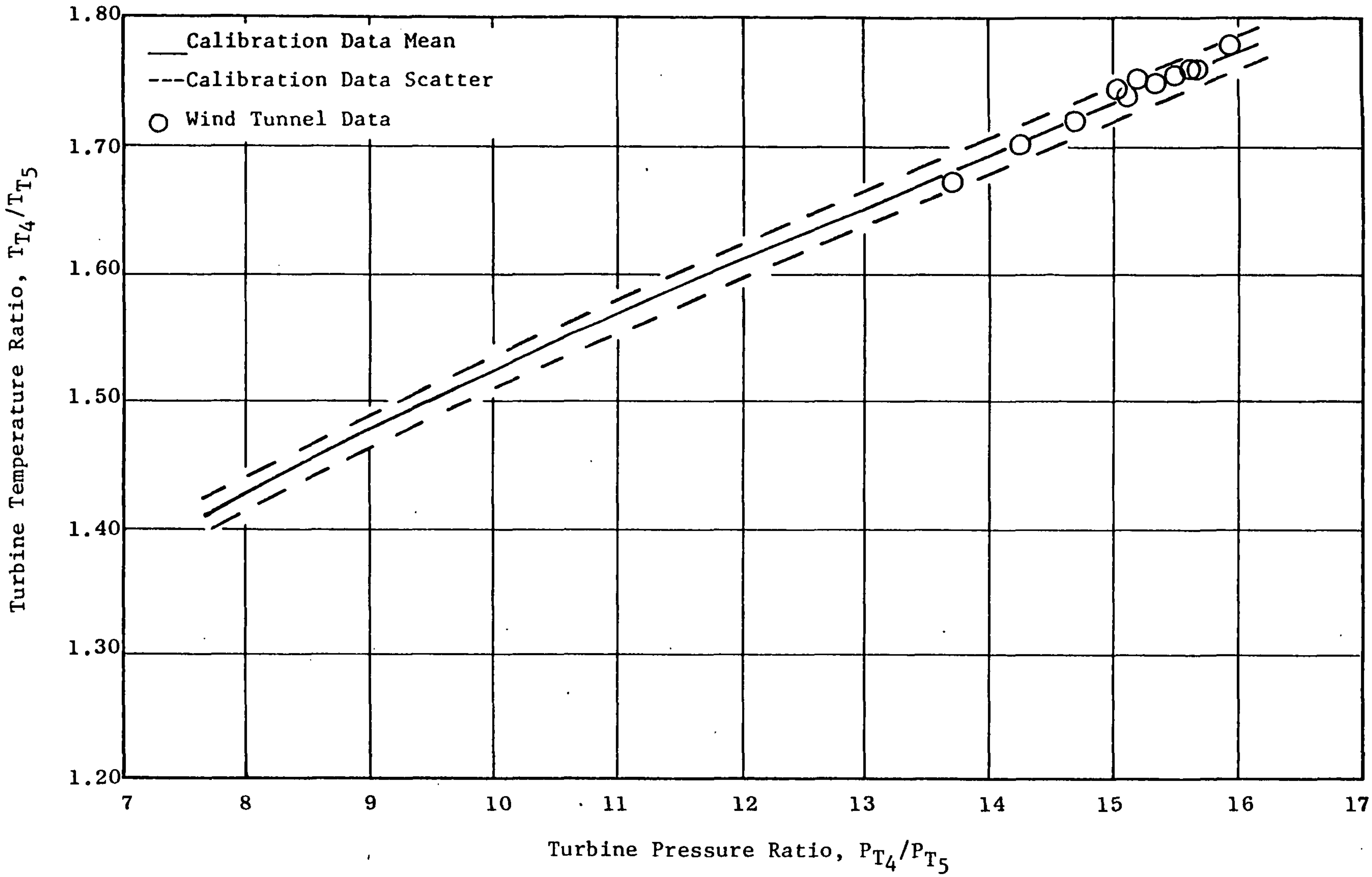

Figure 24e. Long Core Turbomachinery Characteristics.

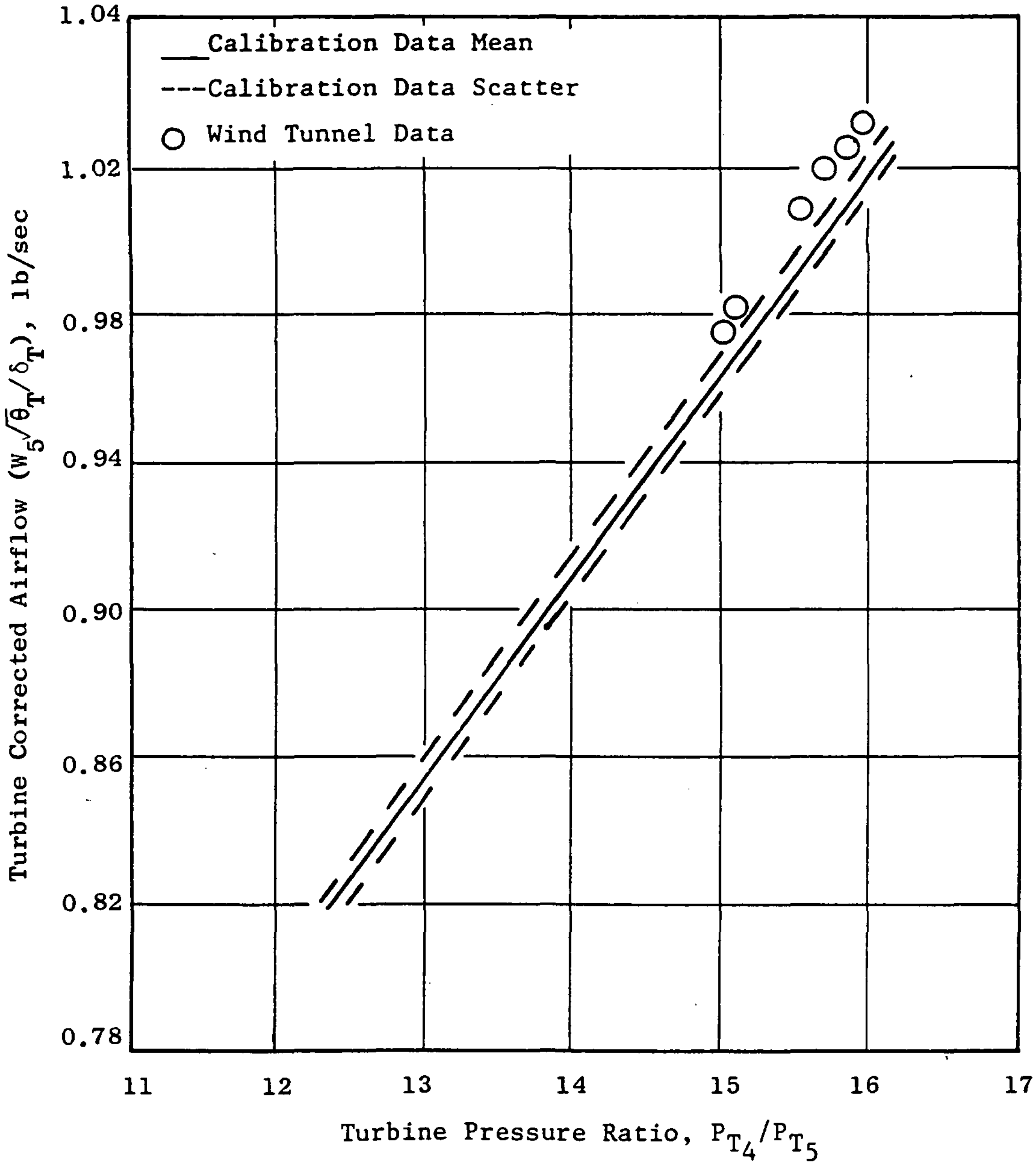

Figure 24f. Long Core Turbomachinery Characteristics.

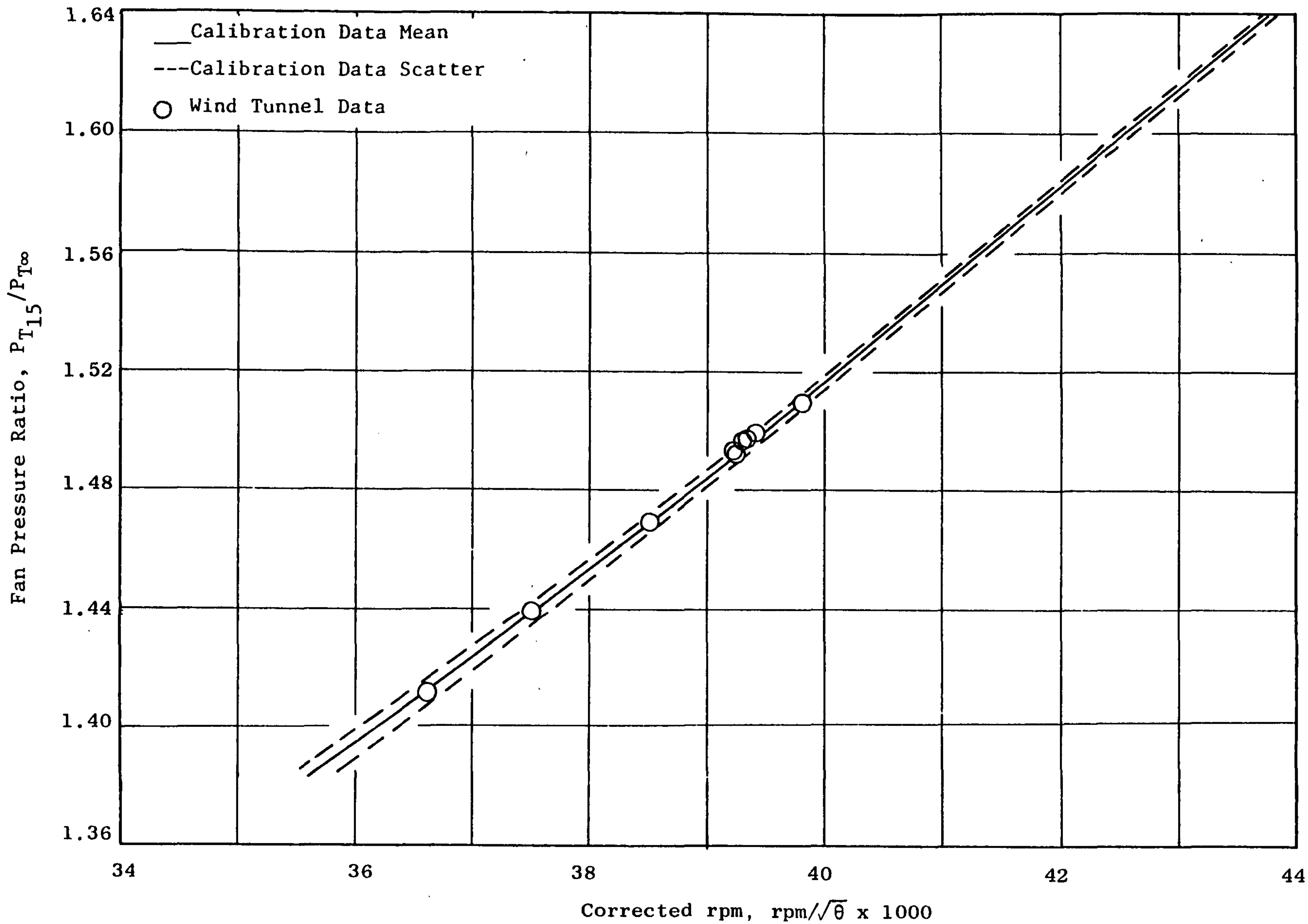

Figure 25a. LDMF Turbomachinery Characteristics.

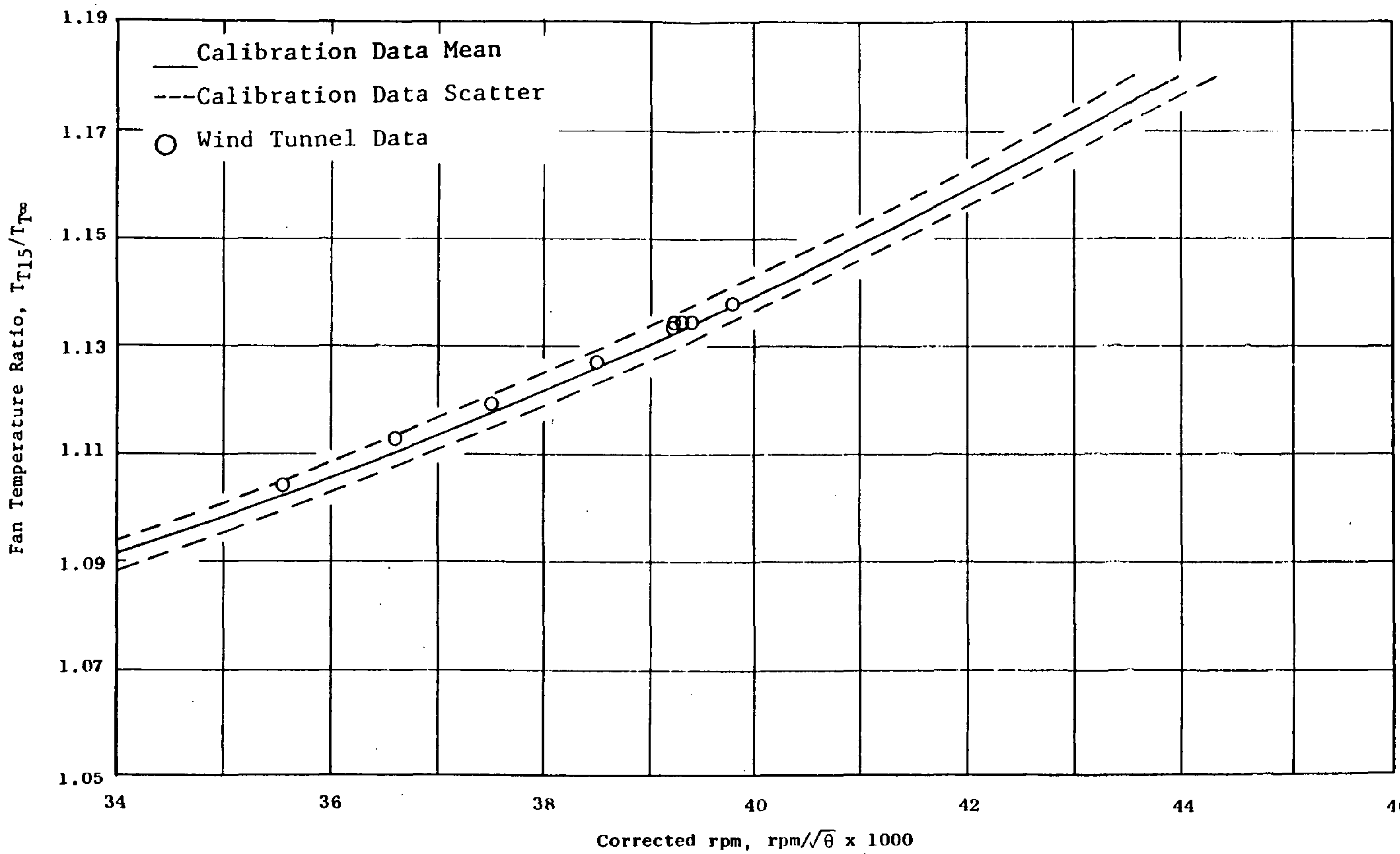

Figure 25b. LDMF Turbomachinery Characteristics.

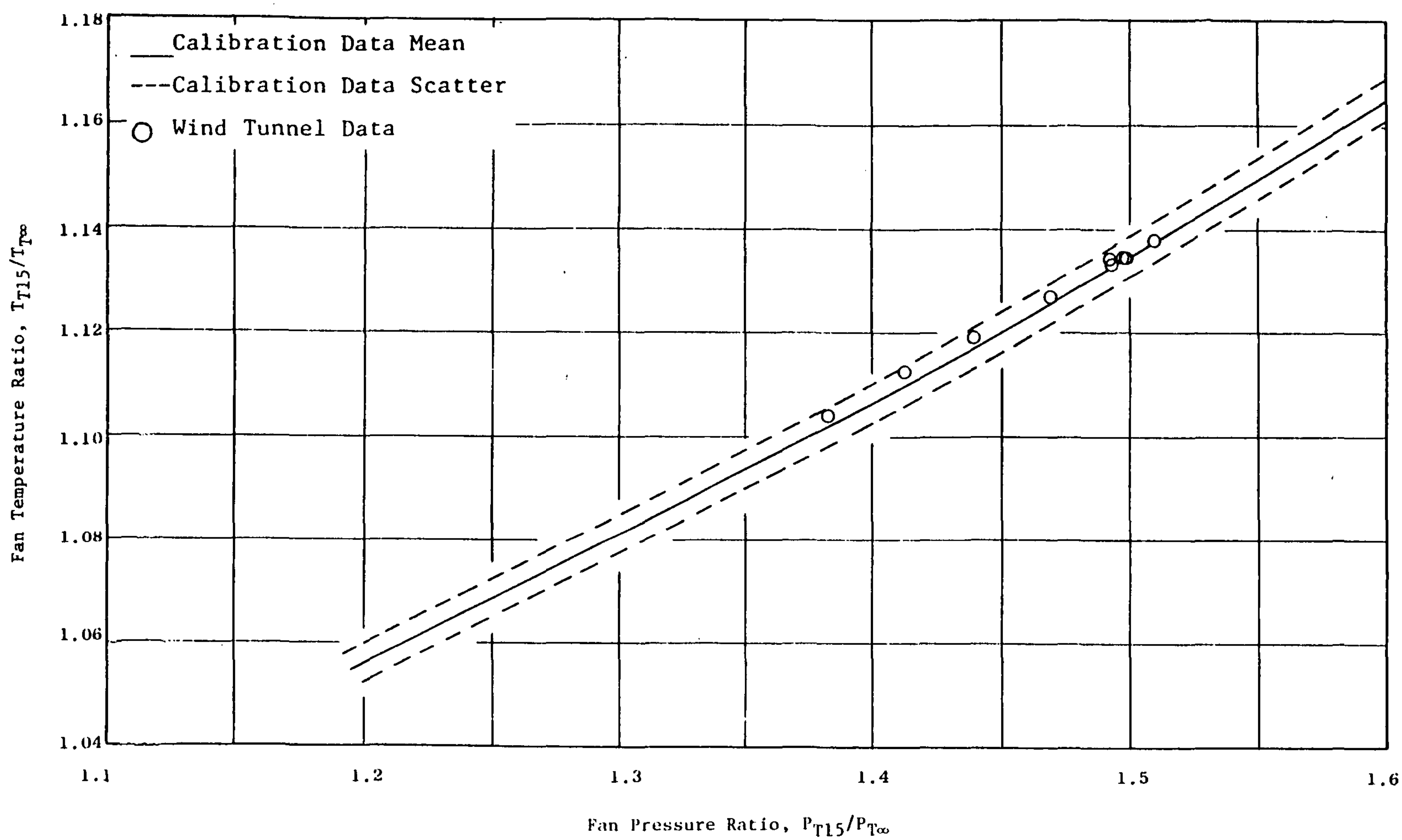

Figure 25c. LDMF Turbomachinery Characteristics.

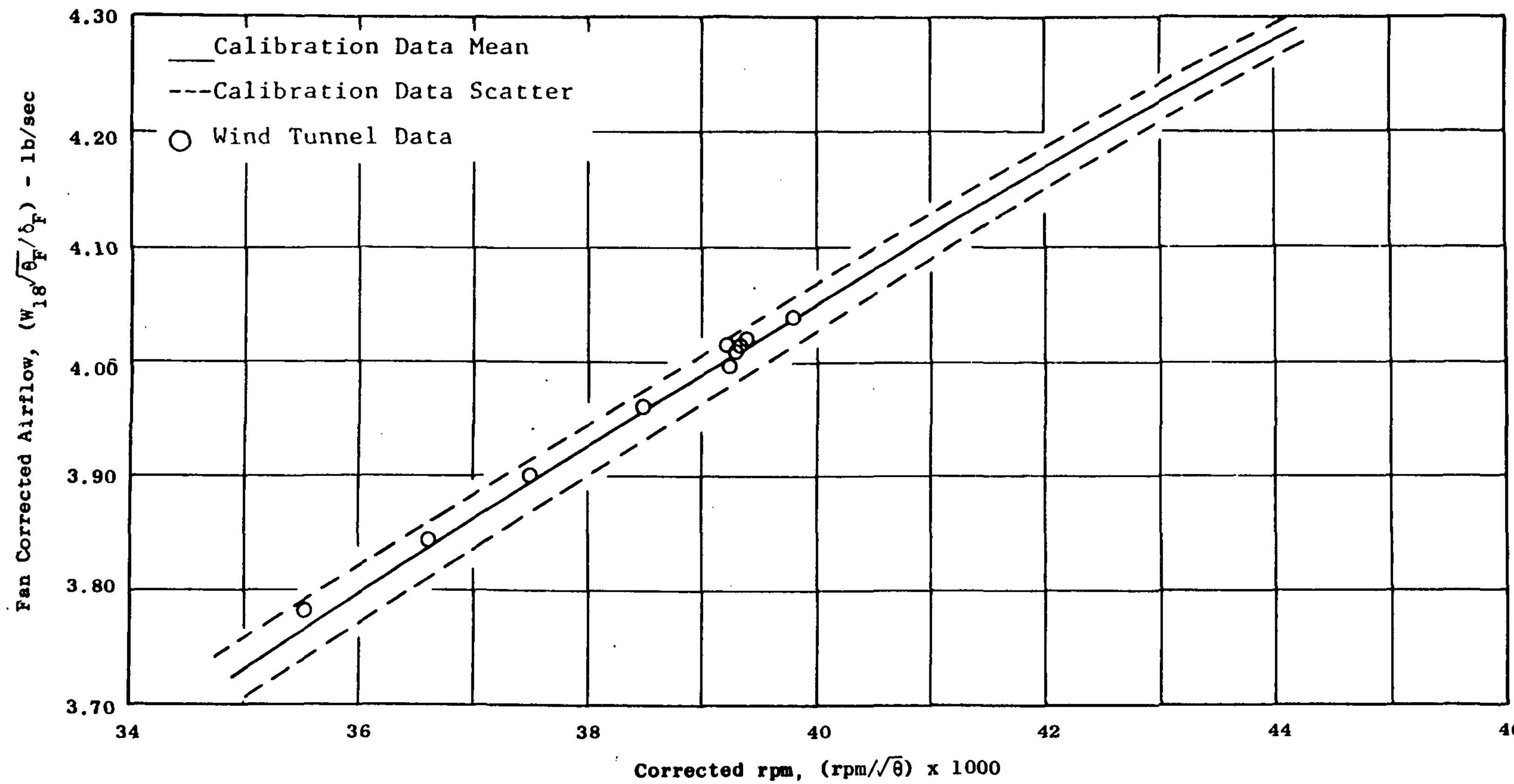

Figure 25d. LDMF Turbomachinery Characteristics.

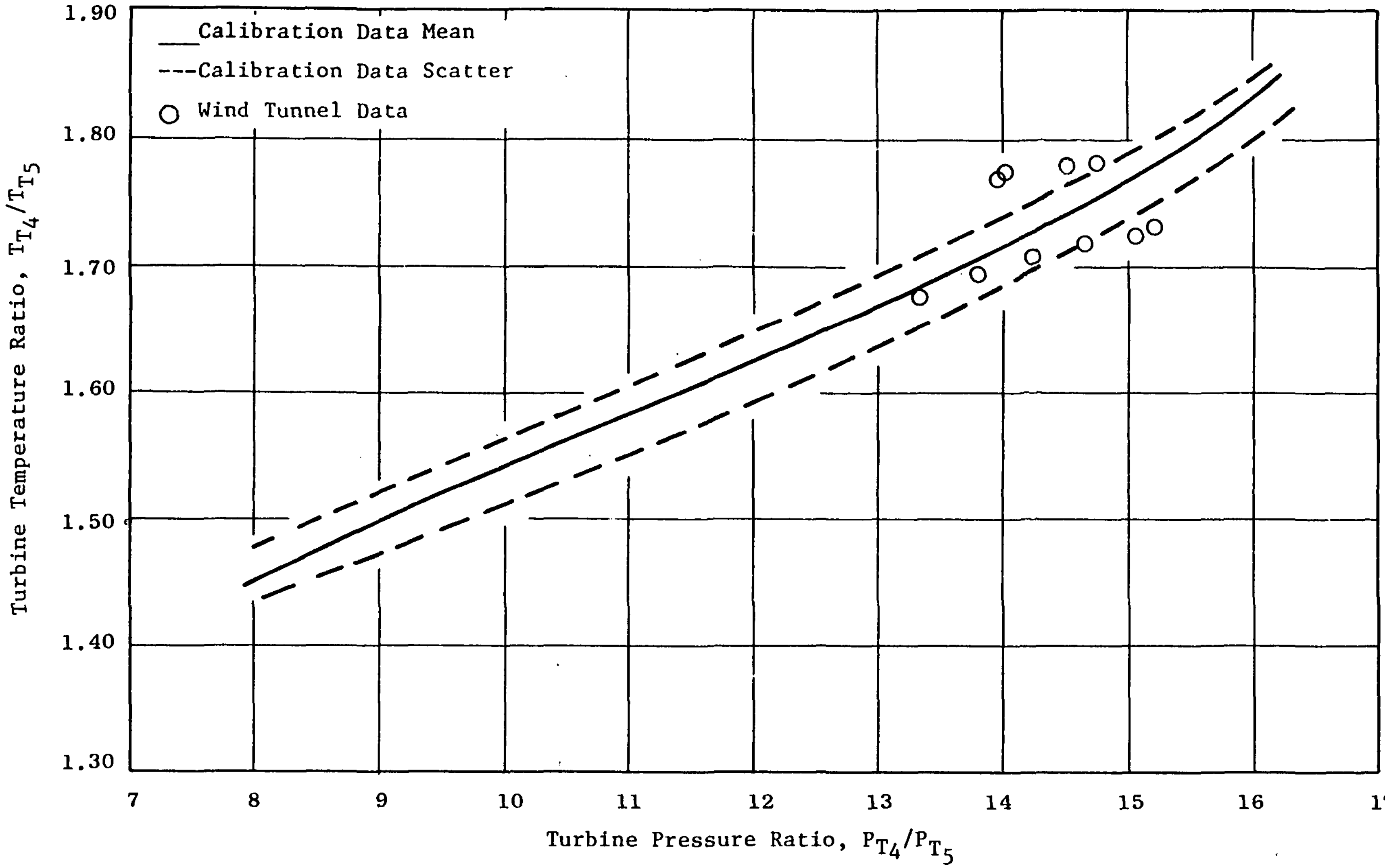

Figure 25e. LDMF Turbomachinery Characteristics.

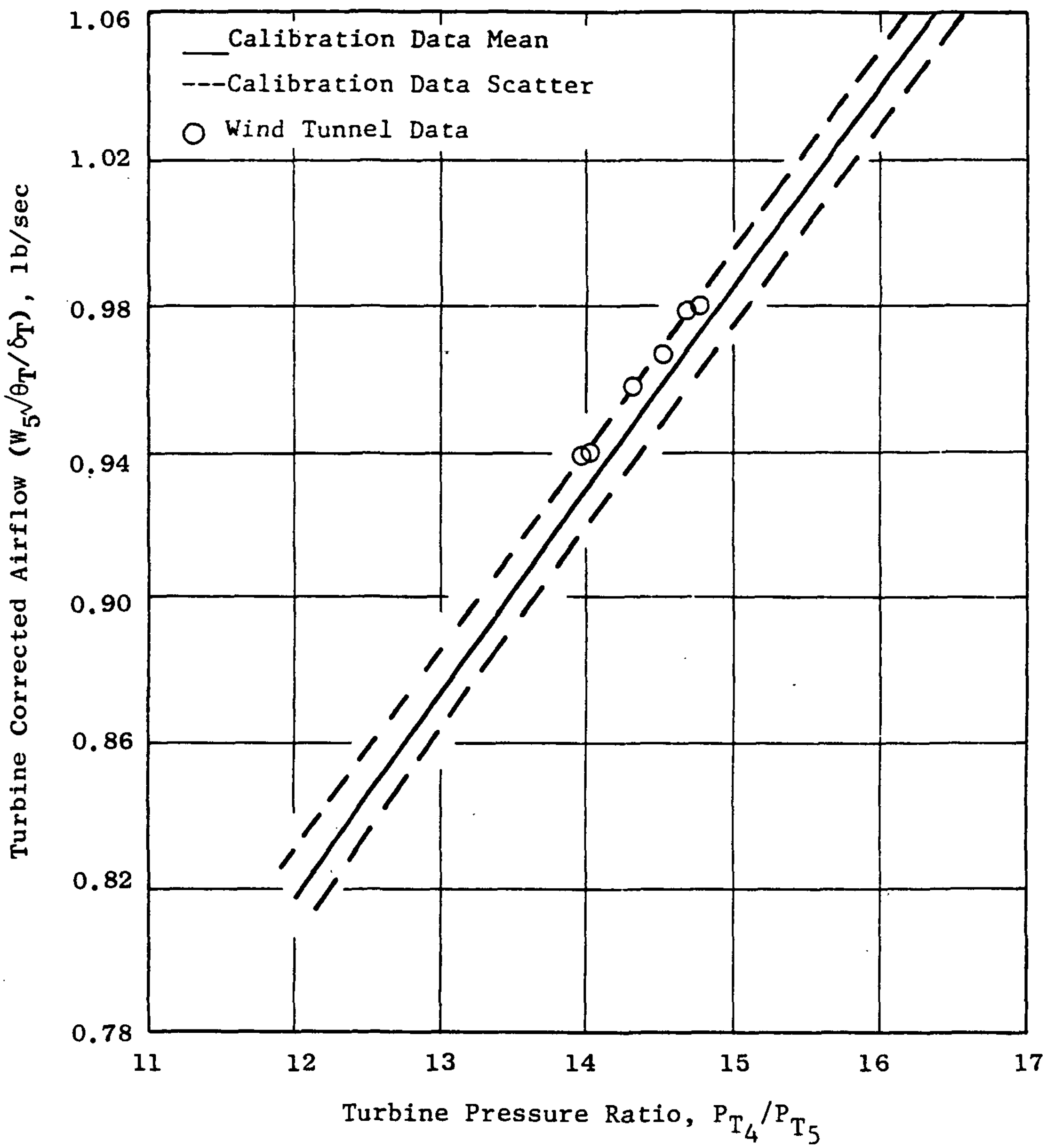

Figure 25f. LDMF Turbomachinery Characteristics.

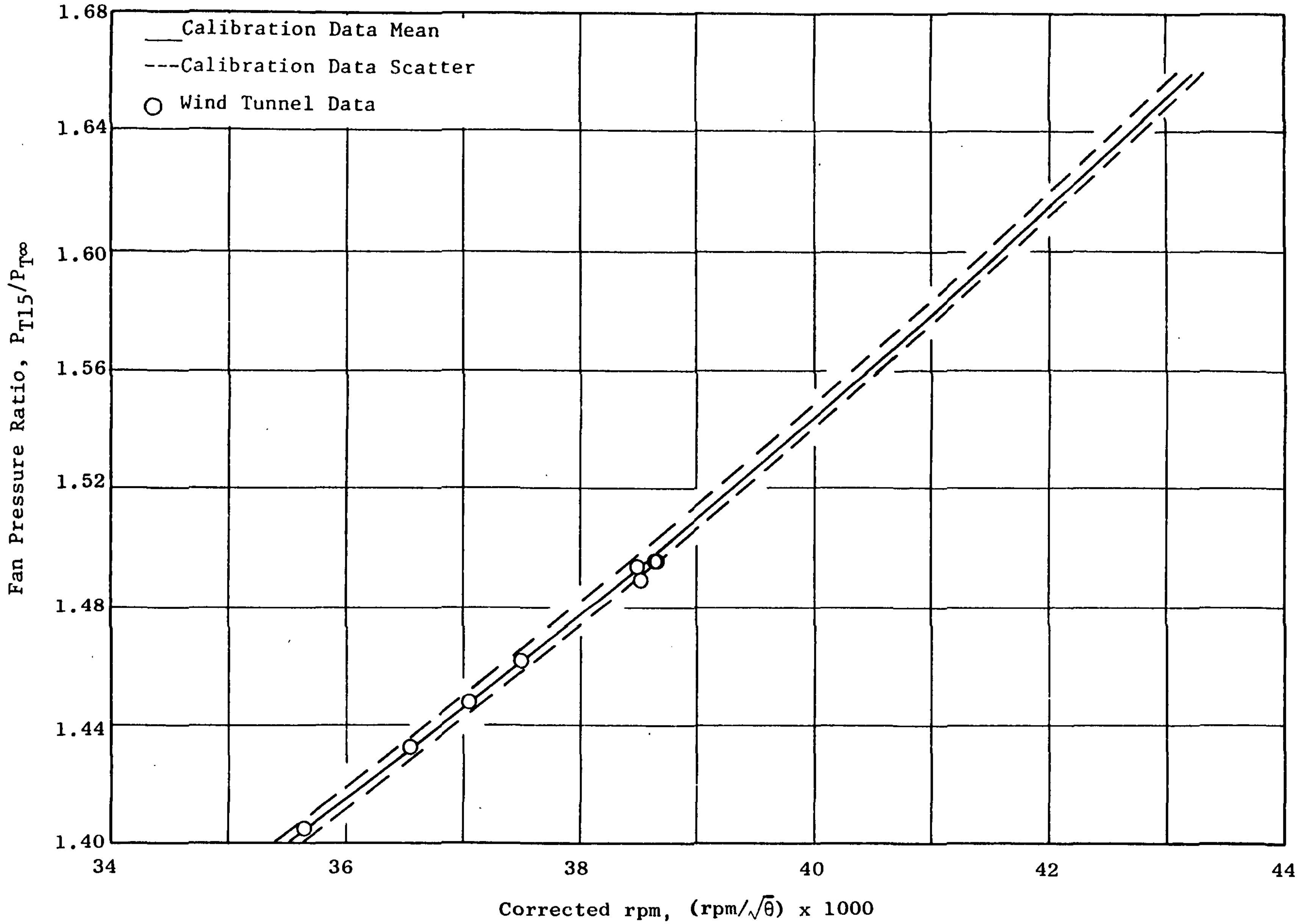

Figure 26a. E^3 Turbomachinery Characteristics.

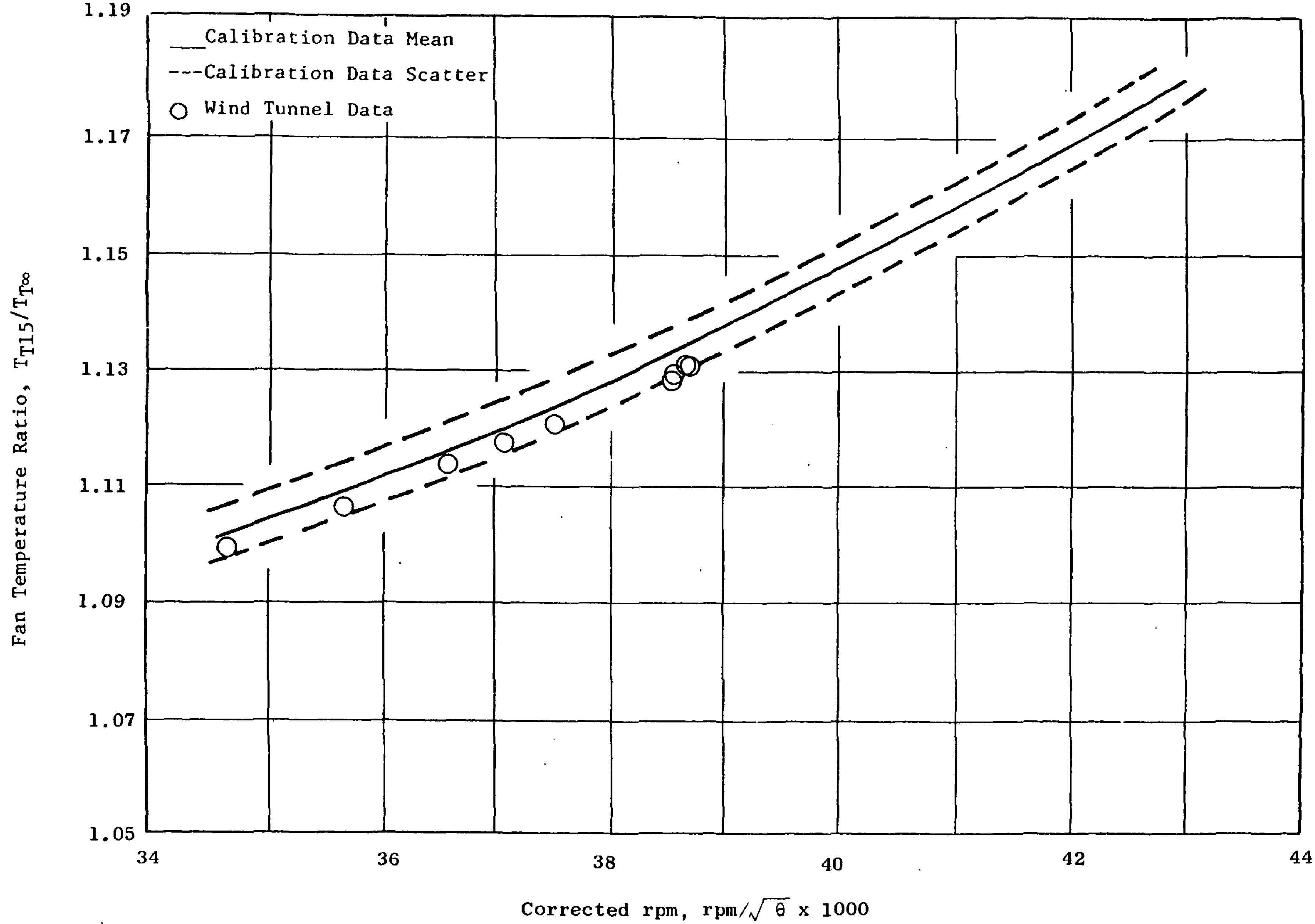

Figure 26b. E^3 Turbomachinery Characteristics.

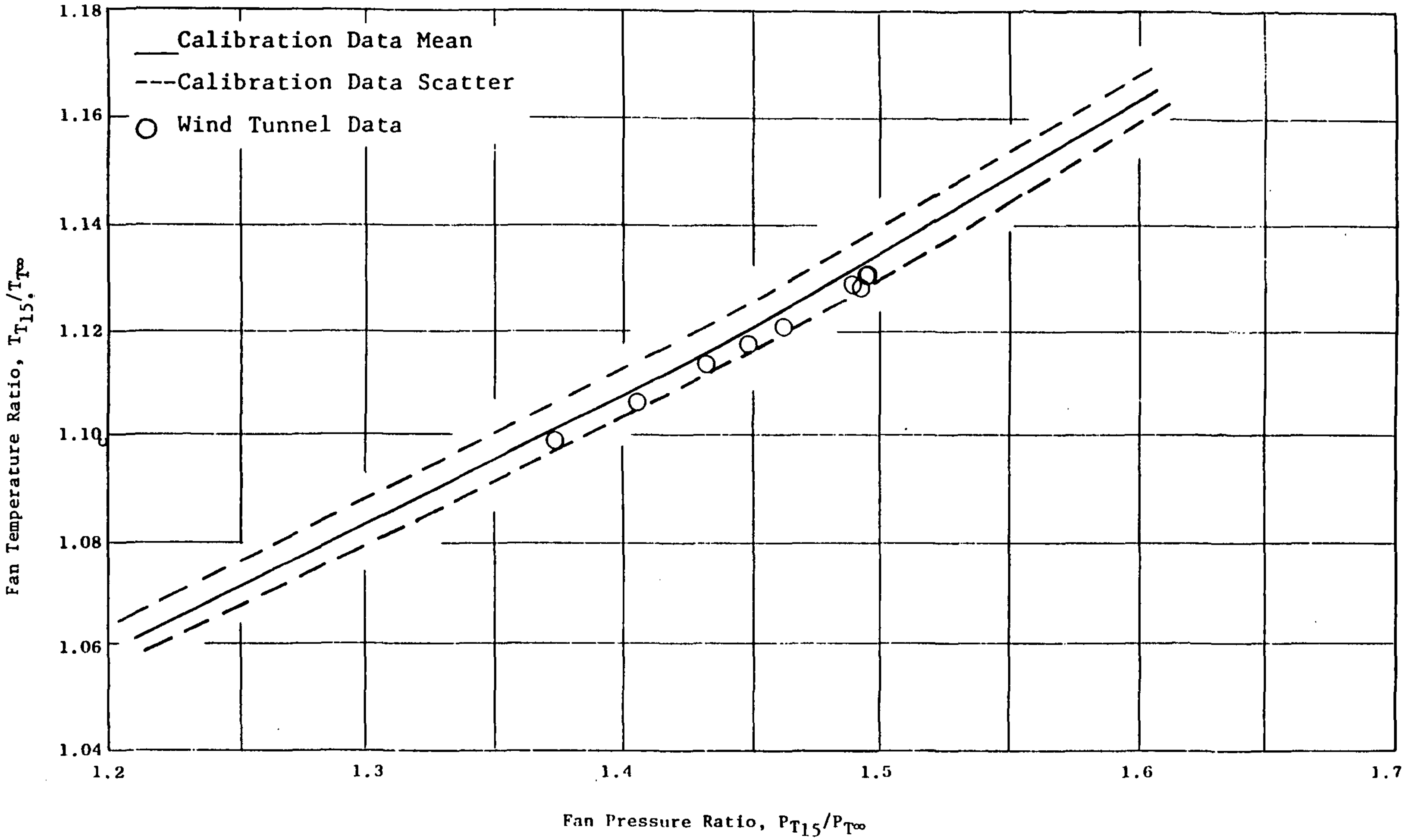

Figure 26c. E^3 Turbomachinery Characteristics.

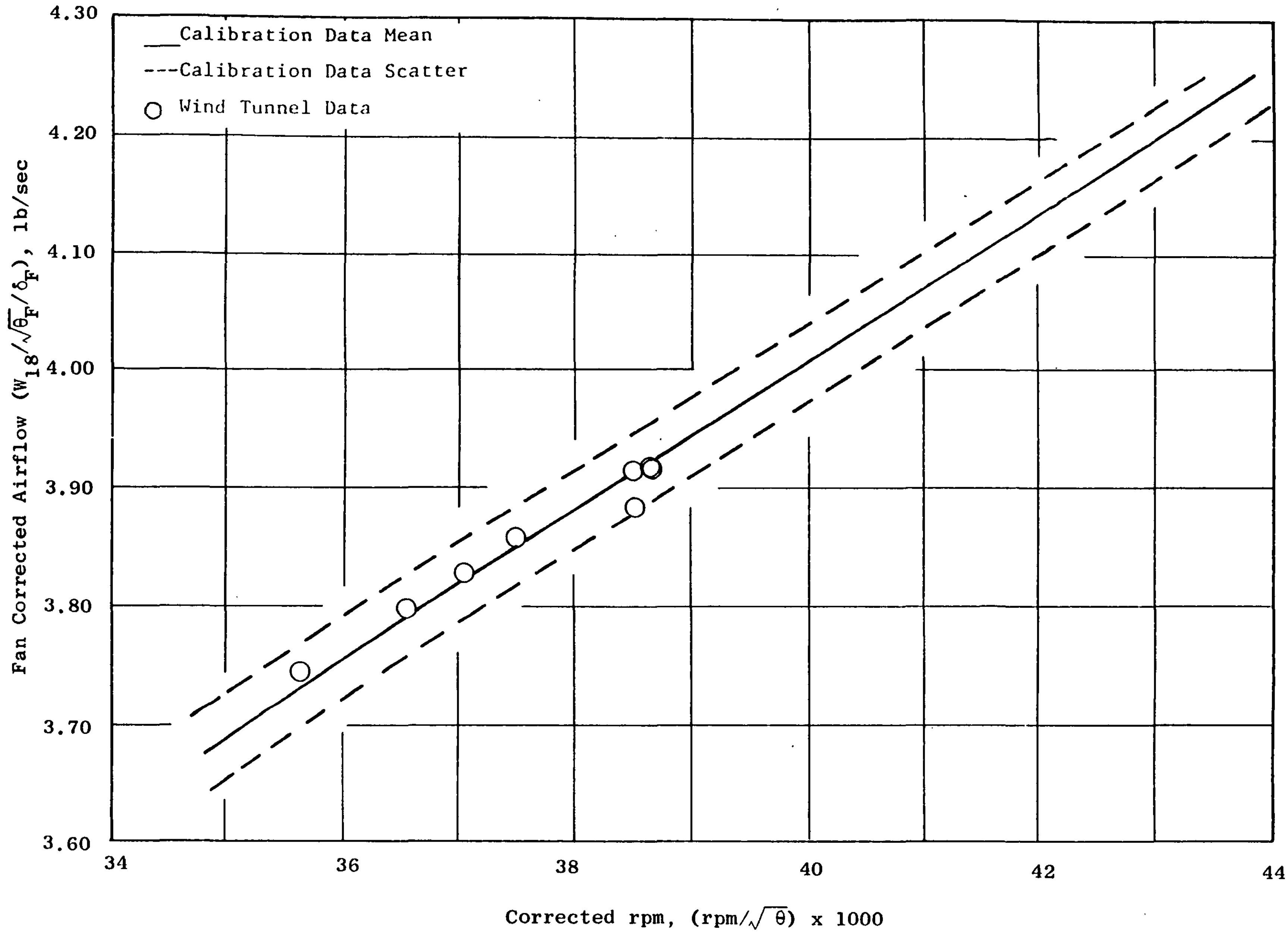

Figure 26d. E^3 Turbomachinery Characteristics.

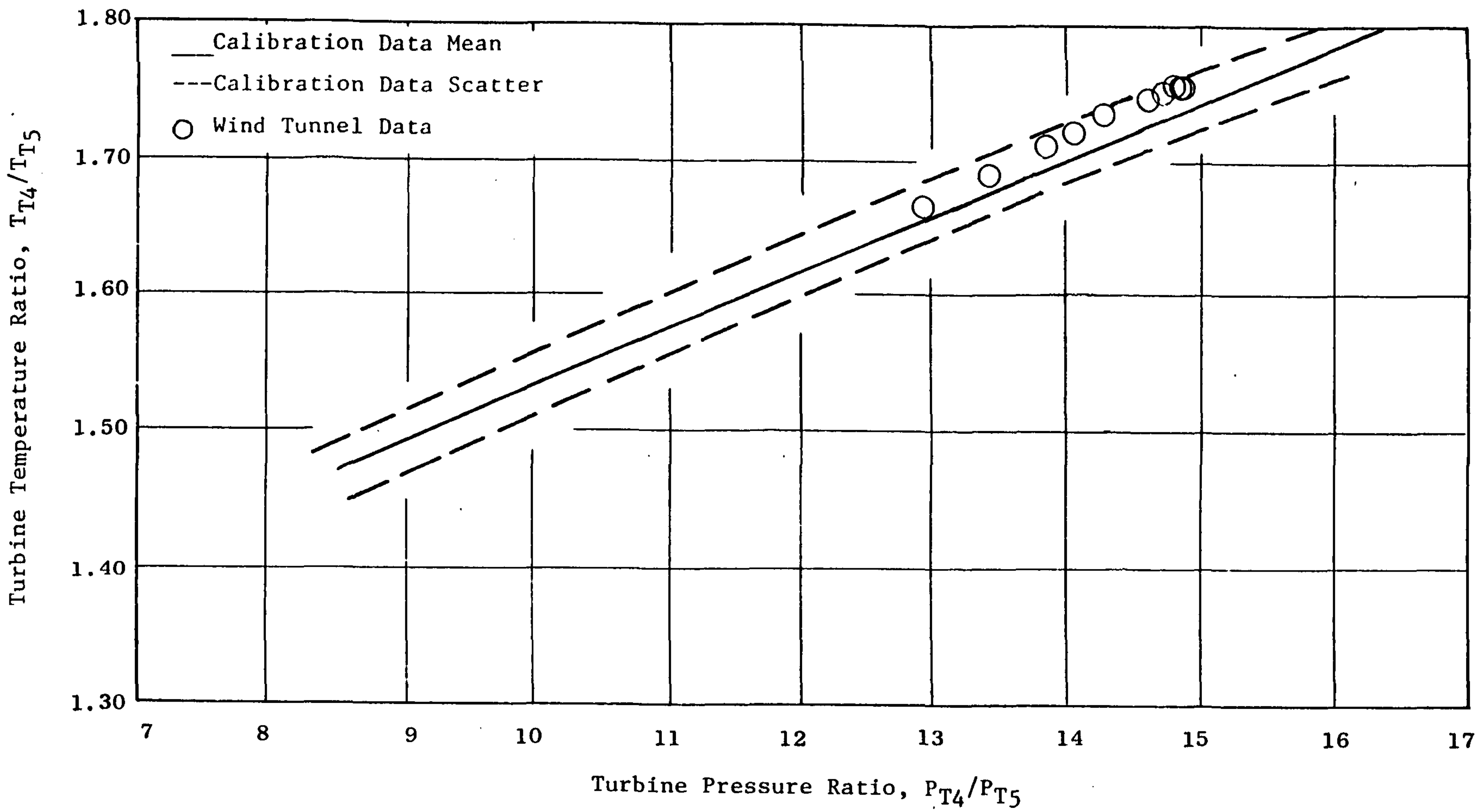

Figure 26e. E^3 Turbomachinery Characteristics.

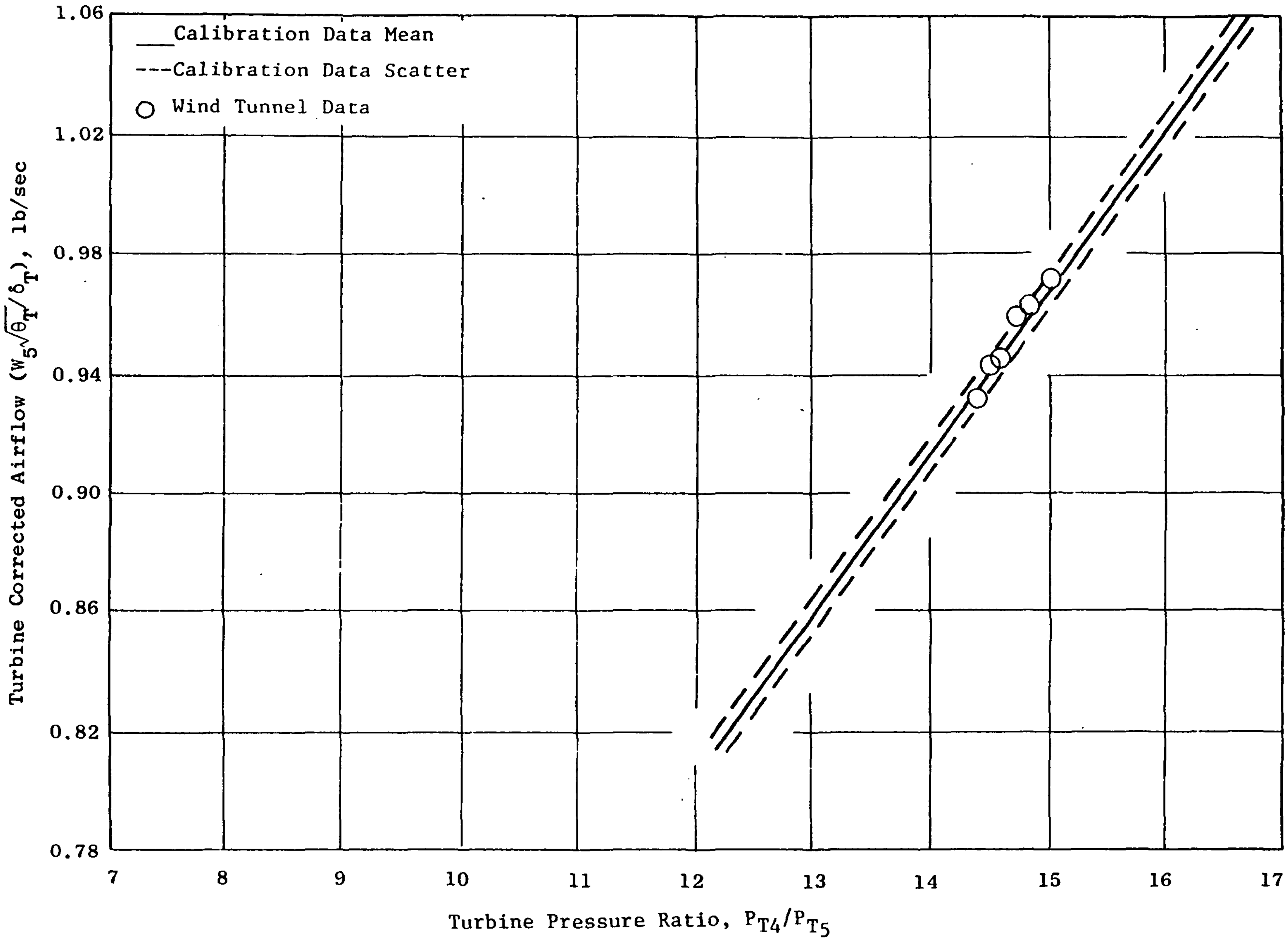

Figure 26f. E^3 Turbomachinery Characteristics.

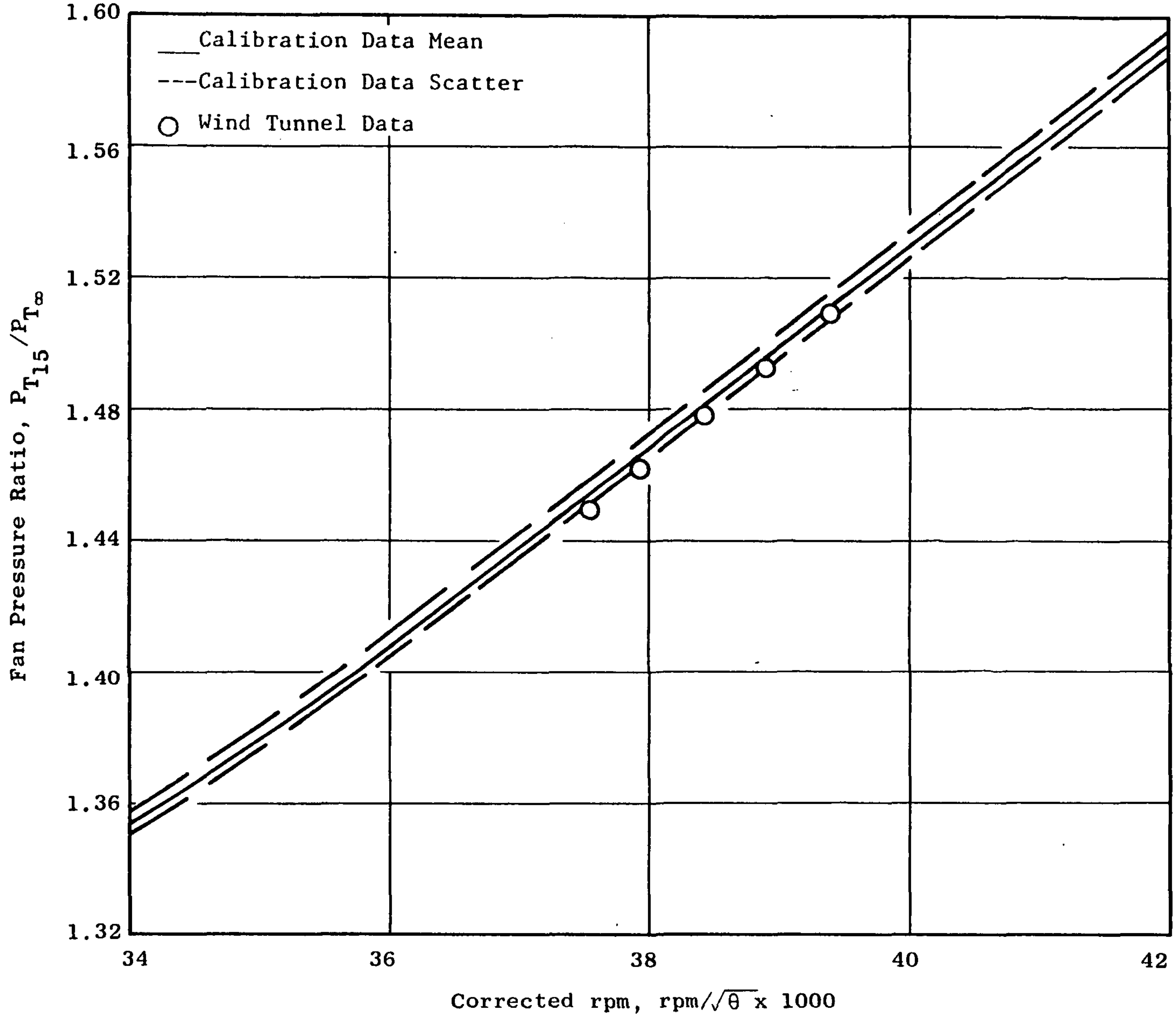

Figure 27a. E^3 Extended Nacelle Turbomachinery Characteristics.

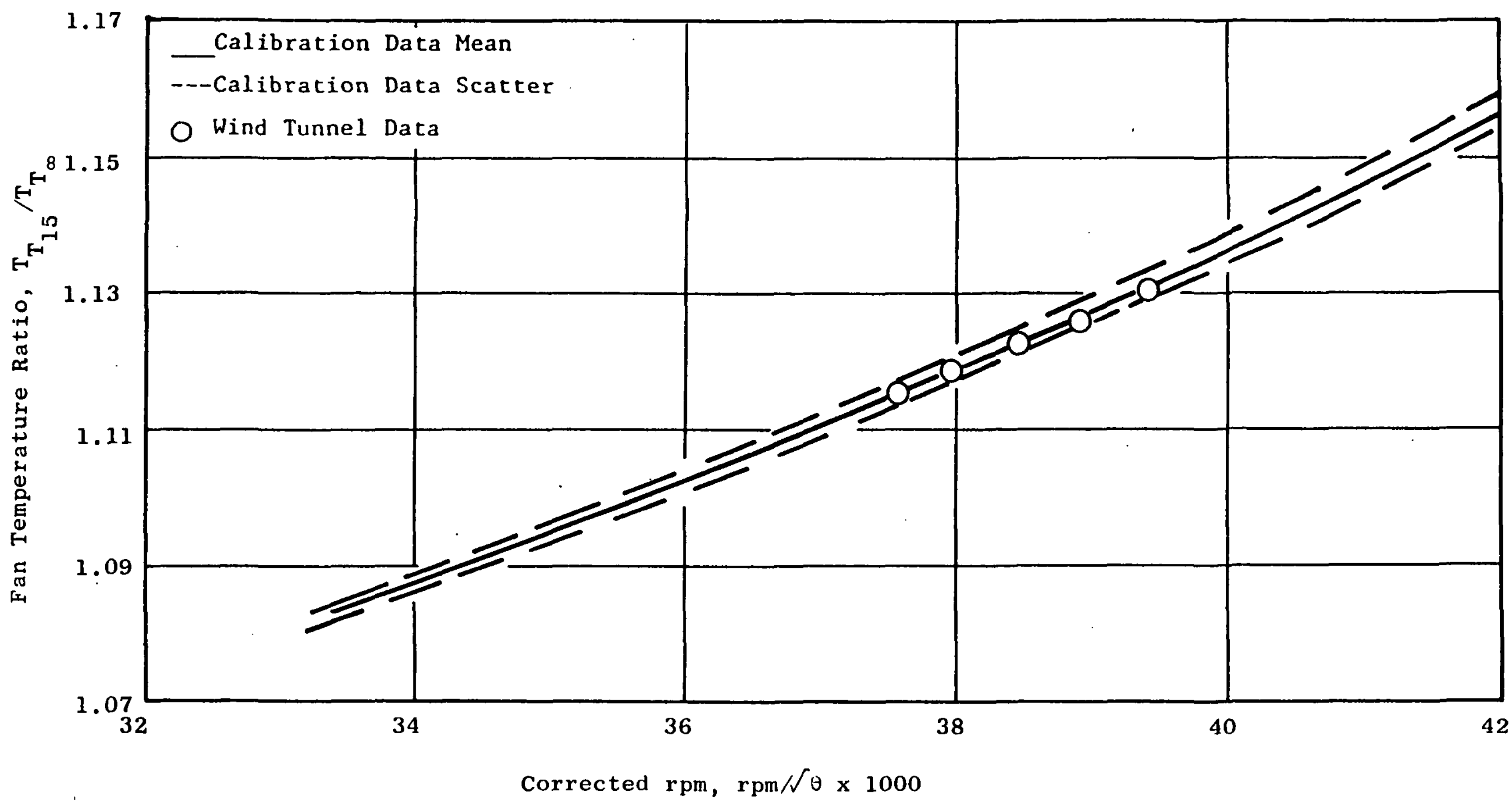

Figure 27b. E^3 Extended Nacelle Turbomachinery Characteristics.

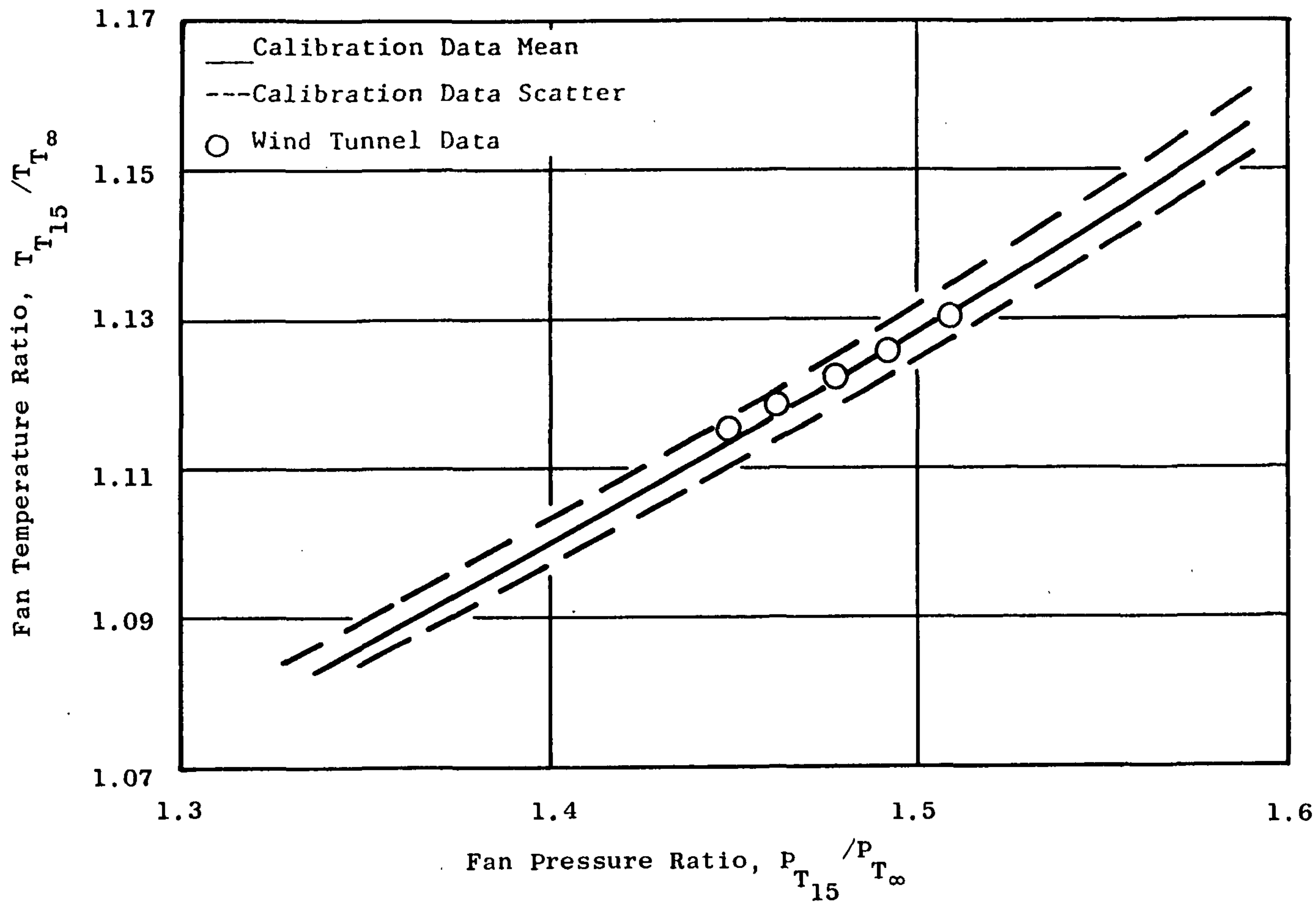

Figure 27c. Extended Nacelle Turbomachinery Characteristics.

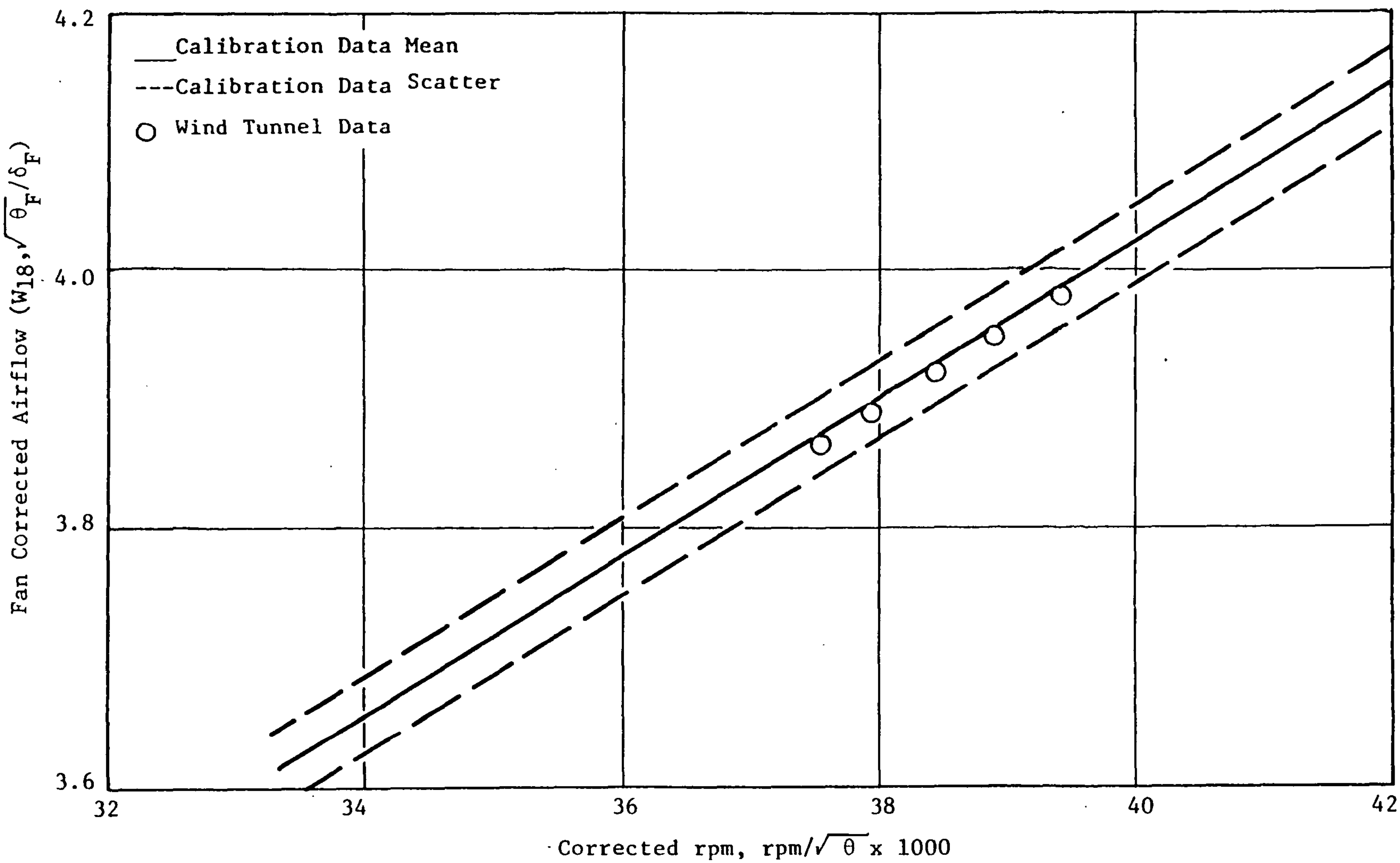

Figure 27d. E^3 Extended Nacelle Turbomachinery Characteristics.

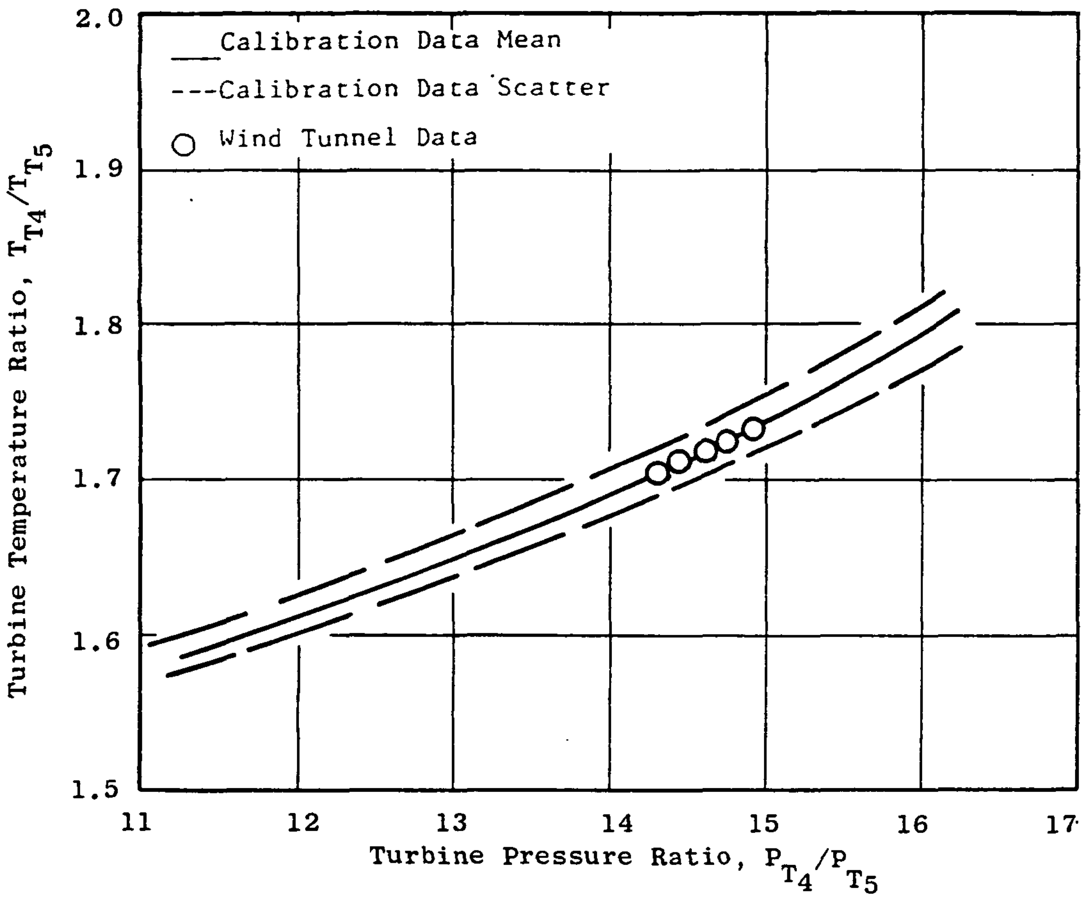

Figure 27e. E^3 Extended Nacelle Turbomachinery Characteristics.

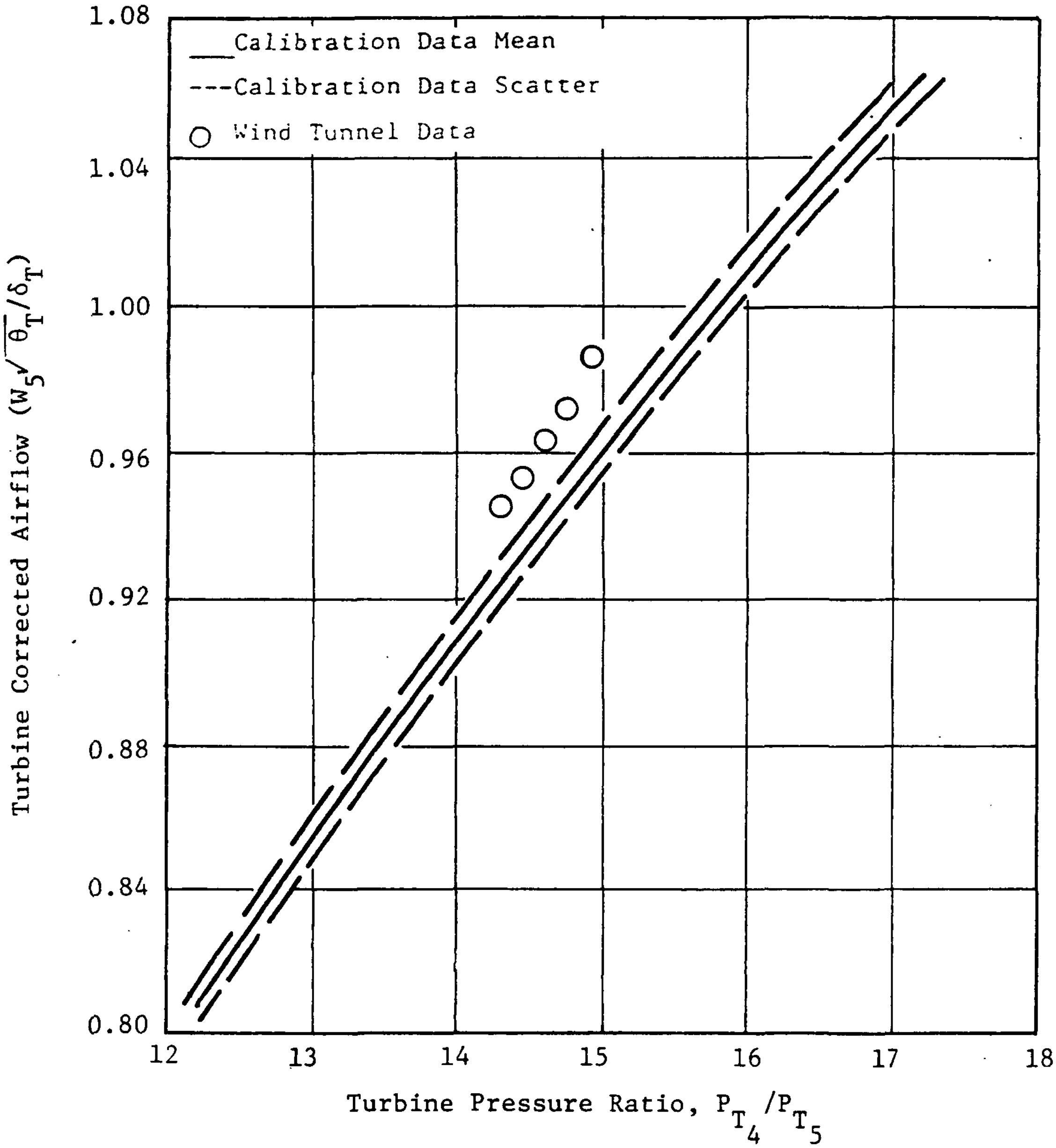

Figure 27f. E^3 Extended Nacelle Turbomachinery Characteristics.

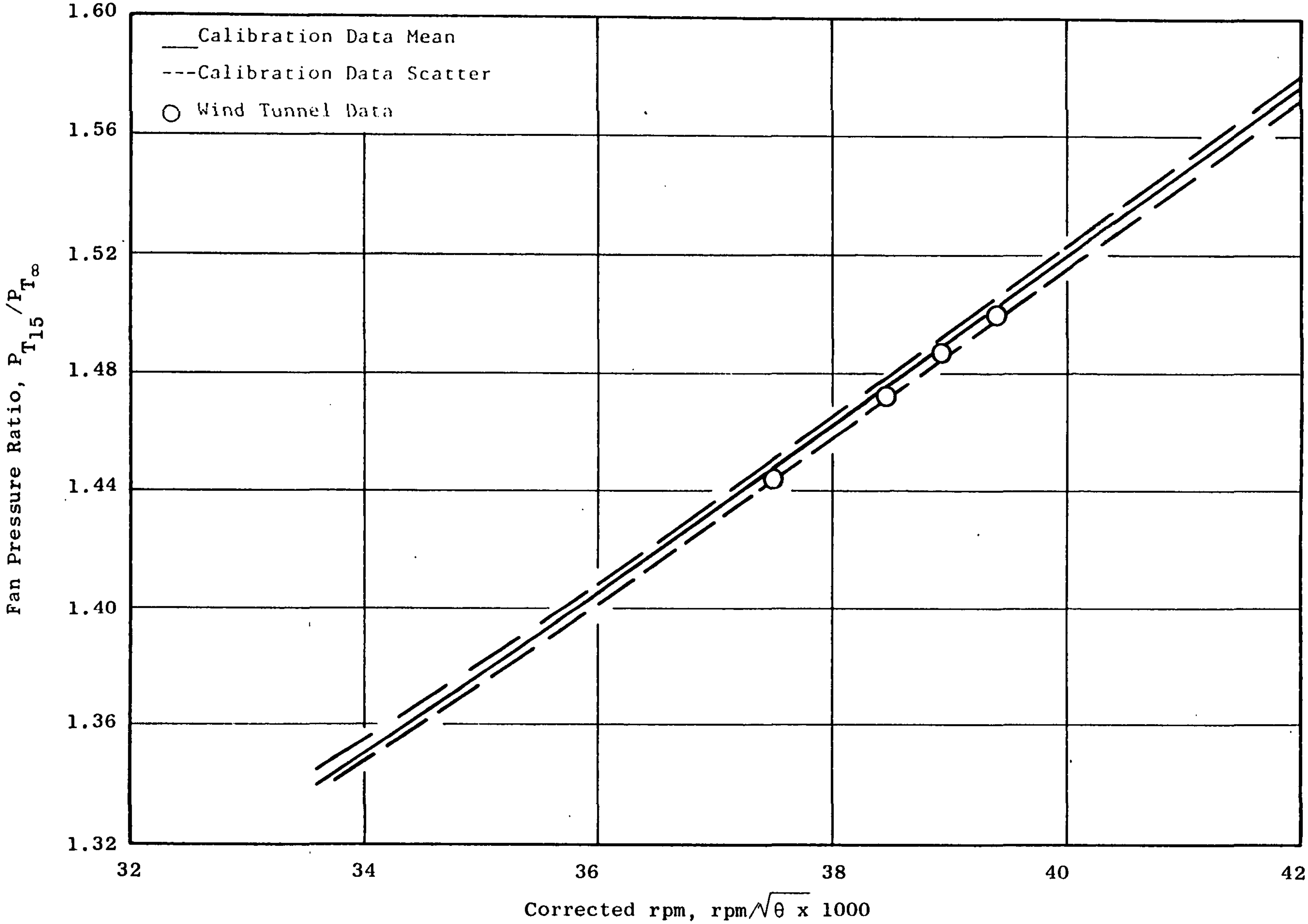

Figure 28a. E^3 Separate Flow Turbomachinery Characteristics.

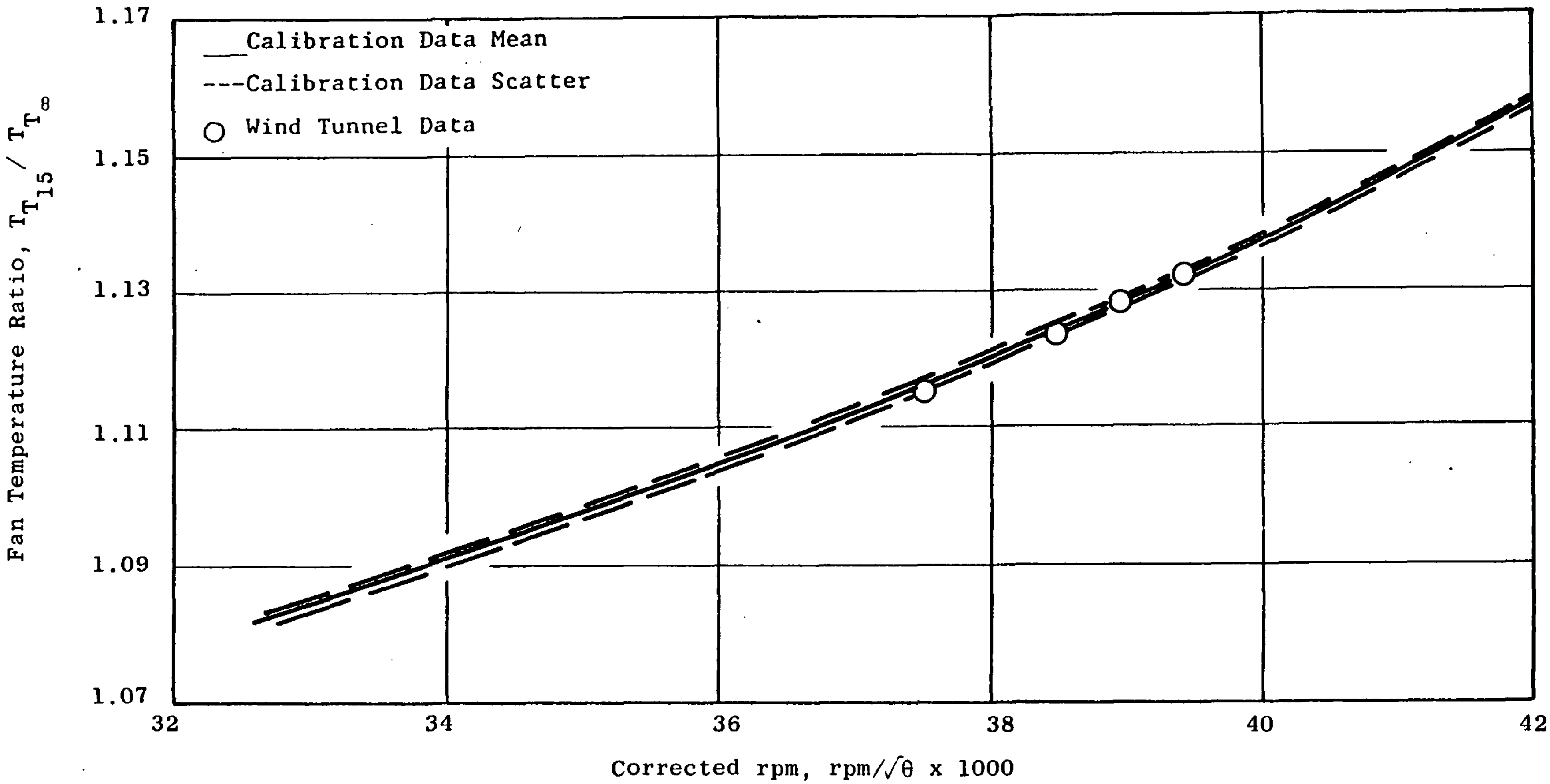

Figure 28b. E^3 Separate Flow Turbomachinery Characteristics.

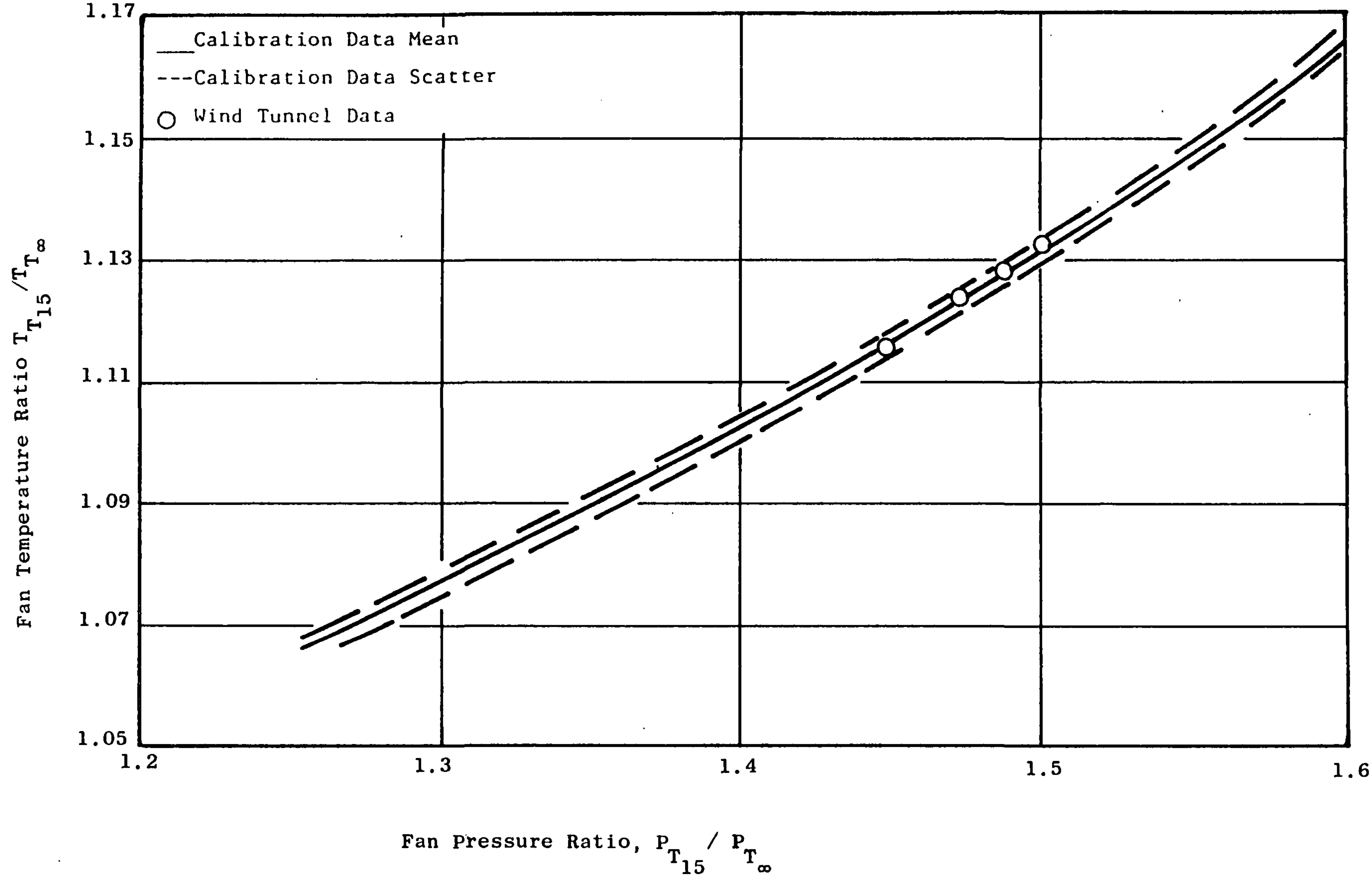

Figure 28c. Separate Flow Turbomachinery Characteristics.

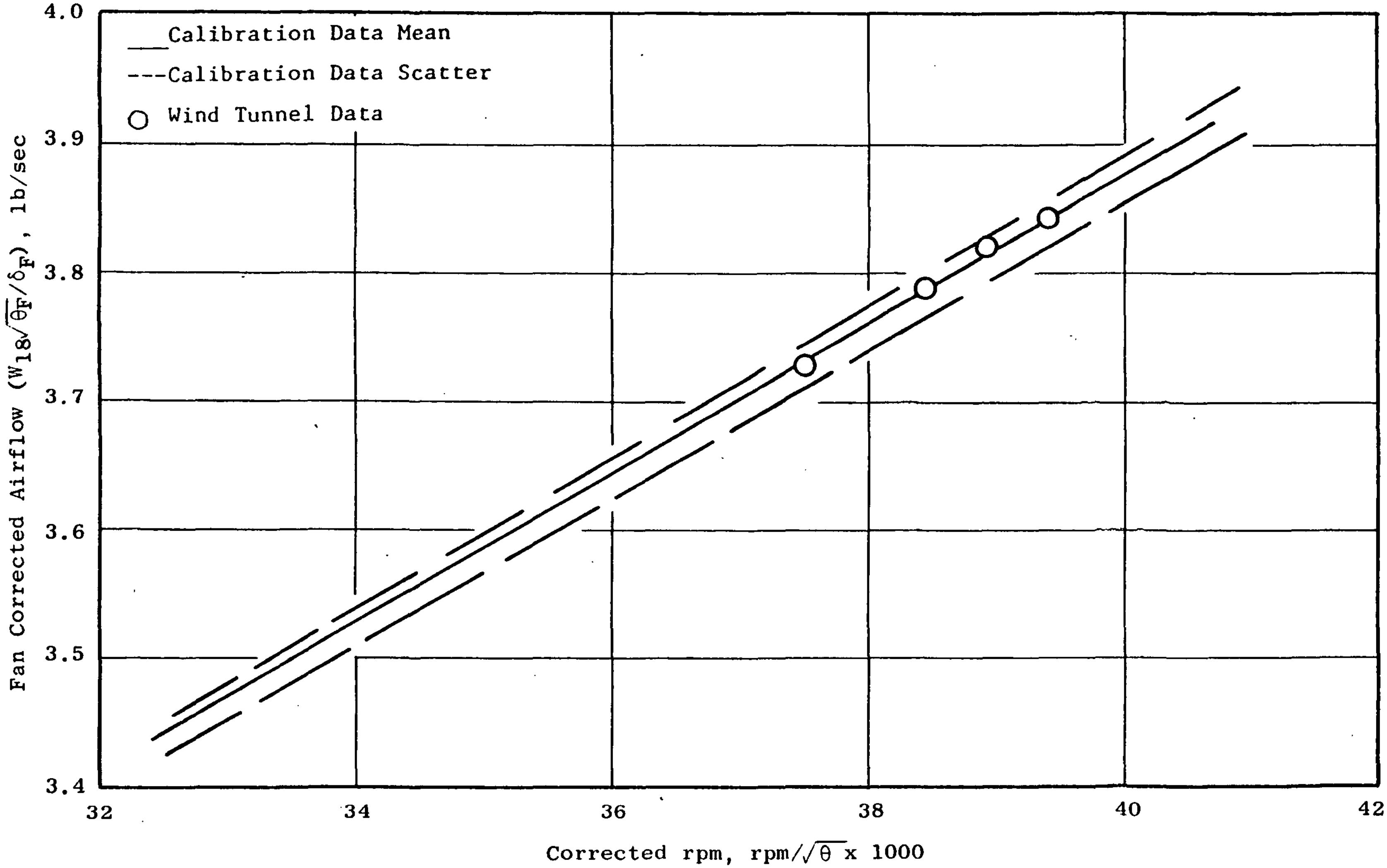

Figure 28d. E^3 Separate Flow Turbomachinery Characteristics.

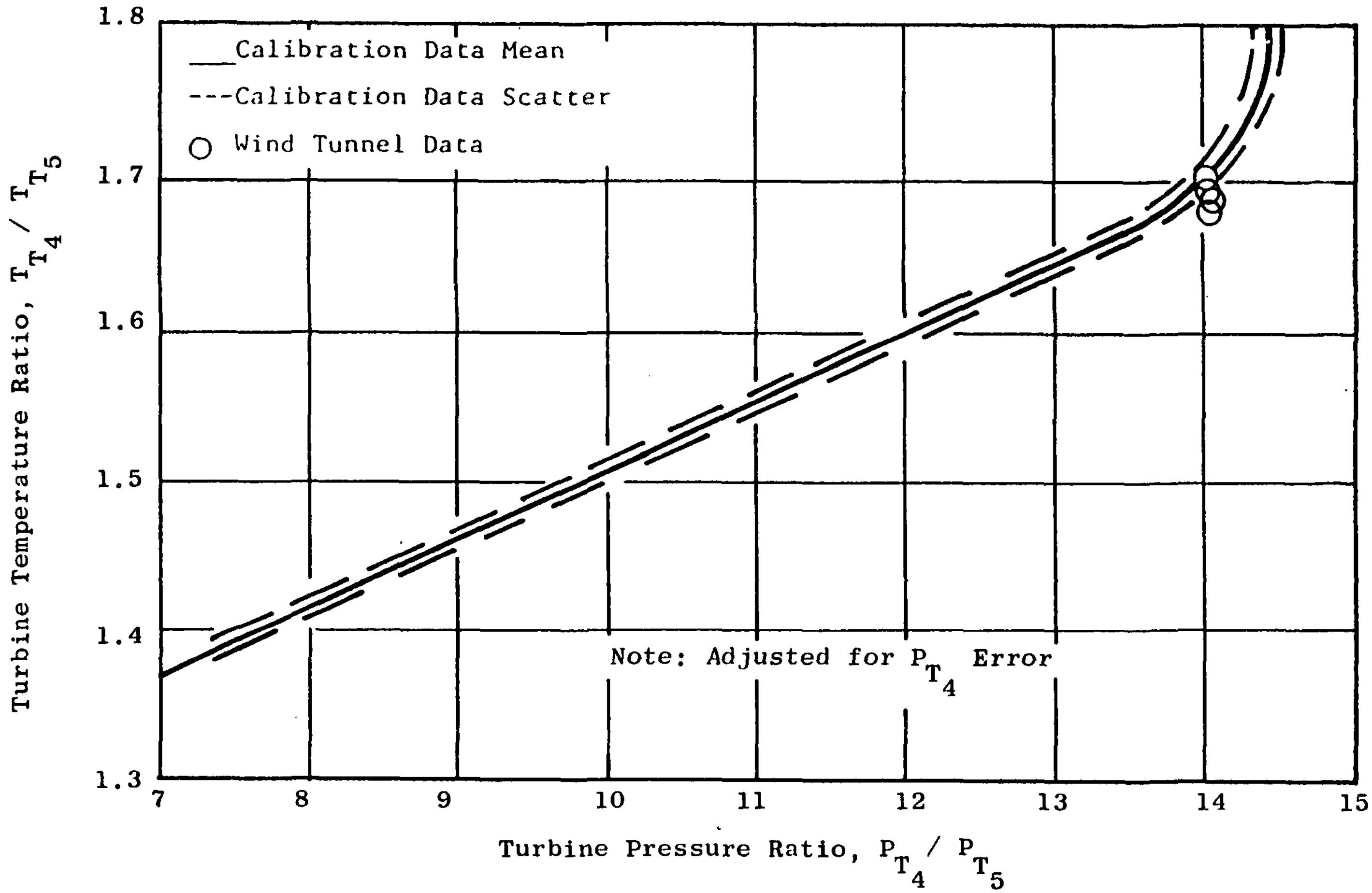

Figure 28e. E^3 Separate Flow Thromachinery Characteristics.

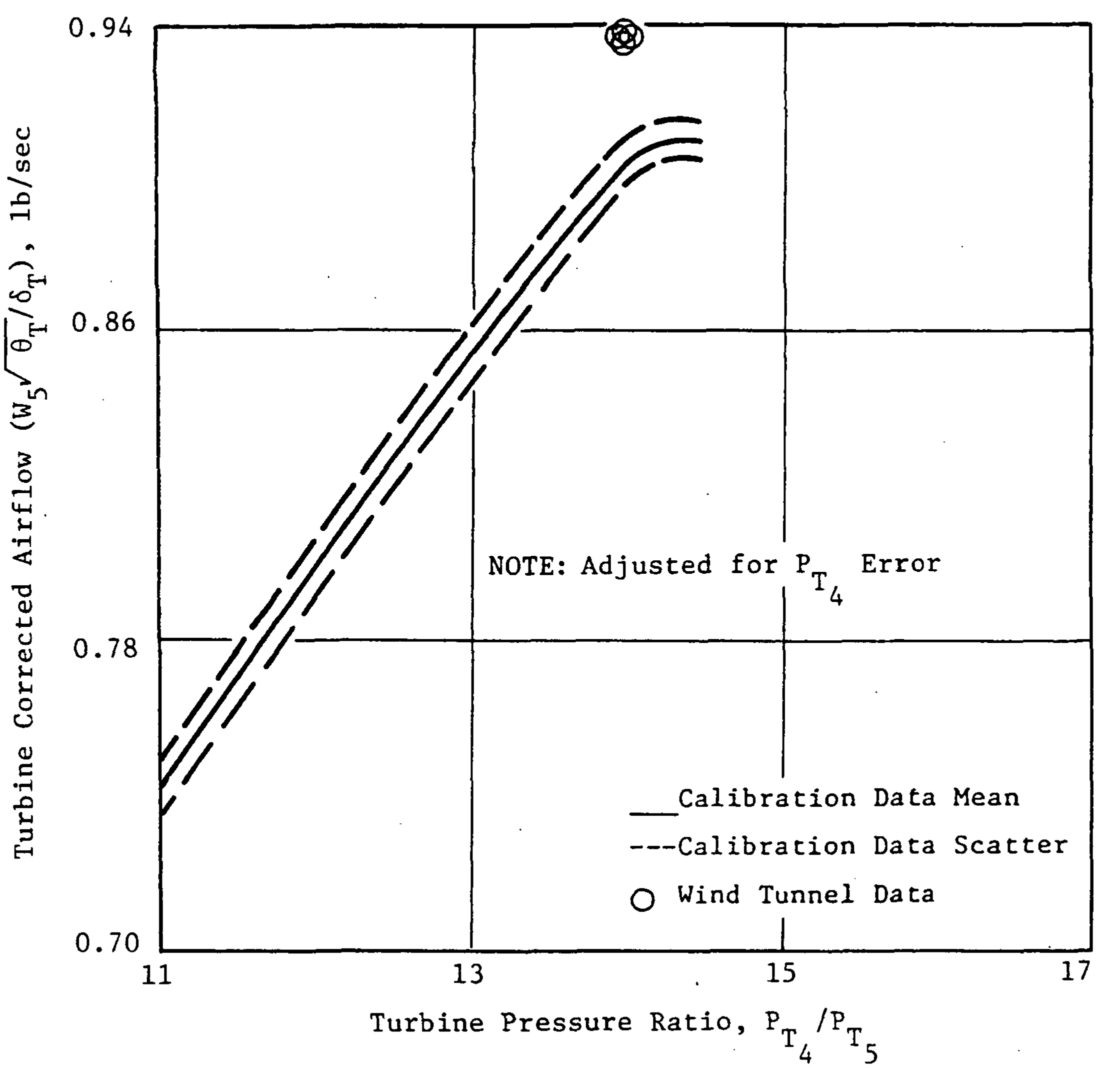

Figure 28f. E^3 Separate Flow Turbomachinery Characteristics.

The core weight flow measurement in the wind tunnel test is high relative to the calibration test (Figures 23f, 24f, 25f, 27f, and 28f).

The wind tunnel data differ as follows:

- CF6-50 Short Core - core weight flow high by 3.0%
- CF6-50 Long Core - core weight flow high by 1.5%
- CF65-50 LDMF - core weight flow high by 1.0%
- E^3 extended - core weight flow high by 3.0%
- E^3 separate flow - weight flow high by 3.0%.

A possible cause for this error could be a bias in the wind tunnel facility flow measuring system.

The fan rake total pressure profiles from the calibration test were normalized and plotted for one condition (M = 0.82, Fan Pressure Ratio = 1.5) to be used in checking the fan rake operation during the wind tunnel test. In addition, these profiles were used as dummy readings in case of a failure of a rake tube during wind tunnel operation. Figures 29 through 34 show the calibration profiles with a sample wind tunnel run plotted for comparison. This check on the rake profiles was done periodically to assure accurate pressure probe readings.

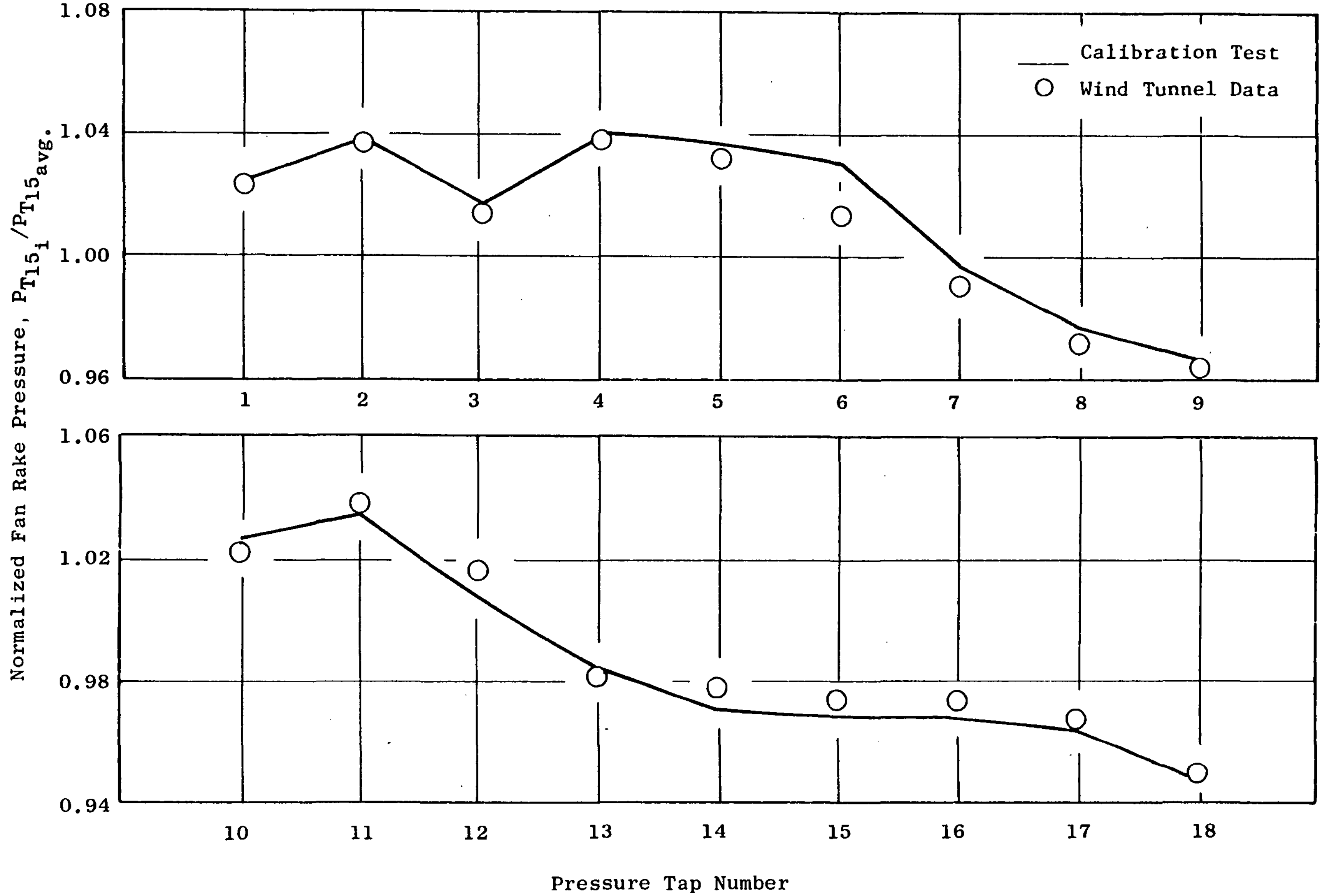

Figure 29. Short Core Fan Rake Pressure Profiles.

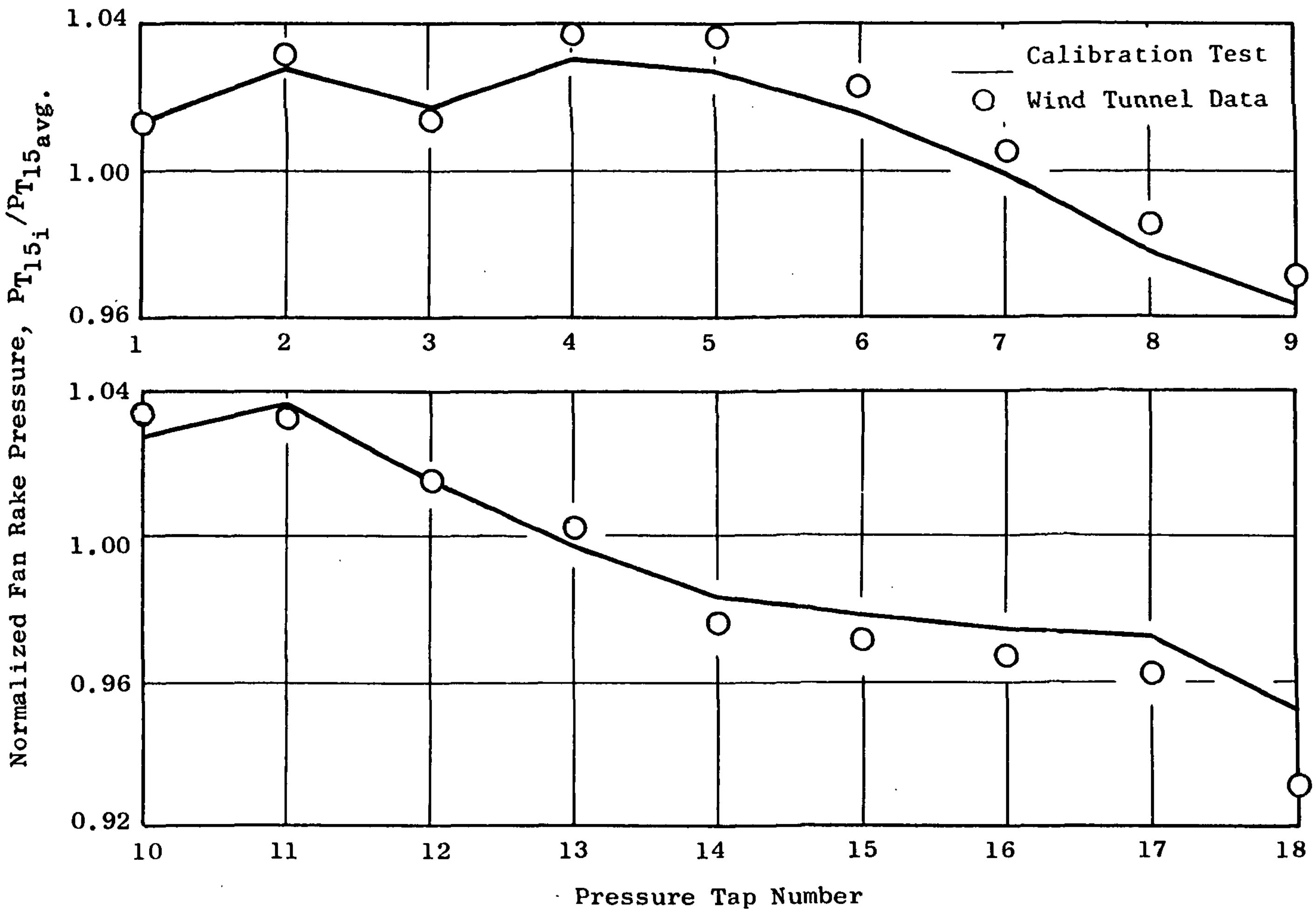

Figure 30. Long Core Fan Rake Pressure Profiles.

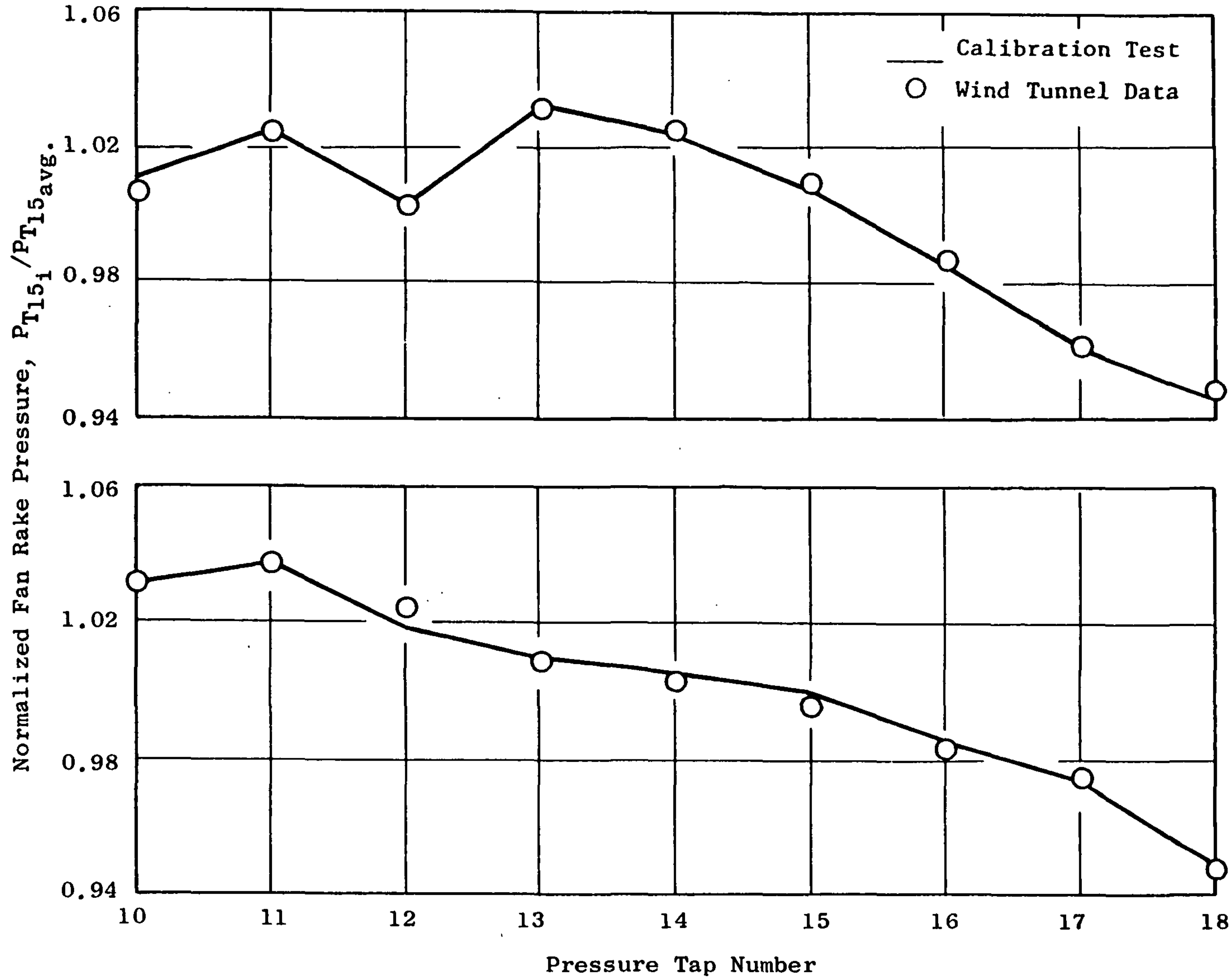

Figure 31. LDMF Fan Rake Pressure Profiles.

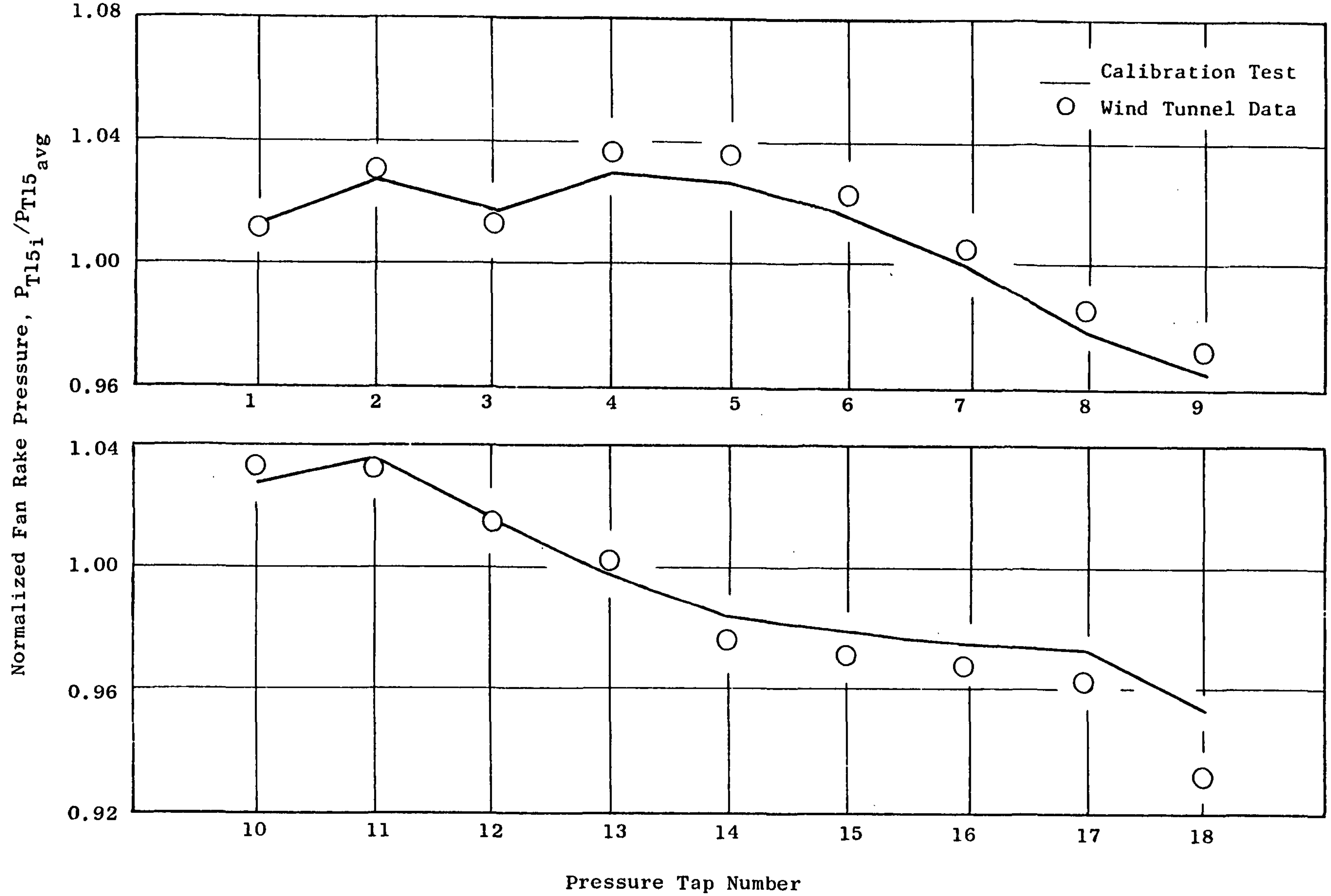

Figure 32. E^3 Fan Rake Pressure Profiles.

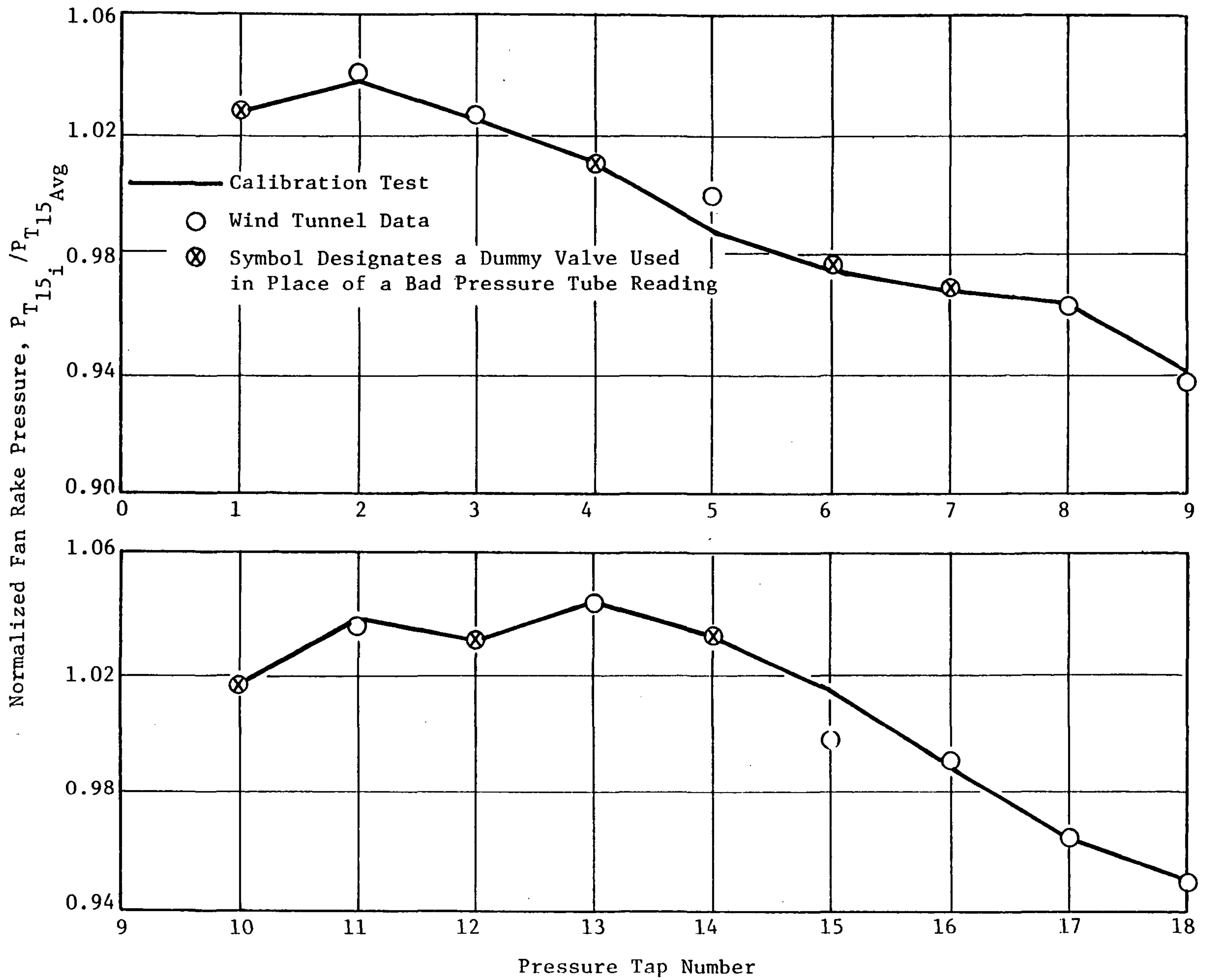

Figure 33. E^3 Extended Nacelle Fan Rake Pressure Profiles.

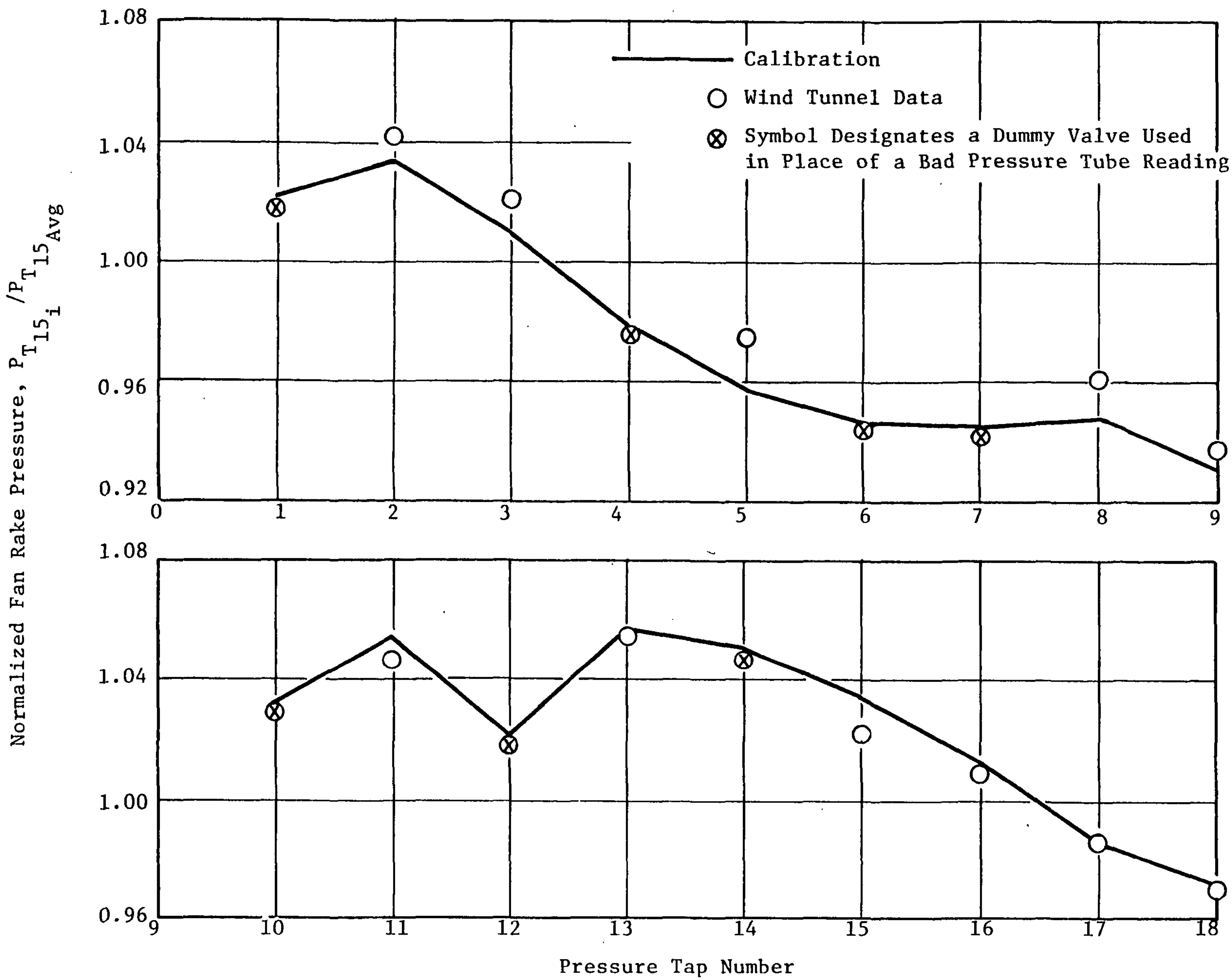

Figure 34. E^3 Separation Flow Fan Rake Pressure Profiles.

REFERENCES

1. Fromm, Eugene H., The Boeing Flight Simulation Chamber for Static Calibrations of Engine Simulators, Presentation at the 45th Meeting of the Supersonic Tunnel Association, April 13, 1976.

Page intentionally left blank

Page intentionally left blank

APPENDIX

NACELLE CONTOURS

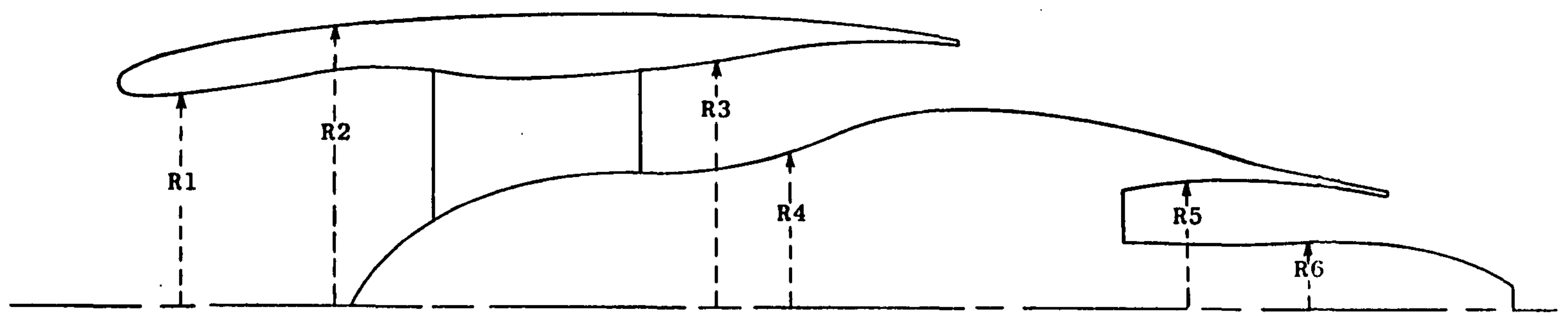

R1 - Fan Cowl Inlet Contours
R2 - Fan Cowl External Contours
R3 - Outer Fan Duct Contours
R4 - Inner Fan Duct Contours
R5 - Outer Primary Duct Contours
R6 - Inner Primary Duct Contours

Nacelle Contour Definition.

FAN COWL INLET CONTOURS (R1)

CF6-50 LONG CORE, SHORT CORE AND LDMF

KEEL		SIDE		CROWN	
Station	R1	Station	R1	Station	R1
4.862	2.730	4.688	2.499	4.513	2.255
4.862	2.706	4.689	2.475	4.517	2.232
4.863	2.697	4.691	2.465	4.519	2.222
4.864	2.692	4.692	2.460	4.521	2.217
4.865	2.685	4.694	2.456	4.523	2.211
4.868	2.677	4.697	2.446	4.527	2.203
4.873	2.663	4.709	2.422	4.533	2.190
4.878	2.652	4.721	2.405	4.540	2.180
4.883	2.643	4.733	2.392	4.547	2.172
4.894	2.627	4.745	2.380	4.553	2.164
4.906	2.614	4.757	2.370	4.560	2.158
4.917	2.602	4.793	2.346	4.566	2.152
4.922	2.597	4.853	2.316	4.573	2.146
4.928	2.592	4.883	2.304	4.585	2.136
4.957	2.570	4.943	2.285	4.598	2.129
4.985	2.552	5.002	2.270	4.660	2.096
5.014	2.536	5.062	2.259	4.722	2.075
5.043	2.522	5.122	2.251	4.844	2.049
5.102	2.499	5.182	2.245	4.906	2.042
5.161	2.480	5.242	2.241	4.965	2.038
5.220	2.465	5.272	2.240	5.025	2.037
5.279	2.452	5.302	2.239	5.085	2.037
5.339	2.442	5.332	2.238	5.116	2.038
5.398	2.434	5.362	2.238	5.145	2.039
5.428	2.431	5.400	2.239	5.175	2.041
5.458	2.428	5.460	2.241	5.205	2.043
5.488	2.425	5.520	2.244	5.235	2.045
5.518	2.423	5.580	2.249	5.281	2.051
5.565	2.420	5.640	2.256	5.328	2.058
5.639	2.416	5.760	2.271	5.376	2.067
5.784	2.413	5.880	2.291	5.425	2.078
5.925	2.413	6.000	2.312	5.475	2.091
6.063	2.416	6.120	2.334	5.526	2.104
6.197	2.422	6.240	2.358	5.577	2.119
6.327	2.430	6.360	2.380	5.630	2.135
6.453	2.438	6.480	2.402	5.738	2.168
6.574	2.447	6.600	2.422	5.850	2.204
6.691	2.456	6.720	2.441	5.966	2.241
6.804	2.465	6.840	2.457	6.026	2.259
6.911	2.473	6.960	2.470	6.149	2.296
7.014	2.480	7.080	2.482	6.277	2.331
7.111	2.486	7.200	2.489	6.409	2.365
7.203	2.491	7.260	2.493	6.547	2.396
7.290	2.495	7.320	2.496	6.689	2.424
7.372	2.497	7.380	2.498	6.837	2.448
7.449	2.499	7.440	2.499	6.913	2.459
7.485	2.500	7.500	2.500	7.068	2.477
7.521	2.500	7.548	2.500	7.229	2.490
9.000	2.500	9.000	2.500	7.311	2.494

FAN COWL INLET CONTOURS (CONT.)

CROWN

Station	R1
7.395	2.498
7.479	2.500
7.548	2.500
9.000	2.500

FAN COWL EXTERNAL CONTOURS (R2)

CF6-50 LONG AND SHORT CORE

Keel Station	Keel R2	Side Station	Side R2	Crown Station	Crown R2
4.862	-2.730	4.688	2.499	4.513	2.255
4.863	-2.741	4.689	2.508	4.514	2.265
4.865	-2.748	4.693	2.524	4.517	2.281
4.866	-2.753	4.697	2.532	4.520	2.289
4.867	-2.758	4.701	2.538	4.524	2.295
4.868	-2.762	4.705	2.543	4.527	2.301
4.870	-2.766	4.708	2.548	4.531	2.306
4.871	-2.769	4.716	2.556	4.537	2.314
4.874	-2.775	4.723	2.563	4.544	2.322
4.876	-2.781	4.730	2.569	4.551	2.329
4.879	-2.786	4.737	2.575	4.557	2.335
4.881	-2.791	4.751	2.585	4.571	2.346
4.884	-2.795	4.758	2.590	4.576	2.351
4.887	-2.799	4.772	2.599	4.591	2.361
4.890	-2.805	4.807	2.619	4.624	2.383
4.894	-2.810	4.842	2.636	4.658	2.403
4.898	-2.815	4.876	2.651	4.691	2.421
4.912	-2.830	4.910	2.666	4.724	2.437
4.923	-2.842	4.945	2.679	4.758	2.453
4.943	-2.859	4.977	2.691	4.791	2.468
4.963	-2.874	5.114	2.736	4.928	2.522
4.983	-2.888	5.249	2.773	5.066	2.568
5.022	-2.912	5.385	2.807	5.203	2.611
5.056	-2.930	5.520	2.837	5.340	2.651
5.089	-2.947	5.655	2.865	5.478	2.687
5.122	-2.962	5.684	2.871	5.508	2.695
5.188	-2.991	5.721	2.879	5.545	2.705
5.253	-3.018	5.786	2.891	5.611	2.721
5.317	-3.043	5.850	2.904	5.677	2.738
5.382	-3.067	5.915	2.915	5.743	2.753
5.511	-3.111	6.044	2.938	5.875	2.784
5.639	-3.152	6.173	2.959	6.007	2.812
5.704	-3.171	6.302	2.979	6.139	2.839
6.031	-3.256	6.430	2.997	6.271	2.865
6.435	-3.342	6.559	3.015	6.403	2.889
6.704	-3.391	6.687	3.031	6.534	2.912
7.108	-3.456	6.944	3.061	6.798	2.955
7.378	-3.494	7.136	3.081	6.996	2.985
7.647	-3.528	7.264	3.093	7.128	3.003
7.917	-3.559	7.392	3.105	7.260	3.020
8.052	-3.572	7.584	7.457	7.457	3.045
8.321	-3.598	7.775	3.135	7.655	3.067
8.591	-3.619	7.903	3.144	7.787	3.081
8.726	-3.629	8.222	3.163	8.117	3.111
8.995	-3.645	8.542	3.179	8.447	3.137
9.265	-3.658	8.860	3.190	8.776	3.158
9.399	-3.663	9.179	3.198	9.106	3.174
9.669	-3.671	9.498	3.203	9.436	3.186
9.938	-3.675	9.817	3.204	9.766	3.192
10.073	-3.676	10.135	3.203	10.096	3.196

FAN COWL EXTERNAL CONTOURS (CONT.)

CF6-50 LONG AND SHORT CORE

Keel Station	Keel R2	Side Station	Side R2	Crown Station	Crown R2
10.343	-3.673	10.454	3.200	10.426	3.196
10.612	-3.665	10.773	3.195	10.756	3.193
10.747	-3.660	11.091	3.188	11.086	3.188
11.016	-3.646	11.219	3.185	11.218	3.185
11.280	-3.626	11.221	3.185	11.400	3.179
11.400	-3.615	11.340	3.181	11.700	3.169
11.640	-3.58	11.400	3.179	12.000	3.157
11.880	-3.559	11.700	3.169	12.180	3.149
12.000	-3.543	12.000	3.157	12.300	3.144
12.240	-3.506	12.180	3.149	12.360	3.142
12.366	-3.484	12.300	3.144	12.600	3.131
12.600	-3.441	12.366	3.142	12.900	3.117
12.900	-3.380	12.600	3.131	13.200	3.101
13.200	-3.315	12.900	3.117	13.500	3.082
13.500	-3.248	13.200	3.101	13.800	3.057
13.800	-3.180	13.500	3.082	14.100	3.026
14.100	-3.111	13.800	3.057	14.400	2.988
14.400	-3.043	14.100	3.026	14.700	2.944
14.700	-2.974	14.400	2.988	15.000	2.897
15.000	-2.905	14.700	2.944	15.120	2.878
15.120	-2.878	15.000	2.897	15.240	2.859
15.240	-2.859	15.120	2.878	15.354	2.840
15.354	-2.840	15.240	2.859		
		15.354	2.840		

FAN COWL EXTERNAL CONTOURS (R2)

CF6-50 LDMF

Station	KEEL R2	CROWN R2	
Same As CF6-50 Long Core			
10.440	3.670	3.214	- Blended into existing inlet
11.040	3.648	3.207	
11.640	3.588	3.186	
12.240	3.486	3.158	
12.840	3.372	3.125	
13.440	3.270	3.125	
14.040	3.174	3.053	
14.640	3.084	3.018	
15.240	3.012	2.983	
15.840	2.945	2.940	
16.440	2.886	2.889	
17.040	2.832	2.834	
17.640	2.779	2.778	
18.240	2.722	2.721	
18.840	2.659	2.660	
19.440	2.593	2.595	
20.040	2.526	2.527	
20.640	2.454	2.453	
21.240	2.370	2.370	
21.840	2.274	2.274	
22.440	2.166	2.166	
23.040	2.048	2.048	
23.490	1.950	1.950	

For Further Definition, Reference G.E. Drawing No's 4013237-726,727,744 & 774

OUTER FAN DUCT CONTOURS (R3)

CF6-50 Long Core

Station	R3
12.550	2.712
12.900	2.750
13.200	2.780
13.500	2.805
13.680	2.823
13.800	2.840
13.980	2.856
14.100	2.860
14.280	2.884
14.400	2.884
14.580	2.885
14.700	2.886
14.880	2.876
15.000	2.869
15.060	2.862
15.120	2.855
15.180	2.847
15.240	2.840
15.300	2.831
15.350	2.825
15.354	2.825

CF6-50 Short Core

Station	R3
Same As Long Core	

CF6-50 LDMF

Station	R3
12.600	2.780
13.200	2.780
13.800	2.780
13.800	2.780
15.000	2.780
15.600	2.780
16.200	2.773
16.800	2.746
17.400	2.704
18.000	2.651
18.600	2.592
19.200	2.528
19.800	2.456
20.400	2.374
21.000	2.291
21.600	2.210
22.200	2.127
22.800	2.044
23.490	1.946

INNER FAN DUCT CONTOURS (R4)

CF6-50 Long Core

Station	R4
12.550	1.647
12.900	1.740
13.200	1.825
13.380	1.870
13.500	1.901
13.680	1.952
13.800	1.986
13.980	2.039
14.100	2.075
14.280	2.133
14.400	2.171
14.580	2.222
14.700	2.250
14.880	2.279
15.000	2.289
15.060	2.291
15.120	2.290
15.180	2.289
15.240	2.286
15.300	2.282
15.360	2.277
15.420	2.272
15.480	2.267
15.540	2.262
15.600	2.257
15.660	2.251
15.720	2.245
15.780	2.240
15.840	2.234
15.900	2.227
16.200	2.196
16.500	2.163
16.800	2.127
17.100	2.088
17.400	2.046
17.700	2.000
18.000	1.952
18.300	1.900
18.600	1.845
18.900	1.787
19.200	1.725
19.500	1.661
19.800	1.596
20.100	1.527
20.400	1.458
20.700	1.388
21.000	1.319

CF6-50 Short Core

Station	R4
Same As Long Core	
15.840	2.234
15.867	2.231
15.900	2.227
16.200	2.192
16.500	2.150
16.800	2.102
17.100	2.048
17.400	1.989
17.700	1.925
18.000	1.857
18.300	1.786
18.600	1.712
18.900	1.635
19.200	1.557
19.500	1.477
19.596	1.451
19.716	1.419
19.836	1.387
19.896	1.371

CF6-50 LDMF

Station	R4
12.600	1.825
13.200	1.825
13.800	1.825
14.400	1.825
15.000	1.825
15.600	1.825
16.200	1.821
16.800	1.812
17.400	1.795
18.000	1.767
18.600	1.718
19.200	1.655
19.800	1.584
20.400	1.506
21.000	1.421
21.600	1.331
22.200	1.240
22.800	1.149
23.400	1.059
23.780	1.006

INNER FAN DUCT (R4) (CONT.)

CF6-50 Long Core

Station	R4
21.120	1.291
21.240	1.264
21.360	1.236
21.480	1.215
21.600	1.203
21.660	1.196
21.720	1.190
21.751	1.186
21.761	1.186
21.792	1.183

CF6-50 Short Core

Station	R4
19.956	1.355
20.016	1.338
20.077	1.322
20.137	1.306
20.197	1.290
20.257	1.274
20.317	1.258
20.340	1.252

OUTER PRIMARY DUCT CONTOURS (R5)

CF6-50 Long Core

Station	R5
18.190	1.500
18.500	1.512
18.780	1.486
18.900	1.465
19.200	1.413
19.500	1.405
19.800	1.397
20.100	1.388
20.400	1.367
20.700	1.335
21.000	1.285
21.120	1.257
21.240	1.230
21.360	1.203
21.480	1.185
21.600	1.175
21.660	1.171
21.720	1.168
21.791	1.167

CF6-50 Short Core

Station	R5
18.190	1.500
18.500	1.512
18.780	1.486
18.900	1.465
19.200	1.412
19.500	1.374
19.560	1.364
19.680	1.345
19.800	1.325
19.920	1.302
20.040	1.277
20.100	1.263
20.160	1.252
20.220	1.244
20.280	1.238
20.340	1.236

CF6-50 LDMF

Station	R5
18.000	1.478
18.600	1.487
19.200	1.466
19.800	1.422
20.400	1.369
21.000	1.311
21.600	1.248
22.200	1.180
22.800	1.107
23.400	1.039
23.780	1.002

INNER PRIMARY DUCT AND PLUG CONTOURS (R6)

CF6-50 Long Core

Station	R6
18.290	0.805
18.500	0.810
18.780	0.816
18.900	0.813
19.200	0.801
19.500	0.816
19.800	0.832
20.100	0.817
20.400	0.794
20.700	0.765
20.760	0.758
20.880	0.744
21.000	0.727
21.120	0.710
21.240	0.691
21.360	0.671
21.480	0.650
21.600	0.628
21.720	0.605
21.840	0.580
21.960	0.552
22.080	0.523
22.200	0.490
22.500	0.392
22.800	0.253
22.860	0.212
22.896	0.183

CF6-50 Short Core

Station	R6
18.290	0.805
18.500	0.810
18.780	0.816
18.900	0.813
19.200	0.801
19.500	0.814
19.560	0.812
19.680	0.824
19.800	0.823
19.920	0.807
20.040	0.780
20.100	0.764
15^{o} cone	
22.280	0.180

CF6-50 LDMF

Station	R6
18.000	0.793
18.600	0.796
19.200	0.736
19.800	0.630
20.400	0.506
21.000	0.372
21.600	0.176
22.200	0.0

FAN COWL INLET CONTOURS (R1)

E^3

KEEL Station	KEEL R1	CROWN Station	CROWN R1
5.3346	2.5223	4.9994	2.2700
5 3351	2.5016	5.0031	2.2496
5.3398	2.4807	5.0112	2.2296
5.3485	2.4598	5.0237	2.2102
5.3613	2.4390	5.0405	2.1915
5.3778	2.4186	5.0614	2.1737
5.3982	2.3986	5.0864	2.1567
5.4224	2.3792	5.1152	2.1410
5.4499	2.3604	5.1477	2.1262
5.4808	2.3426	5.1836	2.1129
5.5148	2.3257	5.2226	2.1009
5.5516	2.3099	5.2646	2.0902
5.5912	2.2953	5.3092	2.0811
5.6329	2.2820	5.3561	2.0734
5.6768	2.2702	5.4050	2.0675
5.7225	2.2597	5.4557	2.0630
5.7696	2.2509	5.5076	2.0603
5.8177	2.2438	5.5605	2.0593
5.8667	2.2384	5.6141	2.0600
5.9161	2.2346	5.6679	2.0622
6.1072	2.2284	5.8750	2.0782
6.2987	2.2309	6.0818	2.1014
6.4909	2.2410	6.2884	2.1307
6.6822	2.2574	6.4949	2.1647
6.8739	2.2789	6.7014	2.2023
7.0655	2.3042	6.9081	2.2421
7.2570	2.3320	7.1149	2.2830
7.4482	2.3613	7.3220	2.3238
7.6391	2.3907	7.5293	2.3631
7.8297	2.4189	7.7370	2.3998
8.0200	2.4448	7.9449	2.4325
8.2100	2.4671	8.1532	2.4602
8.3998	2.4845	8.3616	2.4815
8.5895	2.4959	8.5703	2.4952
8.7790	2.5000	8.7790	2.5000

FAN COWL EXTERNAL CONTOURS (R2)

E^3

KEEL		CROWN	
Station	R2	Station	R2
5.3346	2.5223	4.9994	2.2700
5.3359	2.5313	4.9996	2.2792
5.3411	2.5458	5.0032	2.2943
5.3453	2.5532	5.0066	2.3022
5.3492	2.5589	5.0101	2.3084
5.3530	2.5636	5.0135	2.3136
5.3567	2.5679	5.0169	2.3183
5.3639	2.5751	5.0237	2.3266
5.3710	2.5814	5.0305	2.3338
5.3780	2.5870	5.0373	2.3404
5.3848	2.5921	5.0441	2.3464
5.3984	2.6012	5.0576	2.3574
5.4052	2.6053	5.0644	2.3624
5.4186	2.6130	5.0779	2.3719
5.4517	2.6296	5.1116	2.3931
5.4844	2.6439	5.1454	2.4119
5.5168	2.6567	5.1791	2.4291
5.5491	2.6684	5.2128	2.4451
5.5812	2.6792	5.2465	2.4603
5.6120	2.6890	5.2789	2.4742
5.7391	2.7236	5.4138	2.5253
5.8650	2.7522	5.5487	2.5697
5.9903	2.7771	5.6838	2.6098
6.1151	2.7996	5.8189	2.6468
6.2395	2,8201	5.9541	2.6810
6.2661	2.8243	5.9832	2.6881
6.3001	2.8297	6.0202	2.6972
6.3595	2.8389	6.0851	2.7126
6.4189	2.8478	6.1500	2.7276
6.4782	2.8564	6.2149	2.7420
6.5965	2.8726	6.3447	2.7696
6.7144	2.8877	6.4744	2.7955
6.8321	2.9018	6.6042	2.8197
6.9496	2.9151	6.7340	2.8426
7.0668	2.9276	6.8638	2.8640
7.1838	2.9393	6.9936	2.8841
7.4173	2.9619	7.2533	2.9207
7.5920	2.9758	7.4480	2.9452
7.7083	2.9850	7.5779	2.9601
7.8245	2.9938	7.7077	2.9739
7.9985	3.0061	7.9025	2.9928
8.1723	3.0175	8.0973	3.0095
8.2881	3.0247	8.2272	3.0194

FAN COWL EXTERNAL CONTOURS (CONT.)

KEEL			CROWN	
Station	R2		Station	R2
8.5771	3.0411		8.5519	3.0402
8.8712	3.0554			
9.1777	3.0666			
9.4841	3.0743			
9.7904	3.0787			
10.0970	3.0800			
12.9510	3.0800			
13.5000	3.0744			
14.0000	3.0595			
14.5000	3.0353	Radius = 26.83122	Same As Keel	
15.0000	3.0017			
15.5000	2.9587			
16.0000	2.9062			
16.5000	2.8443			
17.0000	2.7728			
17.5000	2.6916			
18.0000	2.6007			
18.4837	2.5034			
19.0000	2.3946			
19.5000	2.2892	Conical		
20.0000	2.1838			
20.5000	2.0785			
20.9150	1.9910			

FAN DUCT CONTOURS (R3 & R4)

E^3

Outer Fan Duct (R3)		Inner Fan Duct (R4)
Station	R3	R4
13.828	2.720	1.750
14.457	2.720	1.751
15.085	2.720	1.754
15.714	2.715	1.752
16.342	2.694	1.739
16.971	2.647	1.709
17.599	2.569	1.661
18.228	2.466	1.593
18.856	2.351	1.502
19.485	2.236	1.384
20.114	2.124	1.261
20.742	2.009	1.138
20.915	1.979	1.102
21.100	---	1.069

PRIMARY DUCT CONTOURS (R5 & R6)

E^3

Outer Primary Duct (R5)		Inner Primary Duct (R6)
Station	R5	R6
18.228	1.440	0.8100
18.856	1.407	0.7740
19.485	1.325	0.6984
20.114	1.220	0.5840
20.742	1.116	0.4220
20.915	1.087	0.3600
21.100	1.057	0.2840
21.586	--	0.000

FAN COWL EXTERNAL CONTOURS

E^3 EXTENDED NACELLE

Station	R2	
Same as E^3 forward of Station 11.6640		
11.6640	3.0800	Cylinder
12.9510	3.0800	
13.0	3.0799	
13.2	3.0788	
13.4	3.0762	
13.6	3.0721	
13.8	3.0666	
14.0	3.0595	
14.2	3.0509	
14.4	3.0408	
14.6	3.0293	
14.8	3.0162	
15.0	3.0017	Radius = 26.83122 in.
15.2	2.9856	
15.4	2.9680	
15.6	2.9489	
15.8	2.9283	
16.0	2.9062	
16.2	2.8826	
16.4	2.8574	
16.6	2.8307	
16.8	2.8025	
17.0	2.7728	
17.2	2.7414	
17.5315	2.6861	
18.0	2.6050	
18.5	2.5183	
19.0	2.4317	Conical
19.5	2.3451	$y = 5.7236 - 0.17326\ X$
20.0	2.2584	
20.5	2.1718	
21.0	2.0852	
21.5436	1.9910	

FAN DUCT CONTOURS (R3 and R4)

E^3 EXTENDED NACELLE

Station	R3		R4
			Same as E^3
13.765	2.720	Cylinder	
15.085	2.720		
15.714	2.715		
16.342	2.694		
16.971	2.647		
17.599	2.569		
17.8	2.538		
18.0	2.505		
18.2	2.472		
18.4	2.438		
18.6	2.404		
18.8	2.371		
19.0	2.338		
19.2	2.303		
19.4	2.270		
19.6	2.237		
19.8	2.202		
20.0	2.168		
20.2	2.134		
20.4	2.101		
20.6	2.067		
20.8	2.033		
21.0	2.002		
21.2	1.979		
21.4	1.967		
21.5436	1.966		

PRIMARY DUCT CONTOURS (R5 and R6)

Station	R5	R6
Same as E^3		

FAN COWL EXTERNAL CONTOURS (R2)

E^3 SEPARATE FLOW

Same as E^3 forward of Station 11.664

Station	R2	
11.664	3.080	Cylinder
12.413	3.080	
12.704	3.079	
12.994	3.075	
13.285	3.067	
13.575	3.057	
13.866	3.045	
14.156	3.033	
14.447	3.019	
14.737	3.004	
15.028	2.985	
15.319	2.959	
15.609	2.926	
15.900	2.886	
16.190	2.842	
16.481	2.796	
16.655	2.767	

FAN DUCT OUTER CONTOUR (R3)

E^3 SEPARATE FLOW

Station	R3	
13.765	2.720	Cylinder
14.600	2.720	
14.800	2.722	
15.000	2.728	
15.200	2.742	
15.400	2.756	
15.600	2.766	
15.667	2.769	
15.900	2.781	
16.045	2.786	
16.190	2.787	
16.365	2.778	Straight Line
16.500	2.761	$\theta = -7.15886°$
16.655	2.741	

FAN DUCT INNER WALL (R4)

E^3 SEPARATE FLOW

Station	R4	
13.6	1.6500	
13.8	1.7040	Straight Line $\theta = 7.7197°$
14.0	1.7311	
15.0	1.8667	
15.6	1.9480	
15.7200	1.9800	
15.7837	2.0113	
15.8128	2.0279	
15.8418	2.0460	
15.8709	2.0656	
15.8999	2.0866	Radius = 0.600807
15.9581	2.1249	
16.0162	2.1544	
16.0743	2.1766	
16.1324	2.1922	
16.1905	2.2018	
16.2486	2.2056	
16.3067	2.2038	
16.3576	2.1976	
16.4205	2.1871	Straight Line $\theta = -9.43996°$
17.0	2.0908	
17.5	2.0076	
18.0	1.9245	
18.5	1.8414	
19.0	1.7582	
19.5	1.6751	
20.0	1.5920	
20.5	1.5088	
21.0	1.4257	
21.5	1.3426	
21.7440	1.3020	

PRIMARY DUCT CONTOURS (R5 and R6)

E^3 SEPARATE FLOW

Station	R5	R6	
19.403	1.498	---	
19.419	1.500	---	
19.503	---	0.802	
19.519	---	0.805	
19.6	1.510	0.811	
19.7	1.512	0.818	
19.8	1.510	0.823	
19.9	1.508	0.829	
20.0	1.503	0.830	
20.1	1.496	0.830	
20.2	1.488	0.830	
20.3	1.479	0.830	
20.4	1.469	0.830	Cylinder
20.5	1.458	0.830	
20.6	1.447	0.830	
20.7	1.435	0.830	
20.8	1.422	0.830	
20.9	1.409	0.833	
21.0	1.394	0.852	
21.1	1.378	0.879	
21.2	1.363	0.903	
21.3	1.347	0.913	
21.4	1.330	0.911	
21.5	1.312	0.900	
21.6	1.293	0.880	
21.7	1.274	0.856	
21.744	1.265	---	
21.8		0.826	
22.0		0.765	
22.5		0.612	Straight Line
23.0		0.459	$\theta = -17.00°$
23.5		0.306	
24.0		0.153	
24.502		0.0	

NASA Contractor Report 165949
Distribution List
NAS1-15345

	No. Copies
NASA Langley Research Center Hampton, VA 23665 Attn: Report and Manuscript Control Office, M/S 180A	1
James C. Patterson, Jr., M/S 280	40
NASA Ames Research Center Moffett Field, CA 94035 Attn: Library, Mail Stop 202-3	1
NASA Dryden Flight Research Center P. O. Box 273 Edwards, CA 93523 Attn: Library	1
NASA Goddard Space Flight Center Greenbelt, MD 20771 Attn: Library	1
NASA Lyndon B. Johnson Space Center 2101 Webster Seabrook Road Houston, TX 77058 Attn: JM6/Library	1
NASA Marshall Space Flight Center Marshall Space Flight Center, AL 35812 Attn: Library, AS24L	1
Jet Propulsion Laboratory 4800 Oak Grove Drive Pasadena, CA 91103 Attn: Library, Mail Code 111-113	1
NASA Lewis Research Center 21000 Brookpark Road Cleveland, OH 44135 Attn: Library, Mail Stop 60-3	1
NASA John F. Kennedy Space Center Kennedy Space Center, FL 32899 Attn: Library, NWSI-D	1
National Aeronautics and Space Administration Washington, DC 20546 Attn: RJT-2	1
Scientific and Technical Information Facility 6571 Elkridge Landing Road Linthicum Heights, MD 21090	25 plus original